Prepared for:

RIKZ- Rijkwaterstaat

Ecobeach Monitoring project Phase II

Year study

Report

January 2008

WL | delft hydraulics

Z4398.00

Prepared for:

RIKZ- Rijkwaterstaat

Ecobeach Monitoring project Phase II

Year study

C. Brière, A. Cohen, H. vd Boogaard and S. Arens

Report

January 2008

WL | delft hydraulics

WL | delft hydraulics

Client:	RIKZ- Rijkwaterstaat
Title:	Ecobeach Monitoring project Phase II

Abstract:

In order to protect the Dutch coast in an innovative way, the Ecobeach technique (vertical, passive drainage pipes that are regularly spaced on the beach) has been installed in Egmond. During the half-year study, an objective method (statistical model) has been developed to identify the natural behaviour of the beach and dune system in the test area, based on historical data of Coastal State Indicators deduced mainly from Jarkus data.

The overall objectives of the year study are: (i) to improve the statistical model in order to make it able to describe seasonal patterns, (ii) to describe the long-term natural behaviour of the coastal system in the reference area, (iii) and to analyse the behaviour of the beach and dune system in the test area after installation of the Ecobeach modules, with respect to the spatial and temporal references, and then to identify potential effects of the Ecobeach system.

Statistical regression models, including harmonic components to take into account cyclic patterns (sand bar migration, seasonal variations), have been set-up. Comparison between model outputs and observations, obtained after installation of the drainage system, enables the identification of potential effects of the drainage system.

An increase of the MCL and MiCL volumes have been observed between 2006 and 2007 in the test and in the reference areas. The increase of volumes has been predicted by the model and is associated to natural causes (cyclic reappearance of the sand bar). In general, no significant trend break has been noticed in the evolution of Coastal State Indicators.

References:	<begin hier>

Ver	Author		Date	Remarks	Review		Approved by	
	C. Brière		07/01/08		D. Walstra		T. Schilperoort	

Project number:	Z4398.00
Keywords:	
Number of pages:	103
Classification:	None
Status:	Final

Contents

1 Introduction

1.1 Background

The Dutch government is challenging businesses to stimulate innovation. This has led to a proposal by BAM (largest construction firm in The Netherlands) to the Minister of Public Works to protect the Dutch coast in an innovative way with the Ecobeach technique, which has been developed in Denmark by the Skagen Innovation Centre (SIC). It is an easily installable system that consists of vertical, passive drainage pipes that are regularly spaced on the beach (see Appendix A for more details). There is no physical understanding yet of the functioning of the system, based on existing knowledge.

The Ministry of Public Works (RIKZ) is now investigating the added value of the proposed technique. This is done under the framework of the WINN program (WAter INnovatiebron). A field experiment is being carried out in Egmond aan Zee (The Netherlands), which started in November 2006. The proposed duration of the experiment is three years. After one year, an evaluation report will be made, based on which will be decided to complete the test for the full three year period or to remove the modules (in case of negative effects of the system on the coastal behaviour). RIKZ and BAM would like to find out more about the functioning of the system and its effects on the coast. For this understanding, good and thorough monitoring is needed, in order to quantify the possible effects of the drainage system. Identification of the effects of the system as opposed to natural variations in the coast is important in that sense.

WL|Delft Hydraulics has set up a monitoring strategy for the field experiment in Egmond, which is called Phase 1 in the Ecobeach project (Cohen and Grasmeijer, 2007). Based on the plan resulting from Phase 1, WL|Delft Hydraulics has made a proposal for the data analysis of monitoring data during the first year , which is called Phase 2. The present report is the product of the analysis after the first year of the monitoring project.

The project team includes coastal morphologists C. Brière and A.B. Cohen, an expert in statistical analysis, H.P.F. van den Boogaard, and a specialist of dune dynamics S.M. Arens. Review of the report has been performed by D.J.R. Walstra.

1.2 Preliminaries

During the half-year study of the Ecobeach project (Brière et al., 2007), the following objectives have been reached:

1. An objective method (statistical model) has been defined to identify the long-term natural behaviour of the beach and dune system in the test area, based on historical data.

40-years historical yearly Jarkus data have been used to predict future coastal evolution of a selection of Coastal State Indicators, under natural conditions:

- in 2007, the 95% prediction interval for the MCL volume of the test area is [1106 m^3/m, 1234 m^3/m], with a mean extrapolated value of 1170 m^3/m.
- strongly correlated, the MCL position is predicted in 2007 in the range of [113.3 m 132.3 m], with a mean extrapolated value of 122.7 m.
- the 95% prediction interval for the MiCL volume in 2007 is [18.64 m^3/m 48.56 m^3/m], with a mean extrapolated value of 33.66 m^3/m.
- the 95% prediction interval of the MiCL position is predicted in 2007 in the range of [30.7 m 47.8 m], with a mean extrapolated value of 39.3 m.
- the 2007 95% prediction interval for the shoreline posistion is [85.04 m, 129.8 m], with a mean extrapolated value of 107.6 m
- for the dune foot position, the 95% prediction interval in 2007 is [-36.20 m, -24.82 m], with a mean predicted dune foot position of -30.51 m.
- in 2007, the 95% prediction intervals for the beach width and the beach volume are of [115.2 m, 160.5 m], and of [154.2 m^3/m, 193.7 m^3/m], respectively, whereas the mean predicted beach width and beach volume are 138 m and 174.1 m^3/m, respectively.
- with respect to the dunes, the analysed data show a large spatial and temporal variability of volume changes. A regression model has also been set-up for the dune volumes. In 2007, the 95% prediction interval is of [1160 m^3/m, 1214 m^3/m], with a mean extrapolated value of 1187 m^3/m.

2. The behaviour of the beach and dune system in the test area during the first half year after installation of the Ecobeach modules, has been investigated with respect to the natural behaviour of the system.

Argus data obtained after installation of the Ecobeach system has been analysed to identify potential effects of the drainage system on the morphology of the intertidal area. After spatial aggregation, the small number of available points appeared statistically inconclusive, and the prediction intervals, for both the MiCL volume and the MiCL position, display exponential shapes, which prevented, at this moment, the comparison of trends of evolution before and after the installation of the system. In this context, it has been highly recommended to consider the extension of the Argus dataset to a longer historical period of about minimum 3 years, with at maximum a 3-months interval. In particular, it was crucial to gather information before the installation of the Ecobeach system. The Argus station provides images since 1996.

Moreover, a dGPS system has also been used over the last 5 years to monitor the studied area. It has been pointed out that dGPS data, provided in an appropriate format, would be clearly useful, as the monitoring project based on this measuring technique is covering the periods May 2002- June 2004 and November 2006 to present, with a monthly measuring frequency. Such dataset would therefore give insight on the (pre- and post-installation of the Ecobeach technique) behaviours of the beach – from the dune foot position to the intertidal beach area.

1.3 Objectives

The overall objective of this study is to identify the effects of the Ecobeach modules on the natural behaviour of the beach and dune system in the test area.

There are three sub-objectives to enable this identification:

1. To improve the statistical model, which has been developed during the first half-year of the project, in order to identify the medium-term behaviour of the beach and dune system, based on historical data.

2. To evaluate the behaviour of the beach and dune systems *in the test area* during the first year after installation of the Ecobeach modules, with respect to the (natural) behaviour of the system before installation of the Ecobeach modules. This evaluation is based on a temporal comparison.

3. To evaluate the behaviour of the beach and dune systems in the test area during the first year after installation of the Ecobeach modules, with respect to the (natural) behaviour of the beach system in an *adjacent reference area*. This evaluation is based on a spatial comparison.

1.4 Outline

The present study consists of the following subjects:

- a description of the test site, the Ecobeach module locations, the reference area and the conditions during the first year of the test (Chapter 2)
- a description of the historical datasets (Jarkus, laser-altimetry, dGPS and Argus datasets) and the Coastal State Indicators and aggregation levels used in the analyses (Chapter 2)
- a description of statistical models that can be used to define both the long- and medium-term natural behaviours of the beach and dune system (Chapter 3)
- the analysis for different aggregation levels of the historical and the current (after installation of the Ecobeach modules) behaviour of the Coastal State Indicators, for both the test and the reference areas, using the statistical models described previously (Chapters 1 and 6)
- conclusions that can be drawn about the effects of the Ecobeach modules on the natural behaviour of the beach and dune system in the test area (Chapter 7).
- recommendations for the remaining years of the Ecobeach project are finally addressed in chapter 8.

2 Test site

Egmond is located in the central part of the Dutch coast, between Den Helder and Hoek van Holland. Figure 2.1 presents the geographical location of the site.

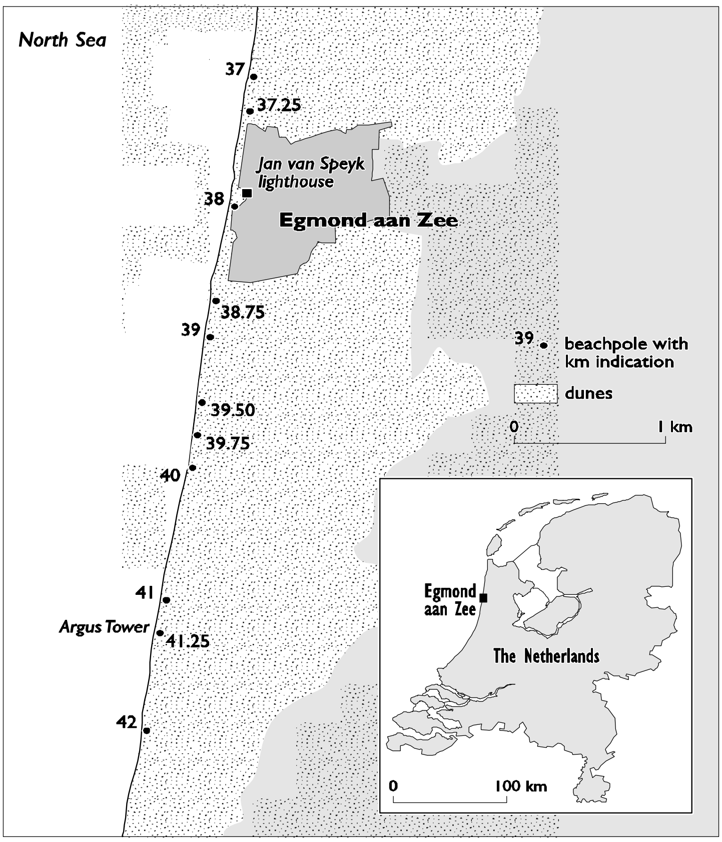

Figure 2.1 Location of Egmond aan Zee in The Netherlands.

2.1 Hydrodynamic conditions

The Holland coast is a mixed-energy coast, according to the classification scheme of Davis and Hayes (1984). A mixed-energy coast implies that both wind waves and tides act on the sandy sediments and induce the morphological responses.

The Dutch coast faces the North Sea and is exposed to sea waves and swell. The tidal wave, which finds its origin on the Atlantic Ocean, enters the basin of the North Sea in the north. The Coriolis force causes the tidal wave to rotate anti-clockwise in the tidal basin. Gradients both in phase and in amplitude occur along the Dutch coast. At Egmond, the general coastline orientation is 8° N (topographic North), which results in 278° N for the shore normal direction. The mean tidal range varies between 1.2 m +NAP during the neap tides to 2.1 m +NAP during spring tides. The tidal peak currents in the offshore zone are about 0.5 m/s, the flood current to the north is slightly larger than the ebb current to the south. The mean monthly offshore wave height has a seasonal character and varies from about 1 m in the summer months (May-August) to about 1.5 to 1.7 m in the autumn and winter (October to January). It can be as large as 5 m at 15 m depth during major storms from southwest or northwest directions.

The wave conditions during the first year of the Ecobeach experiment are shown in Figure 2.2. At the start of the experiment (November 2006), a heavy storm from north-west direction occurred with wave heights of up to 5 m. The remaining November and December months show regular winter conditions. At the end of December (19-27), conditions were weak, with wave heights lower than 1 m. In January 2007, two major storm occurred (11 and 18) from westerly direction with wave heights of approximately 4 m. After that, wave conditions became more moderate for a while, until two major storms occurred in March 2007 (18 and 20). These were the last of the winter season and the spring season has set in since then, with moderate wave conditions. Low-energy conditions remained until July the 6th when a storm occurred (with wave heights of about 3 m). The remaining days in July and August show regular summer conditions. In September, conditions became slightly stronger, with a storm occurring the 10th from westerly direction with wave heights of approximately 3 m. The beginning of October was characterized by low-energy wave conditions.

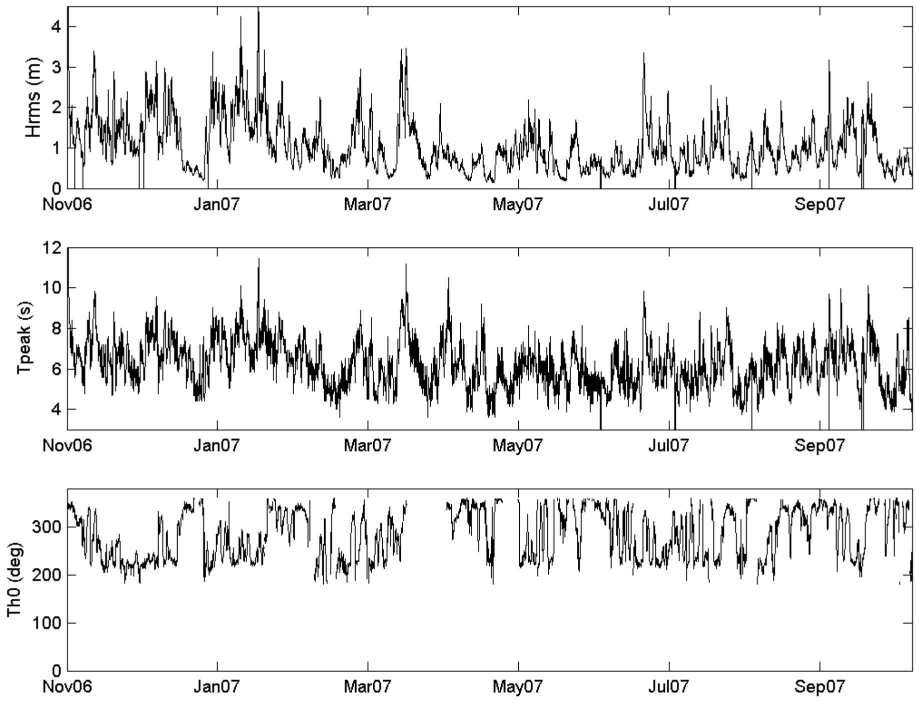

Figure 2.2 Wave conditions (Hrms, Tpeak, Dirp) during the first year of the Ecobeach experiment

2.2 Wind conditions

Most of the winds along the Holland coast come from the North Sea. The prevailing wind direction is southwest (23%), followed by west (16%), east (13%) and northwest (12%) (Stolk, 1989). The storm winds causing the largest wind set-up along the coast are coming from northwest.

Similarly, the prevailing wind directions between November 2006 and October 2007 are southwest, followed by west (Figure 2.3).

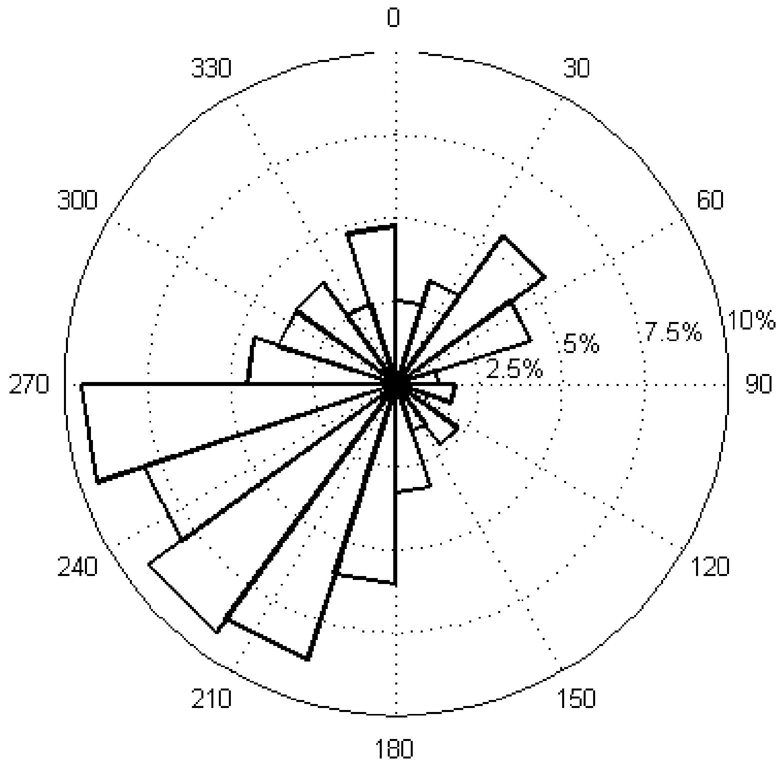

Figure 2.3 Wind rose between November 2006 and October 2007. Wind direction is expressed as the direction from which the wind is blowing.

Wind forcing plays a major role in transferring sediments from the dry beach to the dunes. In order to evaluate its potential influence in time, the temporal wind vectors are plotted in Figure 2.4. The dominant component (southwest) can be found all the time, with a higher occurrence during the winter. The north-easterly component (less than 10%) is obtained mainly during the summer period.

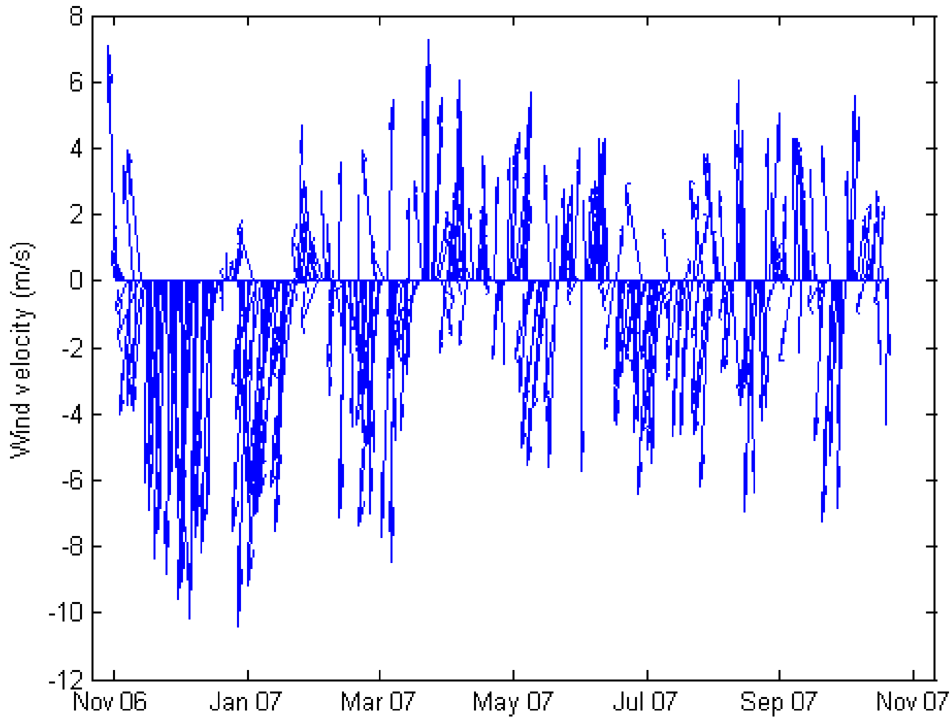

Figure 2.4 Wind velocities. Positive values display northerly winds, whereas the negative ones display southerly winds.

2.3 General behaviour at Egmond-aan-Zee

The large-scale bathymetry can be characterised as a uniform, straight coast with parallel depth contours. The beach width is about 100 to 125 m with a slope between 1 to 30 and 1 to 50. This part of the Dutch coast is typical for the quasi-uniform sandy beaches dominated by breaker bars. Rip channels interrupt breaker bars and small, local bars are present. Two main longshore breaker bars run parallel to the shoreline most of the time. The inner bar is located approximately 400 m from the shoreline at 3 m below mean sea level, whilst the crest of the outer bar is located at about 700 m from the shoreline at 6 m below mean sea level, see Figure 2.5. The inner bar is separated from the outer by a wide trough. Generally the area is characterised by medium well-sorted sands (0.25-0.5 mm), but in the trough between the inner and outer bars, sand is coarse (> 0.5 mm) and has moderate sorting. The cross-shore slope amounts to 1:100 and the median grain size is about 200 µm (Elias et al., 2000 and Van Rijn et al., 2001).

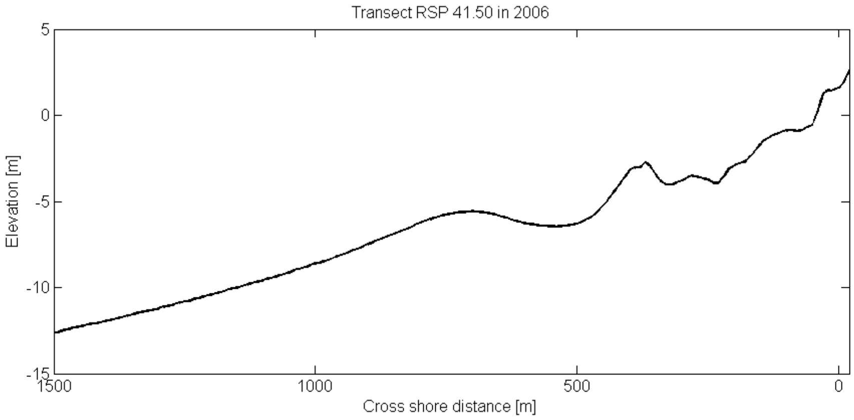

Figure 2.5 A characteristic cross-shore profile at Egmond with the outer bar at x = 700 m, and the inner bar at x = 400m

On large longshore scale (10 km) and on long term (years), the behaviour of the outer and inner bars at Egmond is two-dimensional in the sense that the bars are continuous and of the same form in longshore direction and show the same overall pattern (onshore and offshore migration). On small scale (1 km) and on the short time scale of a storm month, longshore non-uniformities may develop as local disturbances that are superimposed on the overall straight base pattern yielding a three-dimensional morphological system. Rip channels (with length of 200 to 300 m and depth of 0.5 to 1 m) are generated in the crest zone of the inner bar on the time-scale of a few days during minor storm conditions. Rip channels generally are washed out during major storm conditions. Overall, it can be concluded that the net changes at the inner bar and at the beach are relatively small, but larger changes can be observed at the outer bar. The bars show a long-term migration of about 20 to 40 m/year in seaward direction (Van Rijn et al., 2003).

Spatial variations in beach width and volume are due to sand waves. Quartel and Grasmeijer (2006) found variations in beach width of about 40 m over a distance of roughly 300 m, although these variations were not always present. A sand wave crest (large beach width) may contain 5000 m^3 of sand. Sand waves were found to migrate with an alongshore velocity of roughly 250 m/year, but not necessarily in one predominant direction.

At Egmond-aan-Zee, the foredunes are semi-natural. In the past, management mainly consisted of enlarging the dune body by means of sand fences and plantation of marram grass. This part of the coastline is now managed less strictly, and the foredunes are developing more or less freely and natural.

2.4 Test area

Starting in November 2006, a field experiment with Ecobeach modules is being carried out in Egmond aan Zee. The test areas, where Ecobeach modules are installed, are shown in Figure 2.6. The test areas are chosen in such a way that both areas can clearly be monitored with the Argus cameras present in Egmond. There are two Argus video stations located in Egmond, marked with red stars in the figure, the northern one in the Jan van Speijk lighthouse and the other approximately 3 kilometres to the south at the Coast3D tower (built especially for the Argus cameras during the European Coast3D project). The northern test area (marked in red) is located in a region which is heavily nourished during the past years (shoreface and beach). The southern test area (marked in yellow) is located in a fairly undisturbed region. For this reason it is chosen to focus on the southern test area for the analysis of the effects of the Ecobeach modules on the natural behaviour of the beach and dune system, as the natural behaviour of the northern test area is difficult to describe due to the extensive nourishments carried out in the past.

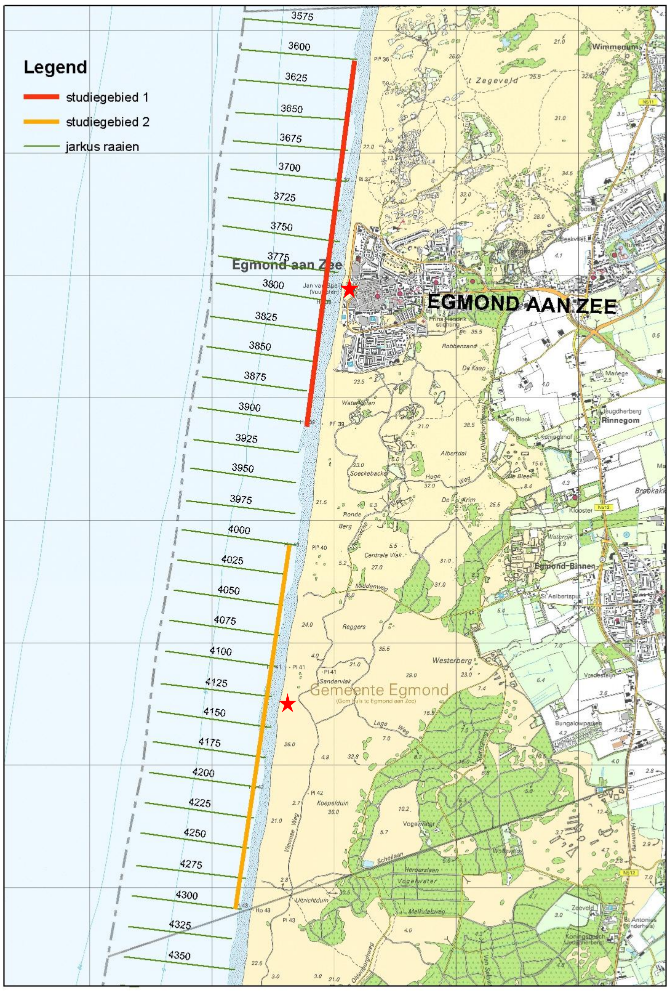

Figure 2.6 Map of the coastal area near Egmond aan Zee. The two Ecobeach test areas are marked in red and yellow, the two Argus stations are shown with red stars. Analysis will focus on the undisturbed southern test area.

For a more extensive description of the morphological behaviour of the test area we refer to the Ecobeach monitoring plan Phase 1 (Cohen and Grasmeijer, 2007).

2.5 Reference area

By comparing the evolution- trends before and after the installation of the Ecobeach modules in the test area, the analysis provides insights on the long-term and medium-term behaviours of Coastal State Indicators only for this specific area. Such temporal analysis does not enable the distinction of potential trend breaks due to particular events to ones induced by the Ecobeach technique. To that end, a reference area has been also considered and results obtained simultaneously for the test and the reference areas are compared. The reference area has been chosen at the south of the test area, and stretches from Beach Pole RSP 43.00 to RSP 46.00. Moreover, no influence of the Ecobeach system is expected in the reference area as the longshore transports are on average directed northward.

3 Data and Coastal State Indicators

3.1 Datasets

The bathymetry and topography at Egmond-aan-Zee have been highly monitored. Sources of data are the JARKUS database, laser-altimetry dataset, dGPS surveys, the ARGUS database, and WESP surveys. As these different datasets are characterized by different monitoring frequencies (from yearly to monthly, and sporadic) and by different precision of the measurement techniques, statistical analysis of Coastal State Indicators can provide information at different time-scales. However, datasets are not directly compatible. It requires long-term datasets, to identify potential effects of the Ecobeach system respective to the natural evolution. It means that answering to the research questions is a long process, and that conclusions can be expected at different time-scales, but should not be given right away based only on a few observations obtained after the installation of the Ecobeach system.

3.1.1 Jarkus data

The bathymetry of the Holland coast (Figure 3.1) is monitored on an annual basis and contained in the JARKUS data base of the Dutch Department of Public Works. The monitoring of this area started in 1963 in the southern part (km 99-km 118). From 1964 on, also the other part of the Holland coast (km 0-km 99) was included in the monitoring program.

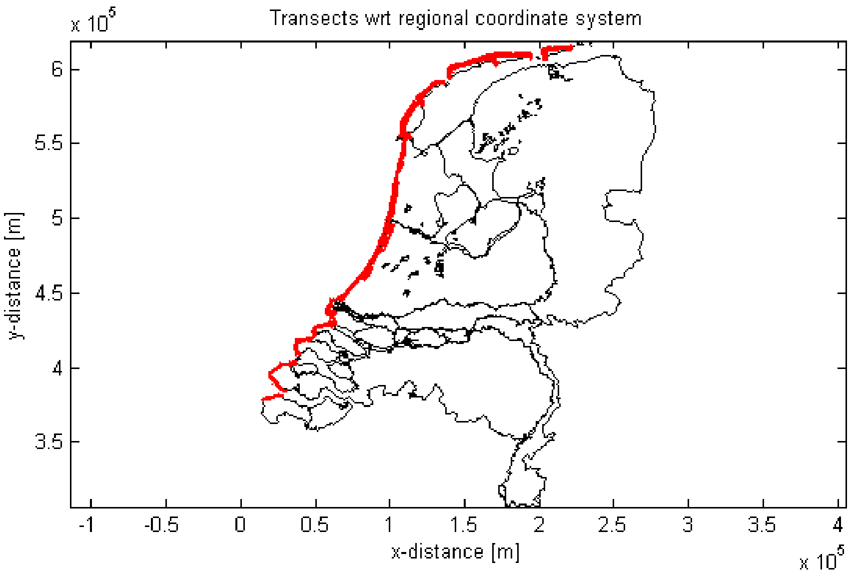

Figure 3.1 Location of Jarkus transects along the Dutch coast

The coastal profiles are measured from the fore dune to approximately 1 km seaward every 250 m alongshore. In areas with groins the alongshore spacing of profile sections ranges between 110 m and 310 m, because profiles are surveyed at locations in between the groins. The alongshore position of cross-shore survey lines is marked by a permanent base line of beach poles (RSP system). The cross-shore distance between consecutive depth measurements ranges from 10 m near the shoreline to 20 m offshore. The sub-aerial part of the profile data (down to the low water line) was initially gathered by levelling, but since 1977 photogrammetric methods are used. The sub-aqueous part of the data (up to the low water line at least) is gathered by sounding.

Profiles are usually surveyed between early April and late September. This implies that the time interval between two successive profile soundings at a particular location may vary between 0.5 and 1.5 year. Furthermore, it implies that the profile sampling has a seasonal bias. Little is known about seasonal changes in surf zone bathymetry along the Holland coast. Generally, spring and summer (April-September) are less stormy seasons than autumn and winter (Kroon, 1994). Nevertheless, Kroon (1994) observed hardly any seasonal differences in the mean profile shape and the width and height of the sweep zone, determined over a 17-year period near km 40. Furthermore, profiles surveyed during a more than average stormy spring may have characteristics of profiles during a less than average stormy winter. Therefore, it is expected that the biased sampling does not cause a strong bias in the shapes of the profiles. Moreover, the analysis of the profiles aims at describing morphological developments that exceed the level of seasonal changes. So, even with some seasonal bias present, long-term trends should become visible anyhow.

In the year study, two parts have been analysed. The first one (so-called test area) stretches from Beach Pole RSP 40.00 to RSP 43.00, whereas the second one (so-called reference area) stretches from Beach Pole RSP 43.00 to RSP 46.00. The datasets cover the period from 1965 to 2007. Data in 2007 are used as observations to be compared to the predictions given by the statistical model.

3.1.2 Laser-altimetry data

Laser scanning is an airborne elevation mapping method that is characterised by a largely automated measuring procedure, where fully digital data collection is followed by a computer-based data evaluation. It is performed with a multi-sensor system with the following main components: laser rangefinder, GPS receiver, and the inertial measurement unit (IMU) recording devices. The density and distribution of “points” hit by the laser is determined by the laser system parameters of pulse frequency, scan frequency and scan angle, in combination with the flight parameters of flying height, aircraft speed, and the distance between the lines. The spatial resolution of the available data is 5 m x 5 m, and the elevation accuracy lies in the order of 0.15 m.

Laser-altimetry data for 1997, 1998, 1999, 2001, 2003, 2004, 2006 and 2007 have been analysed. A small part of the data of 2001, in the northern part of the study area, is missing.

3.1.3 dGPS data

Bed levels have been measured using a differential Global Positioning System (dGPS) with an accuracy of about 25 cm in the horizontal (z and y) and 4 cm in the vertical (z). Between May 2002 and June 2004, the measurements have been carried out around low tide every 4 weeks during spring tide conditions (typical range of 1.8 m), and data have been collected along approximately 20 cross-shore transects with a 50-m alongshore spacing, from Beach Poles RSP 40.00 to RSP 41.00. Additional measurements between transects have been carried out to capture details of small rips. Each transect stretches from just below the momentary water level to well above the dune foot at NAP + 3 m. The lowest bed levels, about NAP – 1.5 m, were reached during low-energy wave conditions.

Since March 2006, the measurements have been carried out using a motor-quad, enabling the coverage of a wider area, from Beach Poles RSP 40.00 to RSP 43.00. The data have been collected along approximately 30 cross-shore transects with a roughly 100-m alongshore spacing. No additional measurements between transects have been carried out to capture details. The transects stretch this time from up the momentary water level to the dune foot at NAP + 3 m. Sometimes, the lowest bed level along a transect does not reach the Mean Sea Water Level at NAP + 0 m. Moreover, the spatial covering of the upper part of the beach (around the dune foot position) in the period 2006-2007 seems not as precise as it was when surveying a smaller area in the period 2002-2004. Such inaccuracies in the monitoring might have induced errors in the interpolation process from samples to grids and in the analysis. It means that the gain in spatial coverage is more or less lost by decrease of quality in capturing details of small rips.

Bed level maps of each survey, which have been created by Kriging interpolation of the bed level measurements, were provided in a grid format by the InfoDesk service of Rijkwaterstaat, and were used to calculate the different Coastal State Indicators.

3.1.4 Argus data

The Shoreline Detection and Elevation models (Aarninkhof, 2003) have been used to define (X,Y,Z) bathymetric points over 1-2 days. First, the horizontal location of the shoreline has been identified based on a raw estimation of the position of the shoreline in terms of image coordinates of the oblique video image. Using the equations for rectification, these screen coordinates are translated into real-world coordinates. The estimation of the elevation of the time-averaged location of the shoreline includes the contribution of four processes which play a role in the inner surf zone. In this respect Janssen (1997) identifies the tidal level, wave set-up, surf beat and swash motions. The still water level is taken immediately outside the surf zone and accounts for the tidal elevation and the wind-induced set-up of the mean water level. The wave set-up of the mean water level in the surf zone, is computed from a wave decay model (e.g. Battjes and Janssen, 1978). The contribution of the oscillating processes surfbeat and swash is modelled by combining empirical expressions for the vertical excursion of surf beat and swash. Wave and tidal information, needed for the shoreline elevation model to compute the shoreline elevation at any moment, is stored in a hydrodynamic database. This database specifically holds the following information: measured water-level, astronomical water-level, root mean square wave height, wave peak period and wave direction.

Assuming that no significant changes occur during the 1-2 days covered each month, a “mean” intertidal bathymetry can therefore be obtained for the selected period. This procedure has been reiterated for each month since March 2003 to October 2007, covering a large period before the installation of the Ecobeach modules (November 2006), and 1 year after the installation of the technique. However, a gap between data occurred from February 2005 to August 2005, due to problem with the cameras caused by lightning struck.

The treatment has been performed to the images recorded at the Coast3D Argus site, covering a coastal stretch of about 3 kms. It means that the medium-term behaviour of Coastal State Indicators has been analysed only for the test area. The reference area can not be seen with sufficient resolution from the Coast3D mast.

3.2 Coastal State Indicators

The objective of the analysis of the data is to aggregate the bathymetric data relevant for the description of the morphological features that change in time and space. In addition, these data should be compressed into only a few variables. This constraint is actually imposed to get an overview over the huge amount of data available along the cross-shore direction. The most compact way to summarise the above mentioned type of information is therefore in terms of sediment budgets and volumes. Moreover, a main characteristic of a nearshore profile is considered to be its “cross-shore position”. This information deals with the accretive or retreating nature of a coast. For example, along an accretive part of a coast the nearshore profile shifts seaward. Therefore, a profile behaviour can be expressed in terms of change in cross-shore position of the profile. For that reason, the monitoring has been designed to give information about the indicators which can describe the state of the coast, based upon volume and position characteristics.

Beach

The MCL -or Momentary CoastLine- (Figure 3.2) represents the momentary horizontal position of the coastline, determined from the (so-called MCL) volume in a cross-shore profile between the dune foot (arbitrary positioned at NAP +3 m) at an elevation *H* above mean low water (mlw) and the depth contour at an equal depth *H* below mlw. The MCL volume and position are computed every year on the basis of annual surveys of bathymetry (named JARKUS for “JAaRlijkse KUStmetingen” or “Annual Coastal Surveys”) along cross-shore profiles with 250 m alongshore spacing. These two CSI give insight on the behaviour of the entire beach.

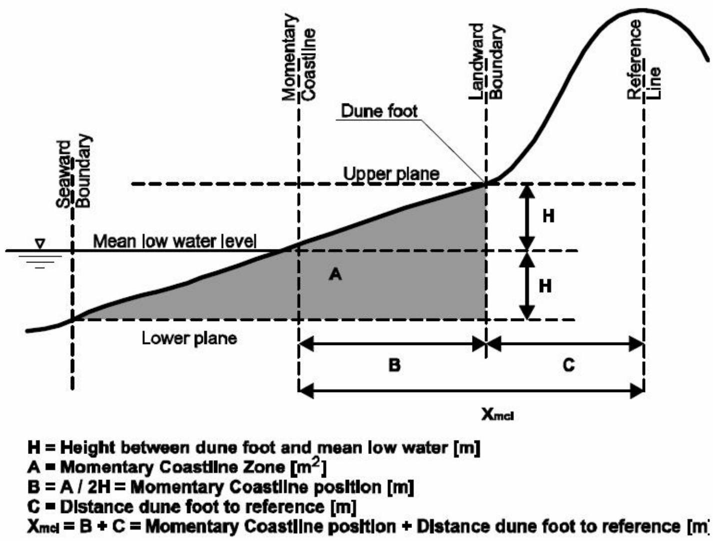

Figure 3.2 Definition sketch of the Momentary Coastline, MCL (Van Koningsveld and Mulder, 2004).

Upper part of the beach

A set of four Coastal State Indicators has been chosen to describe the upper part of the beach. The dune foot position and the shoreline position depend on the location of the NAP + 3 m- and NAP + 0 m- z-levels, respectively. The beach width is computed as the width between the dune foot position and the shoreline position, and is therefore correlated to these two CSI. Finally, the beach volume is defined as the amount of sand (per linear m) included between the NAP + 3 m- and NAP + 0 m- levels with the dune foot position and the shoreline position as landward and seaward boundaries, respectively.

Intertidal beach

The momentary intertidal beach (MiCL) volume is defined as the amount of sand (per linear m) included between the NAP + 1 m- and NAP -0.4 m- levels, with the corresponding x-positions as landward and seaward boundaries, respectively. The corresponding MiCL position is defined following the concept described above for the MCL position. These two CSI (MiCL volume and position) give insight on the behaviour of the intertidal beach.

Dunes

Volumes and volume changes in the dunes are computed from JARKUS-profile data and laser altimetry data which cover the whole area. The border between beach and foredunes is set at NAP + 3 m (dune foot position). Volume changes computed from profile data will be compared to volume changes from laser altimetry data. For two consecutive profiles (distance 250m) the average volume change of the profile data will be calculated. With laser altimetry data the volume change of the whole area between those two profiles will be computed.

Summary

The Figure 3.3 shows a sketch of the Coastal State Indicators evaluated in this study.

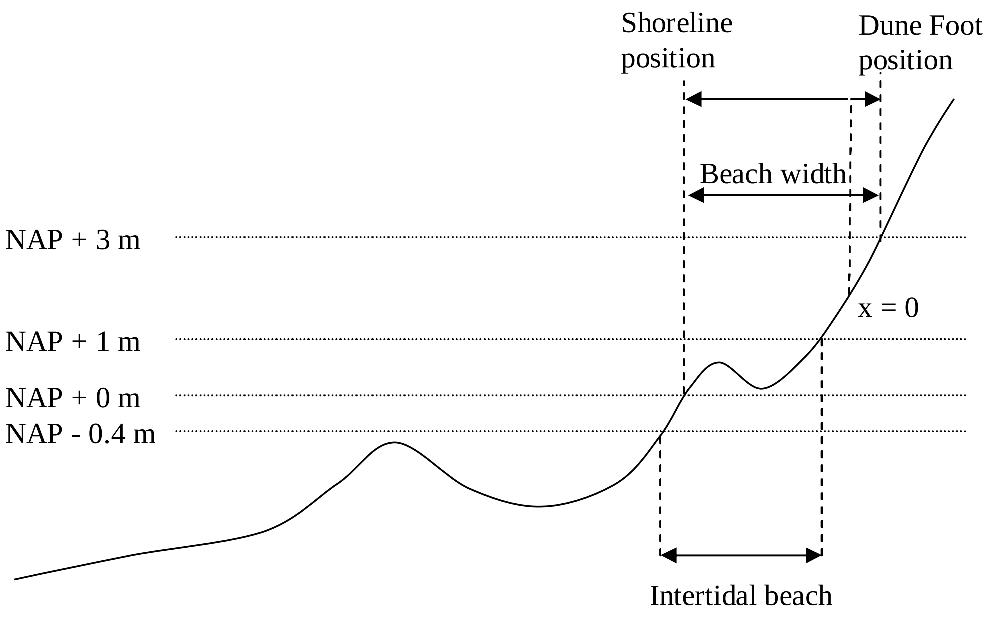

Figure 3.3 Sketch of Coastal State Indicators used in this study

The Table 3.1 summarizes the set of Coastal State Indicators evaluated in this study together with the data that can be used for their quantifications. It is seen from this table that several different measuring techniques can potentially be used for the evaluation of one type of CSI (e.g. MiCL position and MiCL volume). The available measuring techniques have different possible measuring frequencies. The choice for a certain measuring technique can therefore depend on the frequency needed for the analysis of the indicator. Moreover, the second CSI dataset can be also used to validate the model (set up using the first CSI dataset).

Table 3.1 Coastal State Indicators respect to the measurement techniques from which they can be derived.

Part	CSI	Jarkus	dGPS	Argus	AHN
Beach	MCL volume (NAP -20 to 3 m)	X			
	MCL position	X			
Upper part of the beach	Dune Foot position	X	X		
	Shoreline position	X	X	X	
	Beach width	X	X		
	Beach volume	X	X		
Intertidal beach	MiCL volume (NAP -0.4 to 1 m)	X	X	X	
	MiCL position	X	X	X	
Dunes	Volume	X			X

4 Statistical Model

4.1 Outline

For the modelling and forecasting of a time series of a Coastal State Indicator, linear or non-linear parameterised regression models have been set-up. Uncertainties in the model and observations are represented by a random noise. As a consequence *stochastic* rather than deterministic models are used for the description of the temporal evolution of a CSI.

Observed CSI data observed before the installation of the Ecobeach technique are used for the estimation of the model parameters. This identification of the parameters actually represents the model's calibration. The embedding of the regression models in a stochastic environment has the important advantage that apart from estimates for the parameters also (and in a statistically sound way) uncertainties can be derived for these model parameters.

Similarly the uncertainty can be derived in the model's predictions of future Costal State Indicators. These forecasts of a CSI and associated *prediction intervals* can be compared with future measurements to assess whether or not the installation of Pressure Equilibrium Modules has induced a statistically significant effect.

4.1.1 Mathematical formulation

For the half-year study, statistical models have been set-up based upon JARKUS yearly samples. The mathematical formulation of the models reads:

$$Z_t = \Phi\left(t \mid \vec{\Theta} \right) + V_t \tag{4.1}$$

The Z_t in this equation represents the model's prediction of a CSI at a time *t*. The model's prediction is built up of two components, $\Phi\left(\cdot \mid \vec{\Theta} \right)$ and V_t. The $\Phi\left(\cdot \mid \vec{\Theta} \right)$ is a parameterised function of time. It represents the deterministic, long term "systematic" variations in the temporal evolution of a CSI. The V_t in Equation 4.1 is a zero mean random noise. It represents the uncertainties in the modelling of the CSI and/or the uncertainties in the observations. In the present case it is assumed that V_t is a *Gaussian white* noise.

The time series of several aggregated Jarkus based CSI over the period 1965 to 2006 suggested a temporal evolution that often contains a long term. Moreover, in many cases, these CSI time series also suggested the presence of a cyclic component, potentially representing the cyclic coastal bar behaviour. Such a component was modelled by a harmonic time series. More generally, more than one harmonic component may be present, or necessary to represent or approximate a period function, so the mathematical formulation of the statistical models can be generalised to:

$$\Phi\left(t \mid \vec{\Theta} \right) = \alpha_0 + \alpha_1 \cdot t + \alpha_2 \cdot t^2 + \cdots\cdots + \alpha_N \cdot t^N \quad + \sum_{\ell=1}^{L} \left(A_\ell \cdot \cos\left(\tfrac{2\cdot\pi}{P_\ell} \cdot t \right) + B_\ell \cdot \sin\left(\tfrac{2\cdot\pi}{P_\ell} \cdot t \right) \right) \tag{4.2}$$

In that case the vector of model parameters $\vec{\Theta}$ consists of:

$$\vec{\Theta} := \left(\alpha_0 , \alpha_1 , \alpha_2 , \cdots\cdot, \alpha_N \ ; P_1, A_1, B_1, P_2, A_2, B_2, \cdots\cdot , P_L, A_L, B_L \right) \tag{4.3}$$

Parameter P_ℓ denotes the period of the $\ell - th$ harmonic component, while A_ℓ and B_ℓ denote the amplitudes of the cosine and sine functions.

4.1.2 Confidence and prediction intervals

Confidence intervals have been considered to describe the accuracy of (or uncertainty in) the response, $\Phi\left(t \mid \hat{\Theta}\right)$, of the deterministic model component $\Phi\left(\cdot \mid \hat{\Theta}\right)$. *Prediction intervals* (of some confidence level γ, e.g. $\gamma = 95\%$) are a means to quantify the accuracy with which such an observation Z_t can be predicted. In the construction of prediction intervals the uncertainty in both the calibrated model $\Phi\left(t \mid \hat{\Theta}\right)$ (represented by e.g. a confidence interval) and spread of the observation noise V_t (here assumed to be a zero mean white Gaussian random process) have been accounted. For the interpretation of a 95% prediction interval, it must be realised that in a model hindcast or forecast (on the average) 95% of the available observations $\hat{Z}_{t_k}$ are expected to be within the prediction interval.

For more details on general formulations and derivations of the statistical model set-up for the half-year study, the reader is advised to read Appendix B.

4.2 Updated model

The statistical model have been improved in order to represent a cyclic behaviour using a harmonic component with a fixed period. The mathematical formulation of the statistical models remains in the form of Equation 4.2. However, the vector of model parameters $\vec{\Theta}$ consists now of:

$$\vec{\Theta} := \left(\alpha_0 , \alpha_1 , \alpha_2 , \cdots\cdot, \alpha_N \ ; A_1, B_1, A_2, B_2, \cdots\cdot , A_L, B_L \ ; \sigma_V \right) \tag{4.4}$$

Parameters A_ℓ and B_ℓ denote the amplitudes of the cosine and sine functions of the $\ell - th$ harmonic component.

For every harmonic/cyclic component, two unknown model parameters are now involved. The number L of harmonic components that is included in the model must be limited to avoid overfitting. In most of the present applications this L was restricted to $L=1$.

This improvement has been considered in particular to describe the medium-term behaviour of Coastal State Indicators, which in many case display seasonal variations. The cycle of reappearance of these variations occur every year. For that reason, the period P_ℓ of the $\ell-th$ cyclic component is now fixed to 1 year and does not take part of the calibration procedure.

The parameters A_ℓ and B_ℓ, denoting the amplitudes of the cosine and sine functions of the $\ell-th$ harmonic component, remain however unfixed and control the time when a maximum is found. It means that a maximum (or a minimum 6 months later) can be shifted in time from 1 Coastal State Indicator to the other one.

5 Long-term behaviour

In the following sections, Coastal State Indicators are analysed in their aggregated form. The long-term evolutive trends of Coastal State Indicators related to the Momentary Coastline area, the upper part of the beach, the intertidal beach and to the dunes, are successively investigated. To that end, different regression models are proposed for each CSI, and confidence and prediction intervals are evaluated. As the models are set-up based upon Jarkus data, predictions are compared to the observations obtained in 2007. Respective analysis for the reference area and the test area are performed in order to provide spatial and temporal evaluation of the potential effect induced by the Ecobeach Technique.

5.1 Momentary coastline area

5.1.1 Reference Area

Long-term trends of the evolution of the MCL volume and MCL position have been analysed using the complete Jarkus dataset (from 1965 to 2006) setting up a linear regression model (Figure 5.1). Fourier analysis of residuals shows the presence of a cyclic pattern with period of about 16.4 years, which has been included, representing the cyclic behaviour of a migrative sand bar.

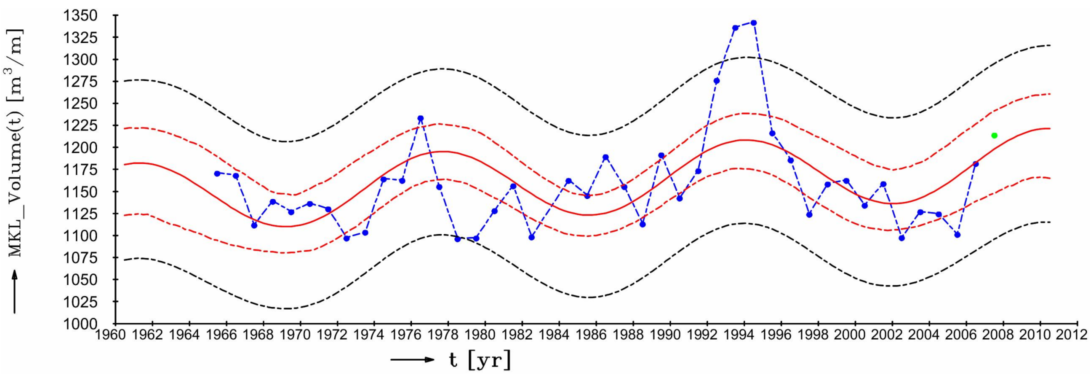

Figure 5.1 Linear regression model (red line), including 1 harmonic component, of the MCL volume based on the Jarkus dataset (blue points), and confidence (red dashed line) and prediction (black dashed line) intervals. The observed Jarkus data of 2007 is included in green.

Moreover, the time-stack image (Figure 5.2) displays a large amount of sand along the cross-shore direction in the range of [100 m; 200 m] during the period 1992-1994. This amount is included in the computation of the MCL volume, resulting in the large values every 14 years. It appears that the offshore migration of the sand bar has a critical influence on the MCL volume, only for the period 1992-1994.

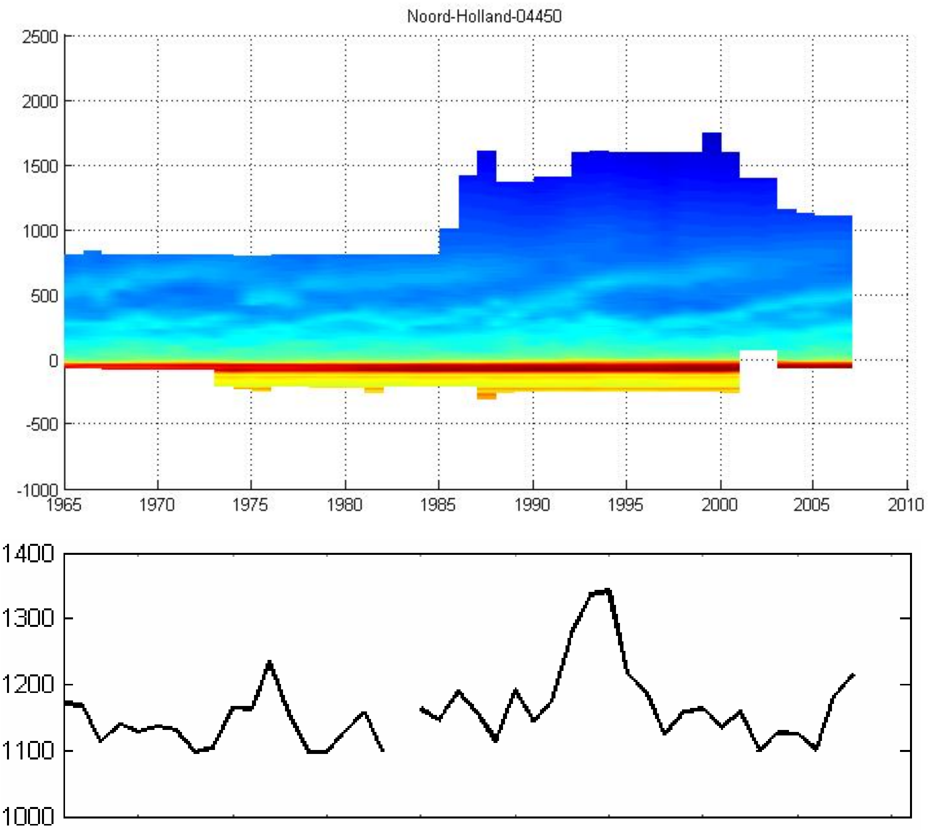

Figure 5.2 Long-term evolution of the bathymetry respect to the cross-shore direction for Transect RSP 44.50, and MCL volume(m^3/m) derived from the Jarkus dataset for the same transect

In order to reduce the prediction interval, a reduced dataset (with values from 1992, 1993, and 1994 which have been removed) has been used. A harmonic function with a period of 14 years has been included to the linear regression model. Results are displayed in Table 3.1 and in Figure 5.3. The model predicts a period of 16.52 years within a skew confidence interval of [13.65 yr, 19.40 yr]. For 2007, the prediction interval is defined with a spread (t=2007) = 34.80 m^3/m; and boundaries (t=2007) = [1088 m^3/m 1225 m^3/m]), whereas the observed 2007 MCL volume is of 1215 m^3/m.

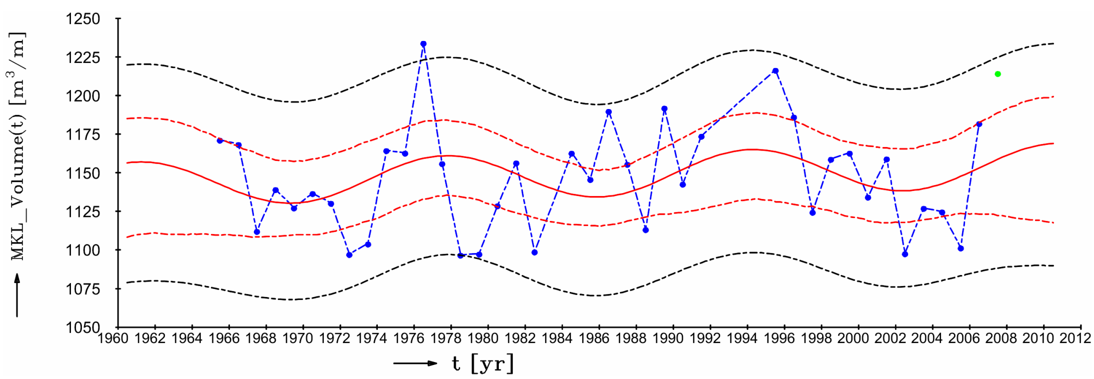

Figure 5.3 Linear regression model (red line), including 1 harmonic component, of the MCL volume based on the Jarkus dataset (blue points) and confidence (red dashed line) and prediction (black dashed line) intervals. The observed Jarkus data of 2007 is included in green.

Table 5.1 List of 95.00% confidence intervals for the parameters based on B-resampling of the model`s residuals, using a linear regression model with no harmonic component

Nr	Name of the uncertain model parameters	RSP Estimate	RSP Spread	Lower_Bound of SKEW Confidence Interval	Upper_Bound
1	alpha0 in Pol. Regres	1149.	5.506	1138.	1159.
2	alpha1 in Pol. Regres	4.965	8.646	-11.98	21.91
3	Period in Harm. Cmp[1]|	16.52	1.469	13.65	19.40
4	A[cos] in Harm. Cmp[1]	-1.187	14.51	-29.63	27.25
5	B[sin] in Harm. Cmp[1]	-14.28	8.208	-30.37	1.806
6	Sigma_V (Spread Noise)	32.45	3.723	25.16	39.75

This model can be used for prediction of the MCL volume (Table 5.2 and Figure C.1). Table 5.2 summarises the mean values and the confidence and prediction intervals for different times. However, this model has to be considered with care, as data have been removed in order to reduce the width of the 95% prediction interval.

The model predicts a MCL volume of 1157 m^3/m in 2007 whereas the observation reaches a higher value of 1215 m^3/m. However, the observation point remains within the prediction interval

Table 5.2 MCL volume: Z(()-statistics and uncertainties (95.00% confidence and prediction intervals) for a list of times tk, using a linear regression model with no harmonic component

Nr	time tk	Obs.	Mean [Z(tk)]	Spread Confid	Lower boundary	Upper	Spread Predic	Lower boundary	Upper
1	2005.5	1101.6	1148.	13.99	1124	1176	33.24	1083	1214
2	2006.5	1182.2	1153	15.61	1123	1183	33.95	1086	1219
3	2007.5	1214.7	1157	17.38	1122	1189	34.80	1088	1225
4	2008.5		1160	18.97	1121	1194	35.62	1089	1229
5	2009.5		1162	18.97	1119	1198	36.26	1090	1232
6	2010.5		1163	20.81	1118	1199	36.63	1090	1234
7	2015.5		1152	19.57	1116	1191	35.94	1082	1223
8	2025.5		1163	24.87	1117	1211	39.08	1087	1238

5.1.2 Test Area

For the test area, long-term trends of the evolution of the MCL volume and MCL position have been analysed (Brière et al., 2007) using the complete Jarkus dataset (from 1965 to 2006) setting up a linear regression model (Figure C.2). Table 5.3 summarises the mean values and the confidence and prediction intervals for different times. Figure C.2 display the Density Probability Functions of the predictions for years 2005, 2006 (hindcasting), and 2007 and 2008 (forecasting).

In 2007, the Jarkus-based MCL volume is of 1225.6 m^3/m, which is higher than the predicted value (1170.0 m^3/m), but still within the prediction interval [1106.0 m^3/m; 1234.0 m^3/m].

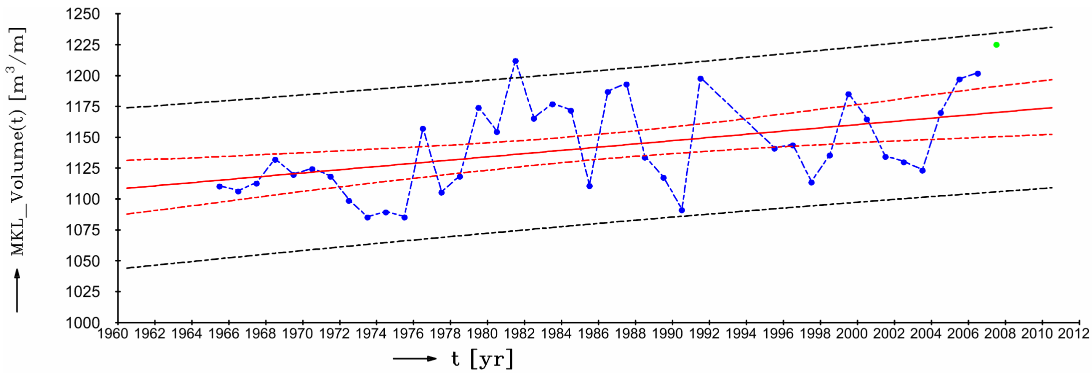

Figure 5.4 Linear regression model (red line) of the MCL volume based on the Jarkus dataset (blue points) and confidence (red dashed line) and prediction (black dashed line) intervals. The observed Jarkus data of 2007 is included in green.

Table 5.3 MCL volume: Z(()-statistics and uncertainties (95.00% confidence and prediction intervals) for a list of times tk, using a linear regression model with no harmonic component

Nr	time tk	Obs.	Mean [Z(tk)]	Spread Confid	Lower boundary	Upper	Spread Predic	Lower boundary	Upper
1	2005.5	1197.5	1167.	9.698	1149.	1188.	32.47	1104.	1231.
2	2006.5	1202.4	1169	10.04	1149.	1190.	32.57	1105.	1233.
3	2007.5	1225.6	1170.	10.39	1150.	1192.	32.68	1106.	1234.
4	2008.5		1171.	10.75	1150.	1194.	32.80	1107.	1236.
5	2009.5		1173.	11.11	1151.	1196.	32.92	1108.	1237.
6	2010.5		1174	11.47	1152.	1198.	33.04	1109.	1239.
7	2015.5		1180.	13.31	1154.	1208.	33.72	1114.	1247.
8	2025.5		1193	17.13	1160.	1228.	35.40	1124.	1263.

5.2 Intertidal beach

5.2.1 Reference Area

The long-term trend of the evolution of the MiCL volume in the reference area has been analysed setting up a linear regression model. Moreover, Fourier analysis of results shows the possible presence of a cyclic pattern with a period of about 14 years. For that reason, a harmonic function has been included in the linear regression model (Figure 5.5). The model calculates a period of 16.67 years within a skew confidence interval of [15.48 yr, 18.15 yr] and the stochastic part is reduced to 7.34 m^3/m.

The model can be used for prediction of the MiCL volume (Figure C.3, Table 5.4). The predicted MiCL volume equals 37.34 m^3/m whereas the confidence and prediction intervals are of [20.12 m3/m 54.42 m3/m]. In 2007 observations have been carried out. The observed MiCL volume has been deduced and equals to 53.9 m3/m, which almost reaches the upper boundary of the prediction interval.

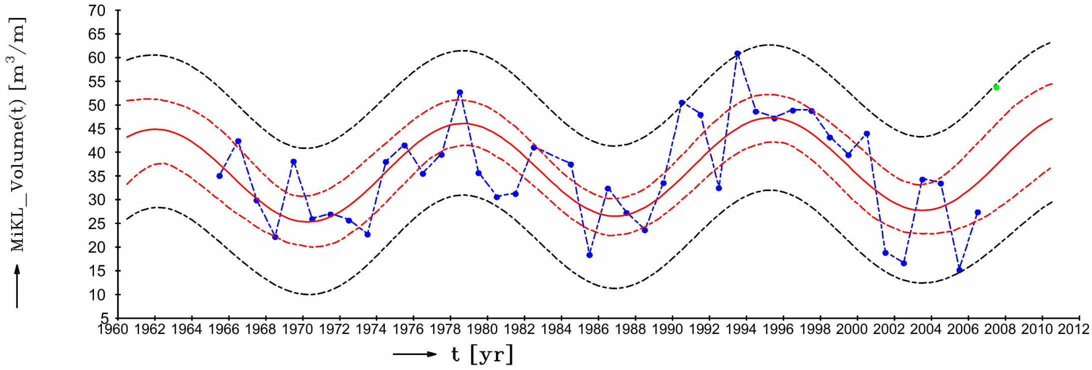

Figure 5.5 Linear regression model (red line), including 1 harmonic component, of the MiCL volume based on the Jarkus dataset (blue points), and confidence (red dashed line) and prediction (black dashed line) intervals. The observed Jarkus data of 2007 is included in green.

Table 5.4 MiCL volume: Z(()-statistics and uncertainties (95.00% confidence and prediction intervals) for a list of times tk, using a linear regression model with no harmonic component

Nr	time tk	Obs.	Mean [Z(tk)]	Spread Confid	Lower boundary	Upper	Spread Predic	Lower boundary	Upper
1	2005.5	15.3	30.65	3.570	24.00	37.90	8.192	14.61	46.80
2	2006.5	27.6	33.71	4.214	25.55	42.04	8.493	17.07	50.41
3	2007.5	53.9	37.34	4.701	27.94	46.02	8.745	20.12	54.42
4	2008.5		41.03	4.899	30.78	49.91	8.853	23.46	58.20
5	2009.5		44.27	4.775	33.91	52.55	8.784	26.75	61.26
6	2010.5		46.63	4.411	36.96	54.46	8.592	29.51	63.29
7	2015.5		40.32	5.027	30.52	49.47	8.924	22.72	57.71
8	2025.5		43.09	7.354	27.62	56.07	10.41	22.16	62.85

5.2.2 Test Area

As shown in Brière et al. (2007), long-term trend of the evolution of the MiCL volume has been analysed setting up a linear regression model including 1 harmonic function (Figure 5.6). The model has calculated a period of 15.77 years within a skew confidence interval of [14.83 yr, 16.88 yr] and the stochastic part has been reduced to 6.31 m^3/m. The model was used for prediction of the MiCL volume (Figure C.4, Table 5.5). In 2007, the prediction interval ranges in [18.64 m3/m 48.56 m3/m] (spread (t=2007) = 7.6 m^3/m). The observed MiCL volume has been deduced from 2007 Jarkus measurements and equals 42.2 m^3/m, whereas the predicted MiCL volume is of 33.66 m^3/m.

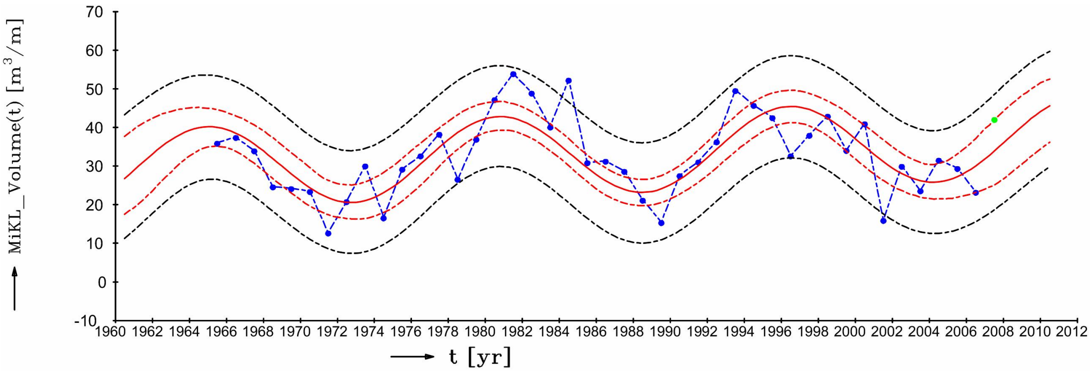

Figure 5.6 Linear regression model (red line), including 1 harmonic component, of the MiCL volume based on the Jarkus dataset (blue points), and confidence (red dashed line) and prediction (black dashed line) intervals. The observed Jarkus data of 2007 is included in green.

Table 5.5 MiCL volume: Z(()-statistics and uncertainties (95.00% confidence and prediction intervals) for a list of times tk, using a linear regression model with no harmonic component

Nr	time tk	Obs.	Mean [Z(tk)]	Spread Confid.	Lower boundary	Upper	Spread Predic.	Lower boundary	Upper
1	2005.5	29.5	27.20	2.829	21.72	33.17	6.964	13.49	40.93
2	2006.5	23.3	29.92	3.539	22.88	37.26	7.282	15.60	44.26
3	2007.5	42.2	33.66	4.163	25.05	41.99	7.605	18.64	48.56
4	2008.5		37.83	4.506	28.29	46.55	7.797	22.32	53.01
5	2009.5		41.82	4.481	32.16	50.30	7.783	26.24	56.89
6	2010.5		45.01	4.121	36.05	52.81	7.582	29.83	59.71
7	2015.5		40.33	4.198	31.62	48.36	7.624	25.24	55.19
8	2025.5		44.75	6.648	29.80	56.91	9.203	25.87	62.14

5.3 Upper part of the beach

5.3.1 Reference Area

In the reference area, long-term trend of the evolution of the beach volume area has been analysed setting up a linear regression model. Moreover, results showed the possible presence of a cyclic pattern with a period of about 14 years. For that reason, a harmonic function has been included to the linear regression model (Figure 5.7). The model calculates a period of 16.58 years within a skew confidence interval of [15.11 yr, 18.78 yr] and the stochastic part is reduced to 12.24 m^3/m. The model can be used for prediction of the beach volume (Figure C.5, Table 5.6). The predicted value is of 168.3 m^3/m whereas the prediction intervals is in the range of [139.5 m^3/m 196.8 m^3/m]. In 2007 observations have been carried out. The observed beach volume has been deduced and equals 173.1 m^3/m, which is in the range of the mean predicted value of the beach volume.

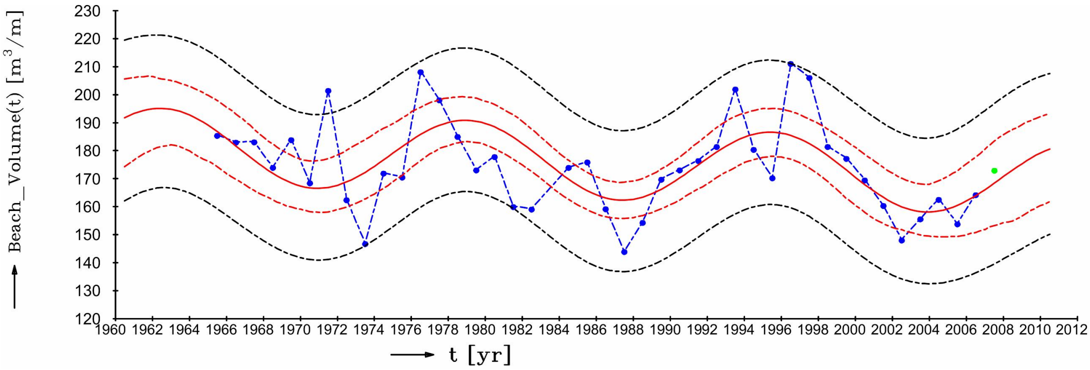

Figure 5.7 Linear regression model (red line), including 1 harmonic component, of the Beach volume based on the Jarkus dataset (blue points), and confidence (red dashed line) and prediction (black dashed line) intervals. The observed Jarkus data of 2007 is included in green.

Table 5.6 Beach volume: Z(()-statistics and uncertainties (95.00% confidence and prediction intervals) for a list of times tk, using a linear regression model with no harmonic component

Nr	time tk	Obs.	Mean [Z(tk)]	Spread Confid	Lower boundary	Upper	Spread Predic	Lower boundary	Upper
1	2005.5	154.0	160.8	5.821	149.4	172.7	13.64	134.0	187.7
2	2006.5	164.4	164.1	6.872	150.8	177.7	14.12	136.4	191.9
3	2007.5	173.1	168.3	7.747	153.2	183.3	14.57	139.5	196.8
4	2008.5		172.7	8.210	154.9	187.6	14.82	143.2	201.5
5	2009.5		176.6	8.178	158.7	190.8	14.80	146.9	205.2
6	2010.5		179.5	7.744	161.8	193.2	14.57	150.1	207.6
7	2015.5		170.7	8.027	154.9	186.5	14.72	141.7	199.6
8	2025.5		169.8	11.90	145.3	190.9	17.14	135.3	202.5

5.3.2 Test Area

As shown in Brière et al. (2007), the beach volume is highly correlated to the beach width, which is defined as the cross-shore stretch between the dune foot position and the shoreline position. The long-term trend of these four Coastal State Indicators have therefore been analysed setting-up a linear regression model including 1 harmonic component (cf. Figure 5.8 for the beach volume). The model can be used for prediction (Figure C.6 and Table 5.7). In 2007, the prediction interval is characterized by a prediction spread = 10.01 m^3/m and a prediction interval in the range of [154.2 m^3/m, 193.7 m^3/m], whereas the predicted beach volume equals to 174.1 m^3/m. Measurements of 2007 show that the beach volume is in the same range, with a observation reaching 168.5 m^3/m.

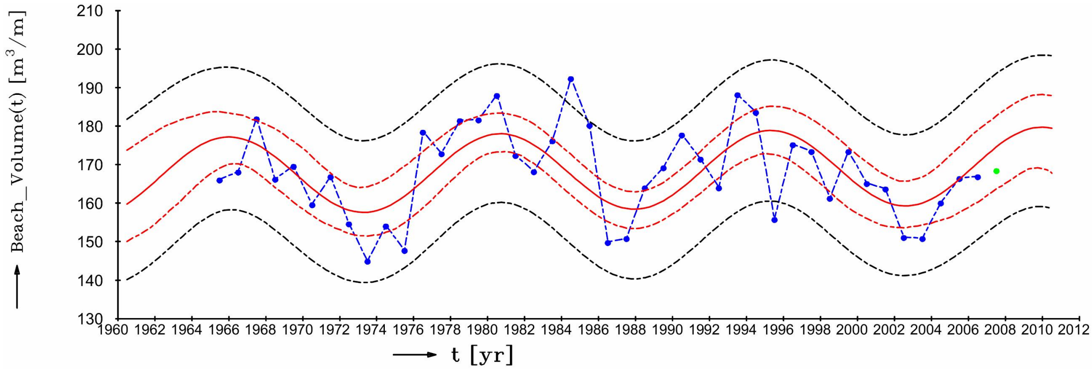

Figure 5.8 Linear regression model (red line), including 1 harmonic component, of the Beach volume based on the Jarkus dataset (blue points), and confidence (red dashed line) and prediction (black dashed line) intervals. The observed Jarkus data of 2007 is included in green.

Table 5.7 Beach volume: Z(()-statistics and uncertainties (95.00% confidence and prediction intervals) for a list of times tk, using a linear regression model with no harmonic component

Nr	time tk	Obs.	Mean [Z(tk)]	Spread Confid.	Lower boundary	Upper	Spread Predic.	Lower boundary	Upper
1	2005.5	166.5	166.1	4.301	157.5	174.8	9.764	147.0	185.4
2	2006.5	167.0	170.2	4.713	160.2	179.2	9.953	150.6	189.7
3	2007.5	168.5	174.1	4.839	163.4	183.0	10.01	154.2	193.7
4	2008.5		177.2	4.764	166.7	186.2	9.977	157.3	196.6
5	2009.5		178.7	4.725	168.8	188.1	9.958	159.0	198.2
6	2010.5		178.7	4.953	167.9	188.2	10.07	158.7	198.4
7	2015.5		163.5	5.385	153.3	175.0	10.29	143.5	184.0
8	2025.5		177.9	7.189	161.7	191.5	11.34	155.1	199.8

The long-term trend of the evolution of the shoreline position has been analysed (Brière et al., 2007) setting up a linear regression model including 1 harmonic component (Figure 5.9). The model is used for prediction of the shoreline position (Table 5.8). The prediction interval ranges in [85.04 m, 129.8 m] (Pred. spread (t=2007) = 11.35 m). are nevertheless quite large compared to the predicted shoreline position (107.6 m). The observed shoreline position has been deduced from measurements carried out in 2007, and equals 75.4 m, which is outside the interval prediction.

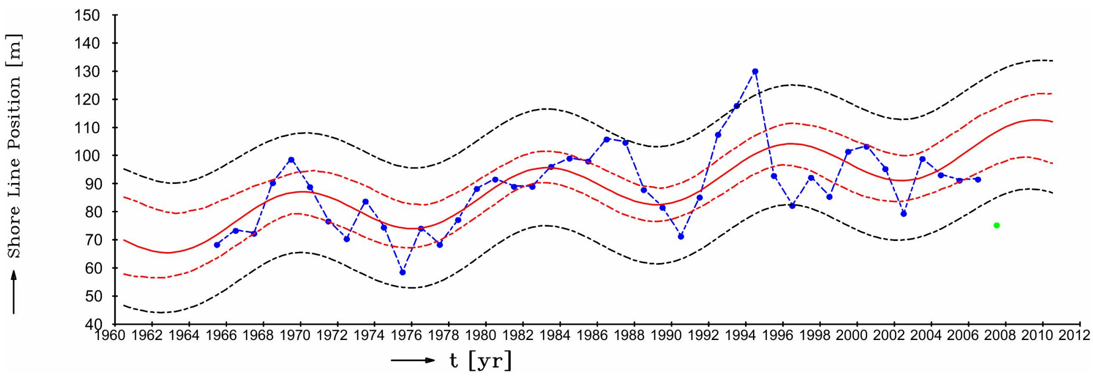

Figure 5.9 Shoreline position : linear regression model including 1 harmonic component (red line) with confidence (red dashed line) and prediction (black dashed line) intervals. Green point displays the observation in 2007.

Table 5.8 Shoreline position: Z(()-statistics and uncertainties (95.00% confidence and prediction intervals) for a list of times tk, using a linear regression model with 1 harmonic component

Nr	time tk	Obs.	Mean [Z(tk)]	Spread Confid.	Lower boundary	Upper	Spread Predic.	Lower boundary	Upper
1	2005.5	91.4	99.48	4.773	90.35	109.5	11.19	77.49	121.6
2	2006.5	91.8	103.8	5.050	93.50	113.8	11.31	81.44	126.0
3	2007.5	75.4	107.6	5.138	96.61	117.3	11.35	85.04	129.8
4	2008.5		110.2	5.258	98.78	120.1	11.40	87.46	132.4
5	2009.5		111.1	5.652	98.93	121.9	11.59	88.03	133.7
6	2010.5		110.5	6.296	96.79	122.4	11.92	86.72	133.7
7	2015.5		100.9	5.766	89.80	113.7	11.65	78.08	124.0
8	2025.5		114.6	9.281	96.21	133.0	13.73	87.66	141.5

Prediction of the shoreline position in 2007 is estimated larger than the observation obtained in the test area, expressing a retreat of the shoreline (Figure 5.9). As the beach volume remains constant between 2006 and 2007 (Figure 5.8), this might suggest a cross-shore exchange in sediment between the lower intertidal zone and the upper intertidal zone, with a steepening of the profile. Nevertheless, the behaviour of the shoreline position is highly dynamic, as the shoreline is located in the intertidal area. Its position is dependent on the period when the surveys have been carried out. This highlights the importance to describe the behaviour of Coastal State Indicators in a shorter-term.

5.4 Dunes

5.4.1 Dune dynamics

The Jarkus profile data have been used for volume calculations of cross sections through the foredunes. Each transect (for the reference and test areas) and years since 1965 to 2007 have been considered to compute the total volume above NAP + 3 m. The laser-altimetry data have been used with 3D Analyst in ArcView for areas in between the Jarkus profiles.

The landward boundary of the dunes is usually considered at the end of the “active” profile. Concerning the test area, the data sets of 1966 to 1972 and 2004, 2006 and 2007 were not covering the whole active area. In those cases the data were supplemented with other data. For 1966 to 1972, the data were derived from the profile of 1973. For 2004, the data were derived form the profile of 2003. For 2006 and 2007, the data were derived form the profile of 2005.

Jarkus-based and AHN-based results have been compared and showed good agreement (see Appendix D).

Long-term description

On the long term, there is a trend of accretion in the dunes. With the inclusion of the 2007 data, all profiles in both the study area (cf Appendix D–1) and the reference area (cf Appendix D–1), except 40.25 in the northern part of the study area, show increasing volumes. This does not necessarily correlate to long term dunefoot migration. Profile 40.25 is the only profile where dunefoot retreat coincides with a volume loss. Profiles 40.50, 40.75, 43.00, 43.25, 43.50, 43.75 and 44.00 all show dunefoot retreat and a gain in volume, which implies that the height of the foredune is changing, probably as a result of aeolian erosion of the dune front after scarping. A large gain in volume occurs between profiles 42.00 and 42.75 and in profle 46.00. In the study area, this coincides with the largest progression of the dunefoot, in the reference area it does not.

Short-term-description

When looking at short term changes, over the period 1997-2006 and 2007 a different picture emerges. The northern profiles now show strong accretion for this period. The spatial variation in the short term is much larger, and also the absolute volume changes are larger. It is clear that, although general trends are clearly visible in the data, the yearly variation is huge. Yearly changes may vary between -100 and +120 m^3/m.year. The large negative numbers are possibly due to years with strong dune erosion. It is very likely that the large positive numbers are somehow related to measurement errors, especially when a year with a very large gain is preceded or succeeded by a large loss. Certainly this is true for profile 45.00 where a huge gain in 1978 is succeeded by a huge loss in 1979. It is very unlikely that volume changes larger than 50-70 m^3/m.year are due to natural aeolian processes, but also these quantities are very large although not impossible. Parts of the process of beach-foredune interaction are still not well understood, and it might be possible that our general concept of aeolian transport underestimates the extremes that may occur. After years with severe dune erosion, often a huge gain of sand at and above the dunefoot is observed (for example in profile 41, 2004-2005; profile 42.50, 1999-2000). This must be related to aeolian transport over the beach, leading to very strong deposition in front of the cliff.

Dune volume variations between 2006 and 2007

The volume changes between 2006 and 2007 have been studied using Jarkus and laser-altimetry data for both the reference and test areas (Figure 5.10). For most of the transects, the volume changes are in the range of [-10 m^3/m; 10 m^3/m]. However, a decrease of the dune volume is noticed between 2006 and 2007 at RSP 41.00. Also, the southern part of the reference area appears quite dynamic during this period, suggesting that the reference area should be extended southward for better description of the dune dynamics in this area.

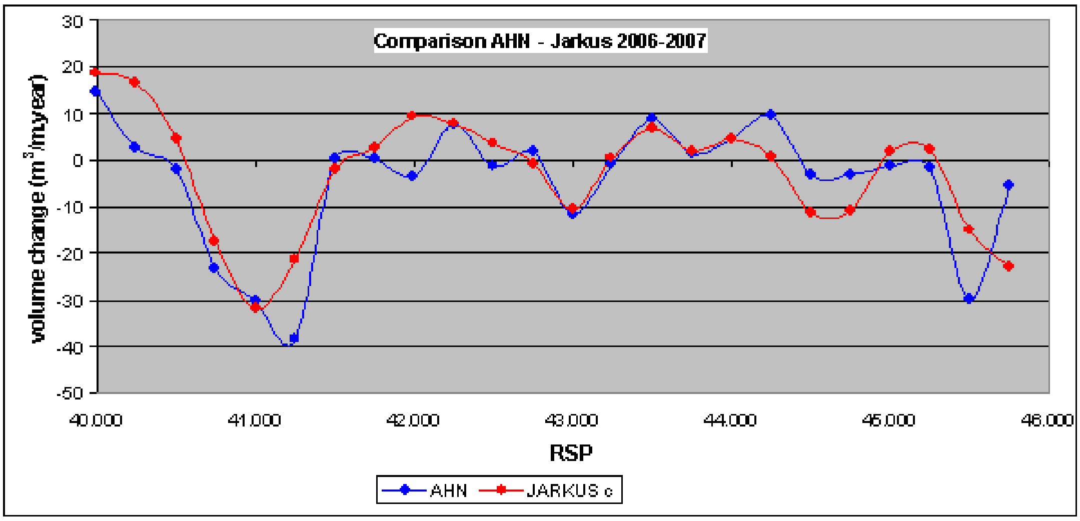

Figure 5.10 Dune volume changes (m3/m) between 2006 and 2007.

For more details on the analysis of the dune dynamics over the period 1965-2007 in the test and reference areas, see Appendix D.

5.4.2 Statistical model

Reference Area

A linear regression model has been set-up to describe the long-term trend of the evolution of the aggregated dune volume obtained from the Jarkus dataset. The model includes a harmonic component, with a period of 15.61 years within a skew confidence interval of [14.39 yr, 17.01 yr]. This cyclic pattern corresponds approximately to the cyclic coastal sand bar reappearance. As shown in Brière et al. (2007) for the test area, the beach is acting as a transferring zone between the dunes and the deeper waters. The results obtained with the linear regression model including 1 harmonic component are displayed in Figure 5.11. Table 5.9 summarises statistics and uncertainties on the confidence and prediction intervals for different times, and Figure C.7 displays the probability functions of confidence and prediction intervals for 2005, 2006, 2007 and 2008. Prediction in 2007 is estimated lower than the observation (1286.8 m^3/m), which remains anyway in the same order of the observation in 2006 (1291.8 m^3/m).

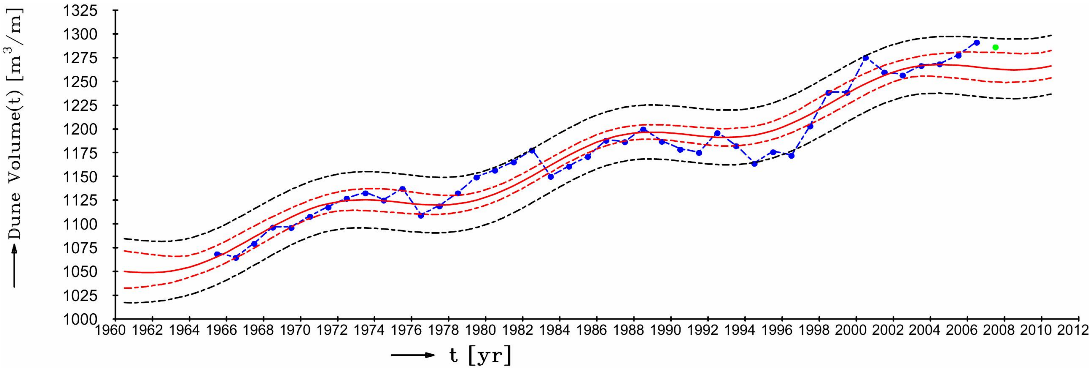

Figure 5.11 Dune volume : linear regression model including 1 harmonic component (red line) with confidence (red dashed line) and prediction (black dashed line) intervals. Green point displays the observation in 2007.

Table 5.9 Dunes volume: Z(()-statistics and uncertainties (95.00% confidence and prediction intervals) for a list of times tk, using a linear regression model with 1 harmonic component

Nr	time tk	Obs.	Mean [Z(tk)]	Spread Confid.	Lower boundary	Upper	Spread Predic.	Lower boundary	Upper
1	2005.5	1278.0	1267.0	7.053	1253	1281	15.54	1236	1297
2	2006.5	1291.8	1265.0	7.759	1251	1281	15.88	1234	1297
3	2007.5	1286.8	1264.0	8.033	1249	1280	16.01	1232	1295
4	2008.5		1263.0	7.876	1249	1279	15.93	1232	1295
5	2009.5		1264.0	7.515	1250	1280	15.76	1233	1295
6	2010.5		1267.0	7.345	1254	1283	15.68	1237	1298
7	2015.5		1312.0	9.190	1294	1329	16.62	1279	1345
8	2025.5		1338.0	10.93	1318	1362	17.64	1304	1373

Test Area

Similar linear regression model has been set-up to describe the long-term trend of the evolution of the dune volume in the test area (Brière et al., 2007). A harmonic component has been added, corresponding approximately to the cyclic coastal sand bar reappearance. The results obtained with the linear regression model including 1 harmonic component are displayed in Figure 5.12. Table 5.10 summarises statistics and uncertainties on the confidence and prediction intervals for different times, and Figure C.8 displays the probability functions of confidence and prediction intervals for 2005, 2006, 2007 and 2008. Observations in 2006 (1193.7 m^3/m) and 2007 (1193.4 m^3/m) are in the range of the model predictions. The behaviour in the test area appears consistent with the one described in the reference area.

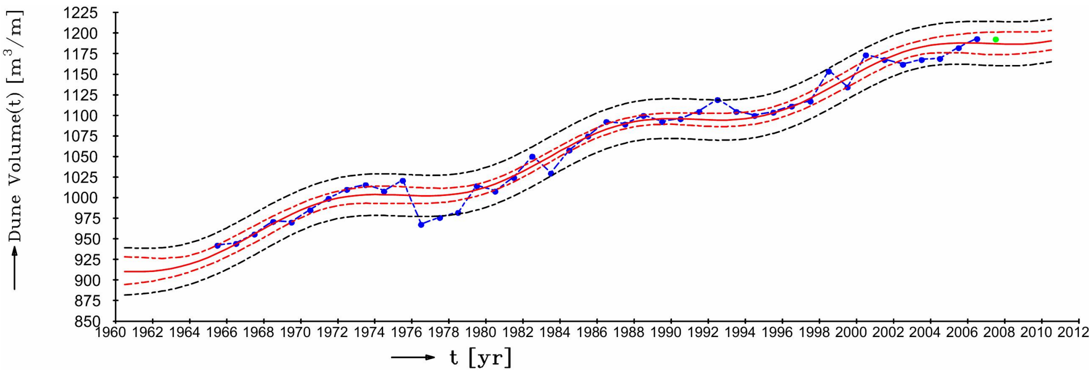

Figure 5.12 Dune volume : linear regression model including 1 harmonic component (red line) with confidence (red dashed line) and prediction (black dashed line) intervals. Green point displays the observation in 2007

Table 5.10 Dunes volume: Z(()-statistics and uncertainties (95.00% confidence and prediction intervals) for a list of times tk, using a linear regression model with 1 harmonic component

Nr	time tk	Obs.	Mean [Z(tk)]	Spread Confid.	Lower boundary	Upper	Spread Predic.	Lower boundary	Upper
1	2005.5	1182.9	1188	5.683	1176	1199	13.05	1162	1214
2	2006.5	1193.7	1188	6.476	1174	1201	13.41	1161	1214
3	2007.5	1193.4	1187	6.908	1173	1201	13.63	1160	1214
4	2008.5		1187	6.871	1174	1201	13.61	1160	1214
5	2009.5		1188	6.454	1176	1202	13.40	1162	1214
6	2010.5		1191	5.974	1179	1203	13.18	1165	1217
7	2015.5		1239	7.998	1222	1255	14.21	1211	1267
8	2025.5		1282	9.492	1264	1302	15.10	1253	1312

5.5 Summary

The results of the model (mean value and prediction interval) and the observations in 2007 are summarized in Table 5.11 and Table 5.12 for a list of Coastal State Indicators used to describe the behaviour of the Momentary Coastline Area, the intertidal beach, the upper part of the beach, and the dune system, for the reference and test area, respectively.

Based on the analysis of long-term evolution of these Coastal State Indicators, the following conclusions can be drawn:

- on the MCL and MiCL volume and position

- an increase of the MCL and MiCL volumes have been observed between 2006 and 2007 in the test area.
- this increase of the volumes has been predicted (see Brière et al., 2007) using a harmonic component, representing the cyclic coastal sand bar migration, to model the long-term trend of the Coastal State Indicators (e.g. Figure 5.6 for the MiCL volume).

- by comparing long-term trends for the MCL and MiCL volumes in the reference and the test area, no significant trend break can be seen in the test area with respect to the reference area. In both cases, the mean predictions of 2007 underestimate the observed data.
- similar conclusions can be drawn for the MCL position (i.e. observations in the range of the upper boundary of the prediction interval, for both the reference and the test areas), whereas the observed MiCL positions in 2007 are in the range of the predicted ones for both the reference and the test areas.

- on the upper part of the beach

- in the upper part of the beach, no significant trend break can be seen for the beach volume and for the dune foot position, by comparing results obtained in the reference and test areas. For these two Coastal State Indicators, observations of 2007 are in the range of the mean predicted values.
- however, for the shoreline position, the mean prediction of 2007 overestimates the observation obtained in test area, which displays a retreat of the shoreline (Figure 5.9). As the beach volume remains constant between 2006 and 2007 (Figure 5.8), this might suggest a cross-shore exchange in sediment between the lower intertidal zone and the upper intertidal zone. Nevertheless, the behaviour of the shoreline position is highly dynamic, as shoreline is located in the intertidal area, and therefore subject to dependence on the period when the surveys have been carried out. This highlights the importance to describe the behaviour of Coastal State Indicators in a shorter-term.

- on the dune dynamics

- the changes of dune volumes between 2006 and 2007 are in the range of [-10 m^3/m; 10 m^3/m]. No trend break suggesting an increase of the dune volume in the test area can be noticed between 2006 and 2007. Moreover, a decrease of the dune volume is obtained at Beach Pole RSP 41.00. Also, the southern part of the reference area appears quite dynamic during this period, suggesting that the reference area should be extended southward for a better description of the dune dynamics in this area.

Table 5.11 Prediction intervals and observations of a list of Coastal State Indicators for year 2007 in the reference area

Reference Area	**Momentary Coast line**		**Intertidal beach**		**Upper part of the beach**				**Dunes**
CSI	MCL Vol. (m^3/m)	MCL Pos. (m)	MiCL Vol. (m^3/m)	MiCL Pos. (m)	Beach Vol. (m^3/m)	Shore Line Pos. (m)	Dune Foot Pos. (m)	Beach Width (m)	Dunes Vol. (m^3/m)
Pred. 2007	1157.0	155.5	37.34	69.18	168.3	128.9	3.15	127.4	1264.0
Lower boundary	1088.0	147.4	20.12	56.64	139.5	109.0	-3.77	105.4	1232.0
Upper boundary	1225.0	163.6	54.42	81.96	196.8	148.8	10.04	149.3	1295.0
Obs. 2007	1214.7	163.1	53.9	74.4	173.1	131.0	2.4	128.6	1286.8

Table 5.12 Prediction intervals and observations of a list of Coastal State Indicators for year 2007 in the test area

Test Area	**Momentary Coast line**		**Intertidal beach**		**Upper part of the beach**				**Dunes**
CSI	MCL Vol. (m^3/m)	MCL Pos. (m)	MiCL Vol. (m^3/m)	MiCL Pos. (m)	Beach Vol. (m^3/m)	Shore Line Pos. (m)	Dune Foot Pos. (m)	Beach Width (m)	Dunes Vol. (m^3/m)
Pred. 2007	1170.0	122.7	33.66	39.3	174.1	107.6	-30.5	138	1187.0
Lower boundary	1106.0	113.3	18.64	30.7	154.2	85.0	-36.2	115.2	1160.0
Upper boundary	1234.0	132.3	48.56	47.8	193.7	129.8	-24.8	160.5	1214.0
Obs. 2007	1225.6	129.9	42.2	38.7	168.5	75.4	-31.9	107.3	1193.4

6 Medium-term behaviour

Sandy beaches function as a natural sediment buffer for coastal systems. Periods of accretion and erosion of this sediment buffer alternate over time and are generally coupled to low- and high-energy wave conditions. Low wave conditions supply sediment for the beach to accrete, while high-energy wave conditions erode sand from the beach by offshore direct currents as undertow. Storms are possible throughout the year, but the frequency and the intensity of storm occurrence is higher during winter months than during summer months.

Seasonal variations
In general, the increase in storm frequency and intensity starts around October and lasts until approximately March. During the summer (April to September), storms are less frequent and less intense. The cumulative effect of these storm events and of the low-energy events leads to seasonal patterns in beach behaviour. In this chapter, the objective is to evaluate the ability of the updated statistical models to detect a seasonal cyclic behaviour, with a period of 1 year, in the evolution of the Coastal State Indicators. Such description would lead to a better representation of the medium-term (over a few years) behaviour of these Indicators and increase the accuracy of the model predictions, enabling a more accurate evaluation of the Ecobeach technique.

Wave impact
Normally, the response of the beach to high-energy wave conditions is faster than to low-energy wave conditions (Wright and Short, 1984). The impact of a storm can be immediately seen on the beach. However, the beach needs more time to respond to low-energy wave conditions and to recover. Therefore, the quantification of the relation between the *beach changes* and the *wave characteristics* has been evaluated. If such relation becomes clear, wave parameters might be used to force the statistical models leading to a better representation of the medium-term behaviour of the Coastal State Indicators, and enabling a more accurate evaluation of the Ecobeach technique.

Datasets
At shorter-term, the bathymetry and topography at Egmond-aan-Zee have been monitored using dGPS system and Argus images. These datasets are characterized by approximately similar monitoring frequencies, but by different precision in the measurement techniques, and different spatial coverages. These differences lead to an incompatibility of the datasets (cf paragraph 6.2.1). It requires to perform analysis of the medium-term behaviour of Coastal State Indicators using dGPS and Argus-based datasets separately. It means also that answering the research questions is a long process, and that final conclusions should not be drawn based only on a few observations obtained after the installation of the Ecobeach system.

6.1 Wave influence

The seasonal pattern in beach changes may be due to the differences in intensity and in frequency of storms during summer and winter periods. The quantification of this relation is made by coupling beach characteristics, expressed as the change in the MiCL volume and the beach width, between two successive surveys, with waves over the same period.

Normally, the response of the beach to high-energy wave conditions is faster than to low-energy wave conditions (Wright and Short, 1984). The impact of a storm can be immediately seen on the beach. However, the beach needs more time to respond to low-energy wave conditions and to recover. The recovery time is strongly influenced by the length of the period between two successive storms. Continuously changing wave conditions and short time periods between successive storms events may not allow the beach to adjust to new conditions. Consequently, beaches may have a certain memory in their response and beach morphology may be best related to wave conditions over a few antecedent days, rather than the immediately preceding conditions. Wright et al. (1985) suggested that the beach changes may be related to wave conditions averaged over a few preceding days, but the amount of days was not clear. The offshore wave characteristics are thus expressed as an average of the hourly Hrms during a variable amount of preceding days Td = [2 days; 7 days; number of days between two successive surveys]. Correlations between the wave height and the beach characteristics have been successively investigated using the different amounts of days defined by Td.

Figure 6.1, Figure 6.2 and Figure 6.3 display the scatter plots of the monthly changes of the MiCL volumes calculated based on Argus images versus the averaged Hrms over the 2 days and 7 days before the Argus data acquisition and over the period between 2 successive data acquisitions, respectively. These 3 plots include as well the linear trend and confidence intervals. The decreasing slope of the linear trend means that the MiCL volumes increase for low-energy events (summer period), whereas the MiCL volumes decrease for high-energy events (winter period). When extending the period on which the significant wave height is averaged, the slope of the linear trend increases. However, the correlation factors R^2 ([0.08, -0.33, -0.15]) show that the "best fit" is obtained when considering the average of Hrms over 7 days. In this case, the correlation factor is still weak. Figure 6.2 displays a quite wide cloud and large confidence intervals, showing the difficulty to correlate the beach characteristic, expressed by the MiCL volume, to the wave parameter Hrms.

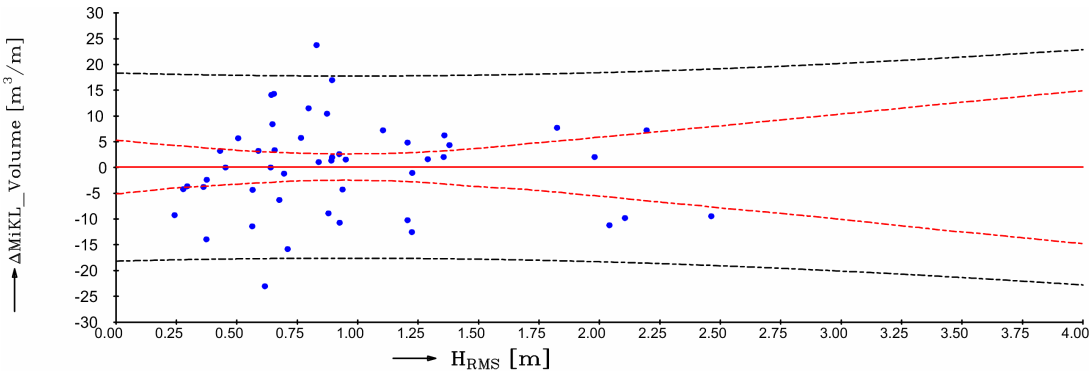

Figure 6.1 Scatter plot of the monthly changes of the MiCL volumes calculated based on Argus images versus the averaged Hrms over the 2 days before the Argus data acquisition.

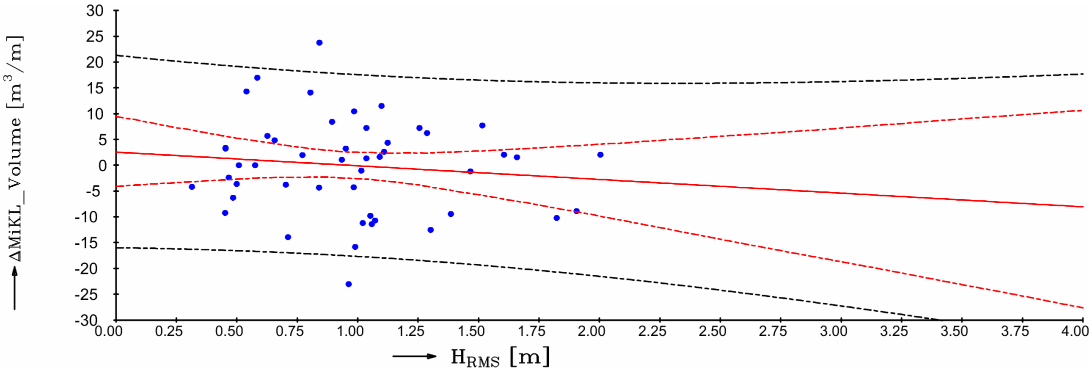

Figure 6.2 Scatter plot of the monthly changes of the MiCL volumes calculated based on Argus images versus the averaged Hrms over the 7 days before the Argus data acquisition.

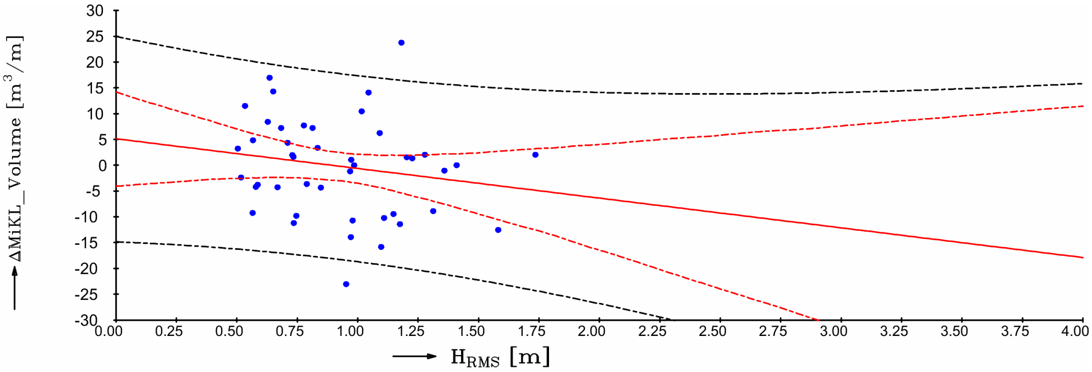

Figure 6.3 Scatter plot of the monthly changes of the MiCL volumes calculated based on Argus images versus the averaged Hrms over the period between 2 successive Argus data acquisitions.

Figure 6.4 and Figure 6.5 display the scatter plots of the monthly changes of the beach width calculated based on dGPS data versus the averaged Hrms over 7 days before the survey and over the period between 2 successive surveys, respectively. Still, the plots include as well linear trends and confidence intervals.

In this case, the beach widths increase for high-energy events (winter period), whereas the beach widths decrease for low-energy events (summer period). This behaviour is usually associated with a flattening of the beach profile during the winter period. But, if a wider beach implies the flattening of the beach, it does not coincide necessarily with a volume loss or gain.

The correlation factors R^2 ([0.25; 0.12]) show that the “best fit” is obtained when considering the average of Hrms over 7 days. In this case, the correlation factor remains weak. Figure 6.4 displays a wide cloud and large confidence intervals, preventing any clear correlation between the beach characteristic, expressed here as the beach volume, with the wave parameter Hrms.

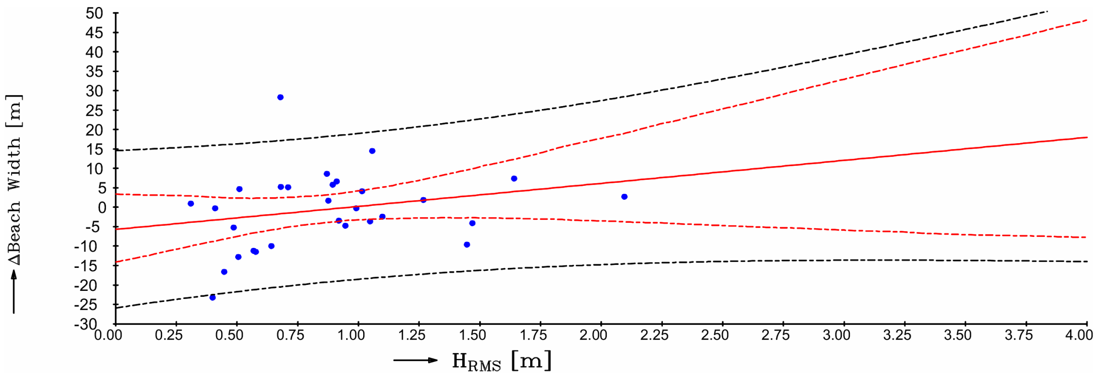

Figure 6.4 Scatter plot of the monthly changes of the beach volumes calculated based on dGPS data versus the averaged Hrms over the 7 days before the survey.

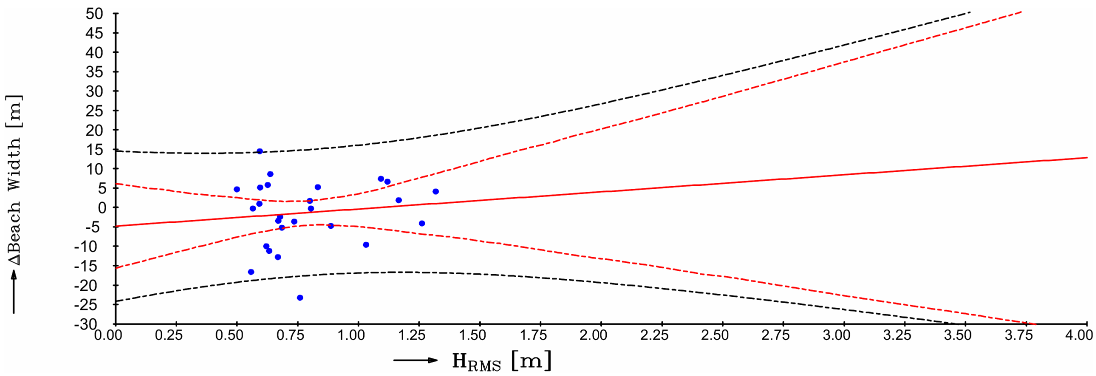

Figure 6.5 Scatter plot of the monthly changes of the beach volumes calculated based on dGPS data versus the averaged Hrms over the period between 2 successive surveys.

Overall, the influence of the seasonal variability in energy conditions and storm-events on beaches remains unclear. No clear relation between beach characteristics and wave parameters can be found. It appears of marginal importance to include any wave schematisation to force the statistical model in order to improve its representation of seasonal patterns. Nevertheless, as explained in paragraph 4.2 and further described in paragraph 6.2, the cyclic variations due to seasons can be included using a harmonic component for the representation of the medium-term behaviour of Coastal State Indicators.

6.2 Seasonal variations

6.2.1 Intertidal beach

Compatibility of datasets

Characterized by different precisions in the measurement techniques, and different spatial covering, the Argus-based and dGPS datasets are not compatible and can not be analysed by merging all data to a single dataset (Figure 6.6). It requires to perform the analysis of the medium-term behaviour of Coastal State Indicators using dGPS and Argus-based datasets separately.

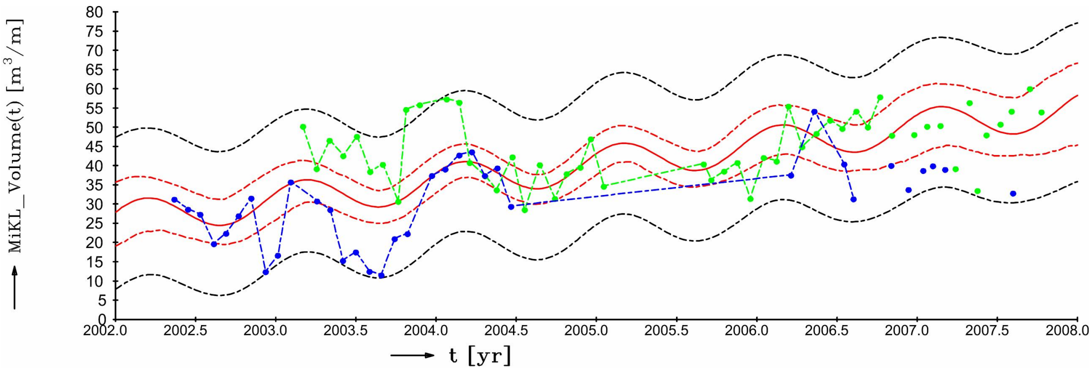

Figure 6.6 MiCL volume : linear regression model including 1 harmonic component (red line), with a fixed period of 1 year. The model is based on the merged dataset including Argus-based data and dGPS data obtained before the installation of the Ecobeach system. The confidence and prediction intervals are displayed with a red dashed line and a black dashed line, respectively. Green and blue points display the Argus-based and dGPS observations, respectively.

Argus-based data analysis

As shown in Figure 6.6, significant MiCL volumes have been obtained using Argus-based data for the winter 2003-2004. These large values might be due to dune erosion induced by storms occurring in the winter 2003-2004 and causing sediment exchange between the upper part of the beach and the intertidal zone, or by a sand wave migrating in front of the Argus station, and increasing therefore the sediment volume during this period. Including these data lead to the unrealistic representation of the medium-term behaviour of the MiCL volume, with a cyclic seasonal period of 1 year and 3 months, and preventing any future accurate assessment of potential effects of the Ecobeach system on the MCL volume. For that reason, the 4 critical points of November and December 2003 and January and February 2004 have been removed from the Argus dataset.

Using the reduced dataset, the medium-term trend of the evolution of the MiCL volume has been finally described setting up a linear regression model (representing the local slope of the long-term trend) and including 1 harmonic component with a fixed period of 1 year (Figure 6.7, Figure 6.8 and Table 6.1). The figures show in particular an increase of the MiCL volumes in the summer periods. Figure 6.7 displays also the long-term evolution predicted by the Jarkus-based model, showing that the linear trend given by the Argus-based model represents quite well the expected annual behaviour.

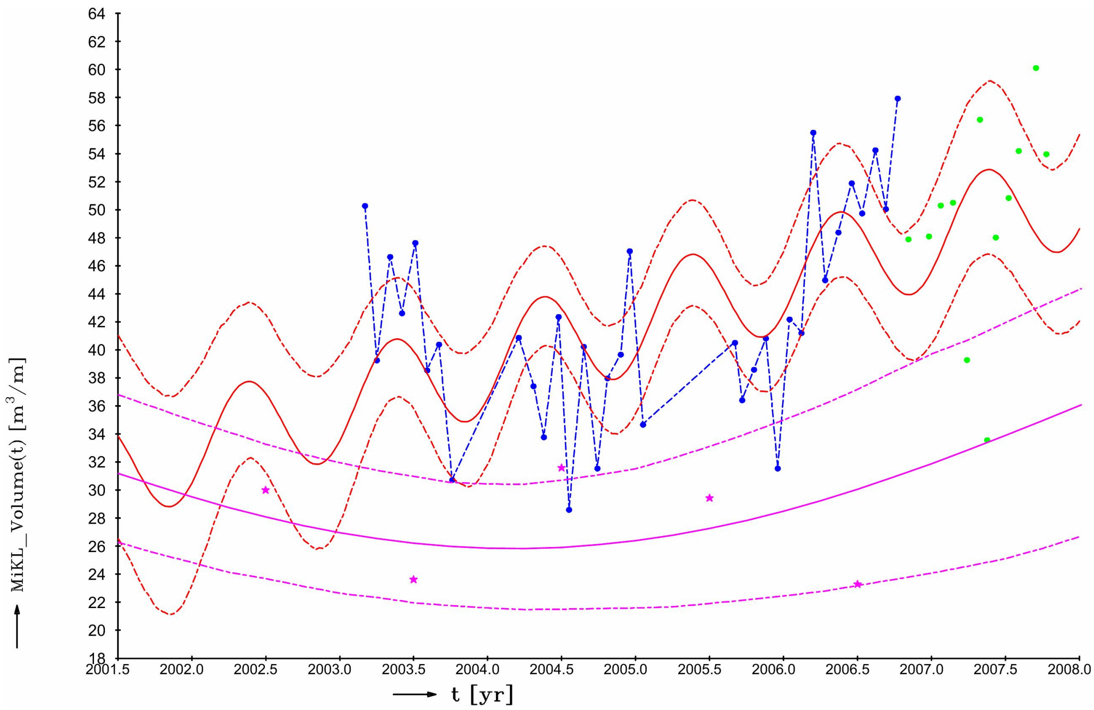

Figure 6.7 MiCL volume : linear regression model including 1 harmonic component (red line), with a fixed period of 1 year. The confidence interval is displayed with a red dashed line. Green points display the Argus-based observations after the installation of the Ecobeach technique. Purple lines describe the long term trend (solid line) and confidence interval (dashed line) based on Jarkus data.

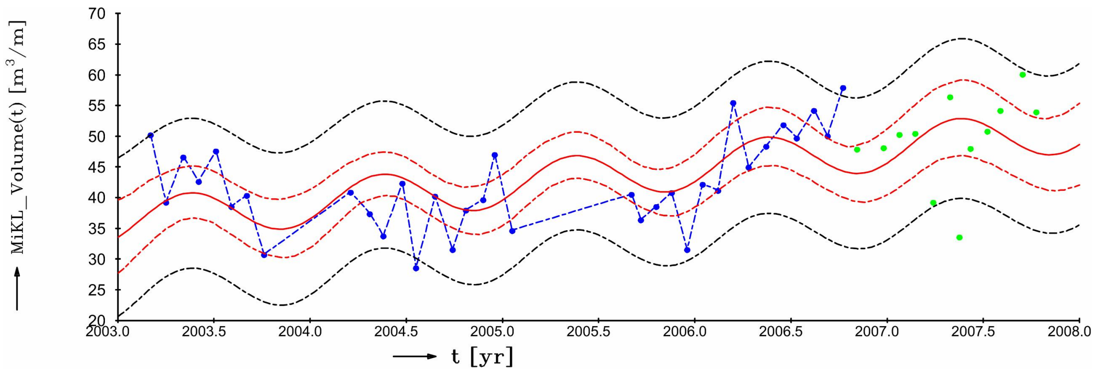

Figure 6.8 MiCL volume : linear regression model including 1 harmonic component (red line), with a fixed period of 1 year. The confidence and prediction intervals are displayed with a red dashed line and a black dashed line, respectively. Green points display the Argus-based observations after the installation of the Ecobeach technique.

Table 6.1 List of 95.00% confidence intervals for the parameters based on B-resampling of the model`s residuals, using a linear regression model with 1 harmonic component

Nr	Name of the uncertain model parameters	RSP Estimate	RSP Spread	Lower_Bound of SKEW Confidence Interval	Upper_Bound
1	alpha0 in Pol. Regres	-15.46	18.19	-51.11	20.20
2	alpha1 in Pol. Regres	62.00	19.53	23.73	100.3
3	Period in Harm. Cmp[1]	1.000	0.10E-04	1.000	1.000
4	A[cos] in Harm. Cmp[1]	2.436	1.623	-0.7444	5.617
5	B[sin] in Harm. Cmp[1]	-2.757	1.466	-5.630	0.1157
6	Sigma_V (Spread Noise)	6.160	0.7470	4.696	7.624

The statistical model is used for prediction of the MiCL volume after the installation of the Ecobeach technique (Figure C.9 and Table 6.2) and can be therefore used to evaluate potential effects of the Ecobeach modules by comparing predictions and observations obtained in 2007.

After the installation of the Ecobeach technique (November 2006), the model predictions and the observations are in the same order. The prediction interval of the evolution of the MiCL volume is in the range of [34.45 m^3/m, 59.77 m^3/m] the 24^{th} of January 2007, with a mean prediction of about 47.09 m^3/m, whereas the observed MiCL volume equals to 50.36 m^3/m. In July the 9^{th}, the observation and prediction remain in the same order. The prediction interval is in the range of [38.76 m^3/m, 64.65 m^3/m] the 24^{th} of January 2007, with a mean prediction of about 51.67 m^3/m, whereas the observed MiCL volume equals 50.88 m^3/m. In both cases, the observations are within the confidence interval, showing that no break can be noticed during the first part of the year. In the autumn 2007, observations diverge slightly from the mean predicted values, displaying an increase of the observed MiCL volume with respect to the predicted ones. However, no significant trend break can be associated to the installation of the Ecobeach modules as all observations in the autumn 2007 remain within the prediction interval.

In total, observations carried out after the installation of the Ecobeach technique show that 92% of the observed MiCL volumes are within the prediction interval. Although the arbitrary choice of the 95% confidence and prediction intervals for the parameters based on B-resampling of the model’s residuals is quite strict, a visual inspection of the data does not show any trend break in the medium-term behaviour of the MiCL volume. Moreover, the small amount of data available after the installation of the Ecobeach system (in a statistical point of view) prevents the statistical representation of the MiCL volume behaviour for the period post-installation of the modules. The desirable comparison of medium-term trends (pre- vs. post-installation) requires to gather more data over a longer period.

Table 6.2 MiCL volume: Z(()-statistics and uncertainties (95.00% confidence and prediction intervals) for a list of times tk, using a linear regression model with 1 harmonic component

Nr	time tk	Obs. value	Mean [Z(tk)]	Spread Confid.	Lower boundary	Upper	Spread Predic.	Lower boundary	Upper
1	17/01/06	42.23	43.59	2.258	39.27	48.26	6.222	31.34	55.86
2	14/07/06	49.78	48.41	2.363	43.93	53.11	6.260	36.09	60.75
3	05/11/06	47.95	43.97	2.297	39.36	48.54	6.236	31.68	56.25
4	25/12/06	48.16	45.29	2.615	40.15	50.71	6.360	32.76	57.82
5	24/01/07	50.36	47.09	2.779	41.69	52.80	6.429	34.45	59.77
6	23/02/07	50.55	49.20	2.911	43.56	55.11	6.487	36.45	62.00
7	29/03/07	39.33	51.35	3.043	45.57	57.51	6.547	38.48	64.25
8	30/04/07	56.49	52.59	3.144	46.62	58.64	6.595	39.64	65.59
9	18/05/07	33.63	52.84	3.178	46.83	59.17	6.611	39.86	65.87
10	18/06/07	48.08	52.69	3.184	46.67	59.00	6.614	39.71	65.73
11	09/07/07	50.88	51.67	3.113	45.70	57.91	6.580	38.76	64.65
12	04/08/07	54.25	50.43	3.009	44.68	56.43	6.532	37.61	63.31
13	15/09/07	60.16	48.25	2.860	42.78	53.98	6.464	35.54	60.99
14	11/10/07	54.02	47.32	2.864	41.78	53.07	6.466	34.60	60.06

dGPS-based data analysis

Using dGPS dataset, the medium-term trend of the evolution of the MiCL volume has been described setting up a linear regression model (representing the local slope of the long-term trend) and including 1 harmonic component with a fixed period of 1 year (Figure 6.9). Table 6.3 summarizes predictions for dates in the winter and summer periods of years 2006 to 2009. Results obtained using the dGPS dataset are more difficult to analyse due to a long gap between June 2004 and March 2006. Moreover, the measurement techniques (by walking or by motor-quad), the spatial covering, and the interval between successive surveys have changed in time, explaining some discrepancies in the general trends displayed in the periods 2002-2004 and 2006-2007.

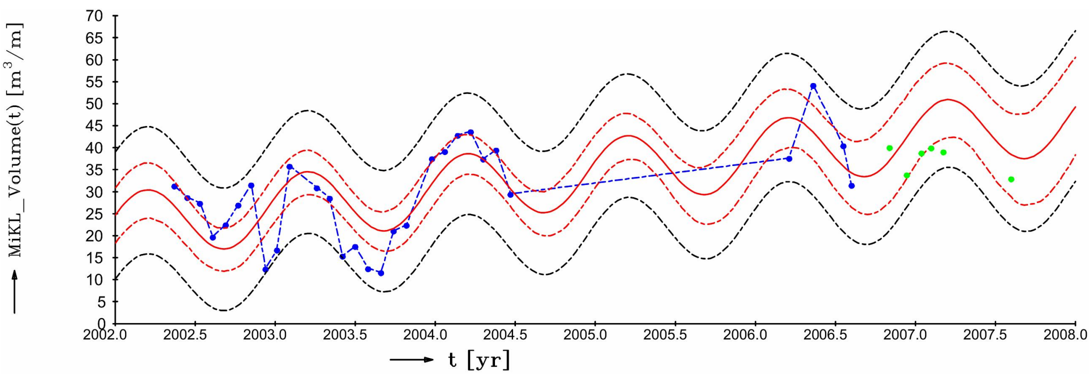

Figure 6.9 MiCL volume : linear regression model including 1 harmonic component (red line), with a fixed period of 1 year. The confidence and prediction intervals are displayed with a red dashed line and a black dashed line, respectively. Green points display the dGPS-based observations after the installation of the Ecobeach technique.

Accepting a higher level of inaccuracy in the predictions, the model can still be used to evaluate potential effects of the Ecobeach modules by comparing predictions and observations obtained in 2007. The general behaviour of the observations is well represented by the model, with however some overestimations of the MiCL volumes by the model. Table 6.3 summarises the model predictions and the observed values for some specific dates. No trend break can be noticed in the dataset. All observations carried out after the installation of the Ecobeach technique are within the prediction interval. Still, the small amount of available data (in a statistical point of view) prevents the statistical representation of the MiCL volume behaviour for the period post-installation of the modules.

Table 6.3 MiCL volume: Z(()-statistics and uncertainties (95.00% confidence and prediction intervals) for a list of times tk, using a linear regression model with 1 harmonic component

Nr	time tk	Obs. value	Mean [Z(tk)]	Spread Confid.	Lower boundary	Upper	Spread Predic.	Lower boundary	Upper
1	20/03/06	37.6	46.92	3.332	40.04	53.26	7.411	32.29	61.44
2	18/07/06	40.5	35.94	3.651	28.52	42.71	7.560	21.01	50.72
3	03/11/06	40.15	37.17	4.691	27.62	46.57	8.113	21.22	53.11
4	12/12/06	33.9	42.46	4.739	32.98	51.69	8.141	26.47	58.48
5	15/01/07	38.9	47.09	4.612	38.13	56.01	8.068	31.23	62.94
6	06/02/07	40.01	49.38	4.481	40.43	57.98	7.993	33.64	65.06
7	06/03/07	39.16	50.93	4.306	42.01	59.19	7.897	35.36	66.39
8	07/08/07	33.0	38.57	4.859	28.85	47.81	8.211	22.35	54.59

6.2.2 Upper part of the beach

Variations in beach characteristics, such as the cross-shore position of the shoreline or the dune foot, and the beach width and volume have been used based on the dGPS dataset to approximate accretion and erosion quantitatively.

Dune Foot Position

Using dGPS dataset, the medium-term trend of the evolution of the dune foot position has been described setting up a linear regression model (representing the local slope of the long-term trend) and including 1 harmonic component with a fixed period of 1 year (Figure 6.10). Table 6.4 summarizes the model predictions and the observed values for some specific dates. In the period 2002-2004, observations show a retreat of the dune foot position in the winter and an offshore migration in the summer, which is well reproduced by the model. In the period 2006-2007, the general behaviour of the observations is not well represented by the model, as the offshore migration of the dune foot position described by the observations is not reproduced by the model. For the dune foot position, a trend break can be clearly seen in the dataset, as all observations since November 2006 are in a range out of the prediction interval. However, it has to be noticed that the measurement techniques (by walking or by motor-quad), the spatial covering, and the interval between successive surveys have changed in time, and might explain the trend break obtained by comparing the periods 2002-2004 and 2006-2007. In particular, the spatial covering of the upper part of the beach (around the dune foot position) in the period 2006-2007 seems not as precise as it was when surveying a smaller area in the period 2002-2004. Such inaccuracies in the monitoring might have induced errors in the interpolation process from samples to grids and in the analysis.

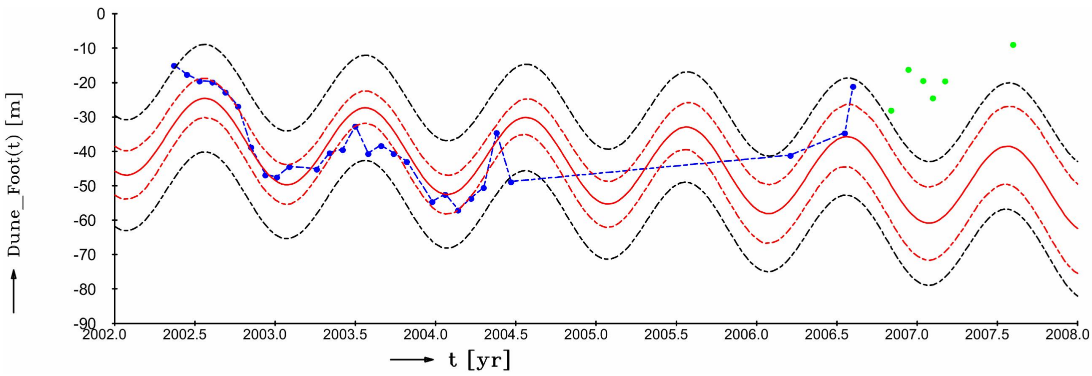

Figure 6.10 Dune Foot position : linear regression model including 1 harmonic component (red line), with a fixed period of 1 year. The confidence and prediction intervals are displayed with a red dashed line and a black dashed line, respectively. Green points display the dGPS-based observations after the installation of the Ecobeach technique.

Table 6.4 Dune foot position: Z(()-statistics and uncertainties (95.00% confidence and prediction intervals) for a list of times tk, using a linear regression model with 1 harmonic component

Nr	time tk	Obs. value	Mean [Z(tk)]	Spread Confid.	Lower boundary	Upper	Spread Predic.	Lower boundary	Upper
1	20/03/06	-41.1	-53.91	4.121	-62.21	-45.76	8.458	-70.58	-37.29
2	18/07/06	-34.5	-35.83	4.449	-44.49	-26.51	8.623	-52.75	-18.80
3	03/11/06	-27.86	-49.96	5.370	-60.45	-39.17	9.132	-67.90	-31.96
4	12/12/06	-16.02	-57.27	5.471	-67.98	-46.39	9.191	-75.35	-39.20
5	15/01/07	-19.3	-60.68	5.431	-71.32	-50.11	9.168	-78.72	-42.67
6	06/02/07	-24.32	-60.83	5.367	-71.47	-50.11	9.168	-78.80	-42.89
7	06/03/07	-19.4	-58.66	5.278	-69.20	-48.18	9.078	-76.52	-40.82
8	07/08/07	-8.7	-38.87	5.827	-50.19	-26.95	9.408	-57.27	-20.22

Beach width

The correlation between sediment volumes and the beach characteristics is not always obvious though. For instance, a flattening of the beach implies a wider beach without coinciding necessarily with a volume loss or gain. The beach width has been described setting up a linear regression model and including 1 harmonic component with a fixed period of 1 year (Figure 6.11). Table 6.5 and Figure C.10 summarize the model predictions and the observed values for some specific dates. The general behaviour of the observations is well represented by the model. Winter periods are characterized by a wider beach compared to the summer periods. No trend break can be noticed in the dataset. All observations carried out after the installation of the Ecobeach technique are included within the prediction interval. Still, the small amount of available data (in a statistical point of view) prevents the statistical representation of the beach volume behaviour for the period post-installation of the modules.

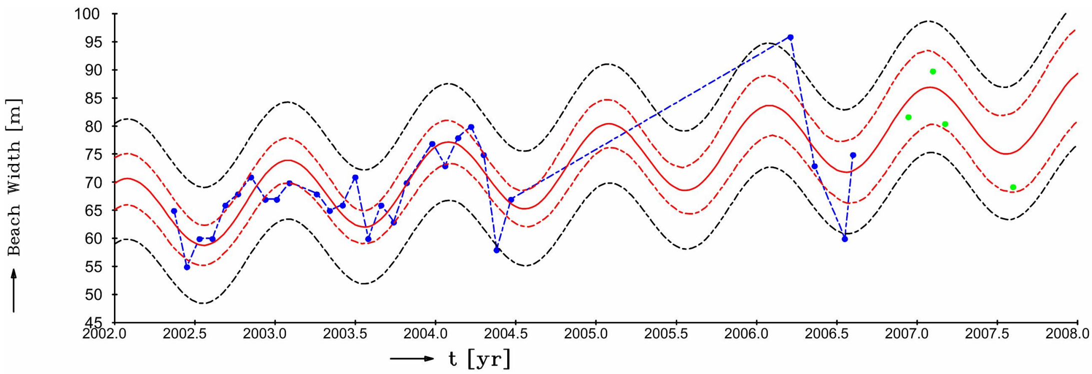

Figure 6.11 Beach width : linear regression model including 1 harmonic component (red line), with a fixed period of 1 year. The confidence and prediction intervals are displayed with a red dashed line and a black dashed line, respectively. Green points display the dGPS-based observations after the installation of the Ecobeach technique.

Table 6.5 Beach width: Z(()-statistics and uncertainties (95.00% confidence and prediction intervals) for a list of times tk, using a linear regression model with 1 harmonic component

Nr	time tk	Obs. value	Mean [Z(tk)]	Spread Confid.	Lower boundary	Upper	Spread Predic.	Lower boundary	Upper
1	20/03/06	96.4	81.52	2.463	76.56	86.28	5.478	70.71	92.35
2	18/07/06	60.8	71.90	2.675	66.39	77.22	5.577	60.88	82.89
3	03/11/06	NaN	80.96	3.490	73.91	87.59	5.959	69.16	92.66
4	12/12/06	81.7	85.25	3.509	77.98	91.93	5.970	73.44	96.97
5	15/01/07	NaN	87.34	3.382	80.43	93.71	5.896	75.69	98.93
6	06/02/07	89.9	87.54	3.266	80.93	93.81	5.830	76.03	99.01
7	06/03/07	80.48	86.47	3.124	80.15	92.33	5.752	75.12	97.79
8	07/08/07	69.2	76.09	3.523	69.07	83.02	5.978	64.27	87.83

6.3 Profiles

The steepness of the nearshore profile, as well as the bar topography, varies over alongshore distances. Spatial aggregation by averaging the CSI-values along the longshore direction has been therefore performed over the tested area (from RSP 40.00 to RSP 43.00) and over the reference area (from RSP 43.00 to RSP 46.00) in order to improve the confidence and the predictability of models, as compression of information minimizes the noise in a timeserie. Moreover, the analysis per profile might be unsuitable to evaluate the overall potential effect of the Ecobeach drains. As an example, Figure 6.12 and Figure 6.13 exhibit different behaviors during the period May 2006 to August 2007. The development of the profile RSP 4150 (Figure 6.12) shows some accretion in the upper part of the beach in the summer 2007 and the bed shape in August 2007 is well developed. On the other hand, the development of the profile RSP 4050 (Figure 6.13) does not show any significant sedimentation in the upper part of the beach during the same period. Although such description appears useful to understand locally the profile developments, the potential effect of the Ecobeach technique has definitely to be evaluated using aggregated CSI values.

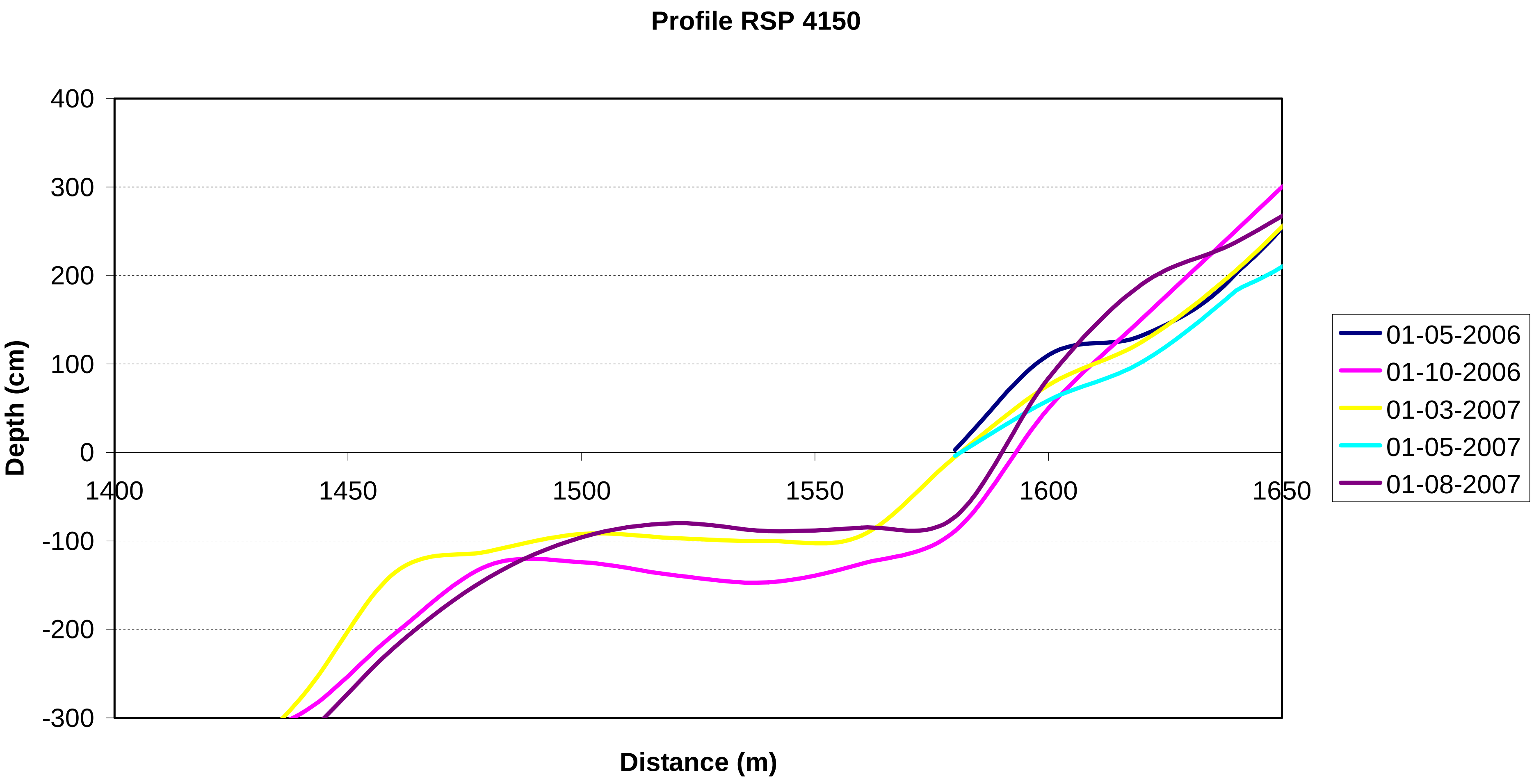

Figure 6.12 Bed levels between May 2006 and August 2007 along a cross-section for profile RSP 4150

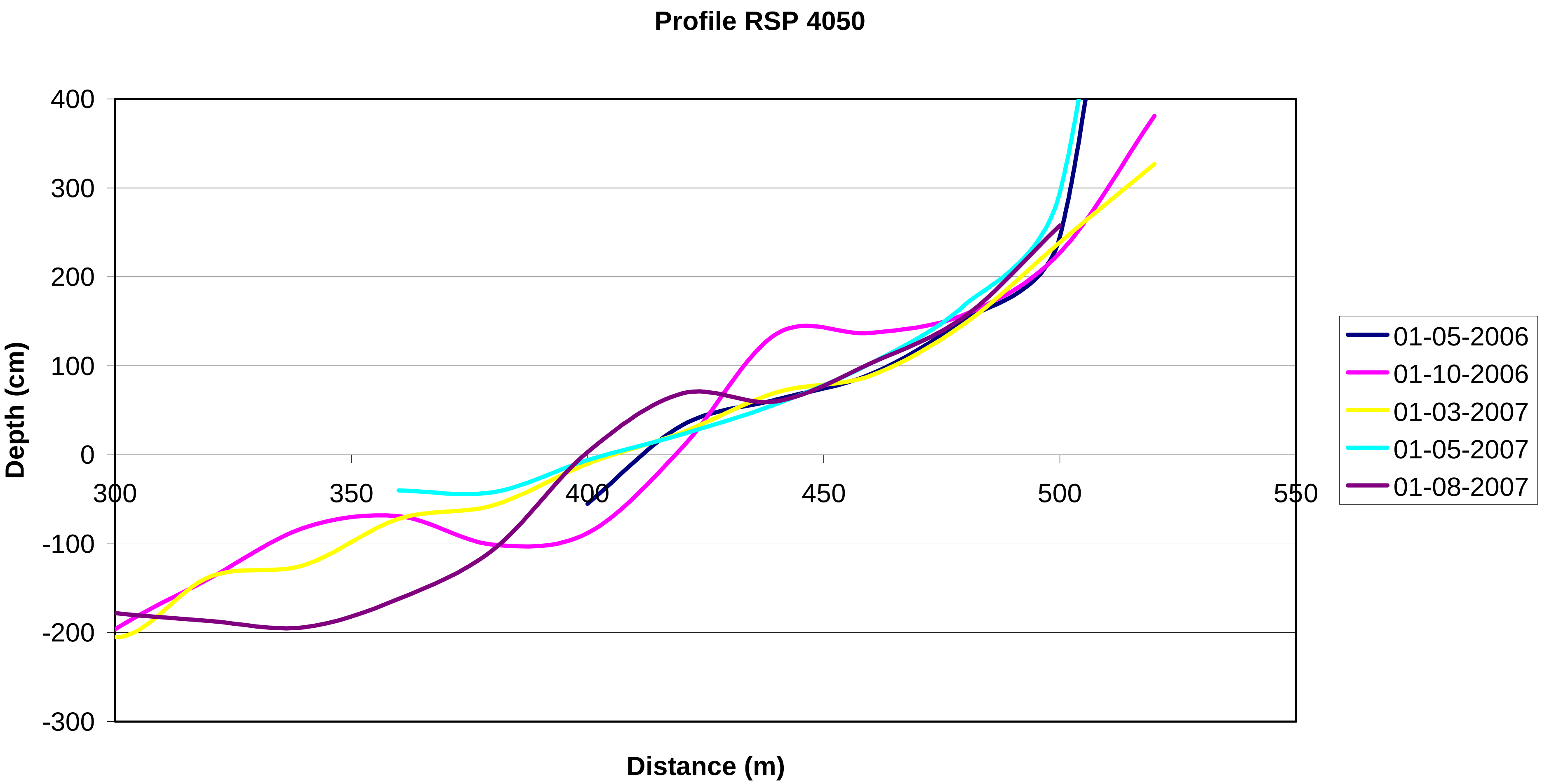

Figure 6.13 Bed levels between May 2006 and August 2007 along a cross-section for profile RSP 4050

6.4 Summary

Variations in beach characteristics, such as the MiCL volume and position, the cross-shore position of the dune foot and of the shoreline and the beach width and volume have been used to approximate accretion and erosion quantitatively.

Based on the analysis of medium-term evolution of these Coastal State Indicators, the following conclusions can be drawn:

- on the wave influence

- correlations between the average of the hourly wave height over [2 days; 7 days; number of days between two successive surveys] and the beach characteristics have been successively investigated.
- no clear relation between beach characteristics and wave parameters can be found. It appears of marginal importance to include any wave schematisation to force the statistical model in order to improve its representation of seasonal patterns.

- on the datasets used

- characterized by different precisions in the measurement techniques, and different spatial covering, the Argus-based and dGPS datasets are not compatible and can not be analysed by merging all data in a single dataset. The medium-term behaviour of Coastal State Indicators has been described therefore using dGPS and Argus-based datasets separately.

- on the MiCL volume and position

- using a reduced Argus-based dataset, the medium-term trend of the evolution of the MiCL volume has been described setting up a linear regression model (representing the local slope of the long-term trend) and including 1 harmonic component with a fixed period of 1 year.
- after the installation of the Ecobeach technique (November 2006), the model predictions and the observations are in the same order. 92% of the observed MiCL volumes remain within the prediction interval. However, the arbitrary choice of the 95% confidence and prediction intervals for the parameters based on B-resampling of the model's residuals is quite strict.
- nevertheless, a visual inspection of the data does not show any trend break in the medium-term behaviour of the MiCL volume.
- results obtained using the dGPS dataset are much more difficult to be analysed as a long gap occurred between June 2004 and March 2006. Moreover, the measurement techniques (by walking or by motor-quad), the spatial covering, and the interval between successive surveys have changed in time, explaining some discrepancies in the general trends displayed in the periods 2002-2004 and 2006-2007.
- the general behaviour of the observed MiCL volumes (based on dGPS data) is well represented by the model. No trend break can be noticed in the dataset. Moreover, all observations carried out after the installation of the Ecobeach technique are included within the prediction interval.

- on the upper part of the beach

- using dGPS dataset, the medium-term trend of the evolution of the dune foot position has been described. In the period 2002-2004, observations show a retreat of the dune foot position in the winter and an offshore migration in the summer, which is well reproduced by the model. In the period 2006-2007, the general behaviour of the observations is not well represented by the model. A trend break can be clearly seen in the dataset, as all observations since November 2006 are in a range out of the prediction interval.
- however, it has to be noticed that the measurement techniques (by walking or by motor-quad), the spatial covering, and the interval between successive surveys have changed in time. In particular, the spatial covering of the upper part of the beach (around the dune foot position) in the period 2006-2007 seems not as precise as it was when surveying a smaller area in the period 2002-2004. Such inaccuracies in the monitoring might have induced errors in the interpolation process from samples to grids and in the analysis.
- the general behaviour of observed beach width based on dGPS data is well represented by the model. Winter periods are characterized by a wider beach compared to the summer periods. No trend break can be noticed in the dataset. Moreover, all observations carried out after the installation of the Ecobeach technique are included within the prediction interval.

- on the statistical method

- the small amount of available data (in a statistical point of view) prevents the statistical representation of the medium-term behaviour of all Coastal State Indicators for the period post-installation of the modules.

7 Conclusions

7.1 Outline

An innovative way to protect the Dutch Coast, the Ecobeach technique, which is an easily installable system that consists of vertical, passive drainage pipes that are regularly spaced on the beach has been installed in Egmond. The proposed duration of the experiment is three years. The overall objective of the study is to identify the effects of the Ecobeach modules on the natural behaviour of the beach and dune system in the test area. It consists more specifically on defining an objective method (statistical model) to identify the natural behaviour of the beach and dune system in the test area and in an adjacent reference area, based on historical data, and on analysing the behaviour of the beach and dune system in these areas after installation of the Ecobeach modules, with respect to the natural behaviour of the system.

7.2 Results

Historical trend analysis relies on the extrapolation of historic data to predict future coastal evolution. Statistical regression models, including possibly harmonic components to take cyclic patterns into account, have therefore been set-up to predict changes for the period when the Ecobeach modules are installed. Comparison between model outputs and observations, obtained after installation of the drainage system, enables therefore the identification of potential effects of the drainage system.

40-years historical yearly Jarkus data enable to predict future coastal evolution of a selection of Coastal State Indicators. These predictions have been compared to observations in 2007:

- on the MCL and MiCL volumes and positions

- an increase of the MCL and MiCL volumes have been observed between 2006 and 2007 in the test and in the reference areas.
- this increase of the volumes has been predicted (see Brière et al., 2007) using a linear regression model including 1 harmonic component, representing the cyclic coastal sand bar migration, to model the long-term trend of the Coastal State Indicators (e.g. Figure 5.6 for the MiCL volume).
- in 2007, the 95% prediction interval for the MCL volume in the test area is in the range of [1106 m^3/m, 1234 m^3/m], with a mean extrapolated value of 1170 m^3/m. Observation in 2007 reaches 1225 m^3/m. However, no trend break between the behaviours in the two areas can be noticed. In both cases, the predictions underestimate the observed data.
- strongly correlated, the MCL position is predicted in 2007 in the range of [113.3 m 132.3 m], with a mean extrapolated value of 122.7 m. Still the model underestimates the observation (130 m). However, the reference area displays similar behaviour.
- the 95% prediction interval for the MiCL volume in 2007 is of [18.64 m^3/m 48.56 m^3/m], with a mean extrapolated value of 33.66 m^3/m. Observation in 2007 is of 42 m^3/m. Behaviours in the reference and test areas look similar.
- the observed MiCL positions in 2007 are in the range of the predicted ones for both the reference and the test areas.

- on the upper part of the beach

- in the upper part of the beach, no significant trend break can be seen for the selected Coastal State Indicators, by comparing results obtained in the reference and test areas. In general, observations of 2007 are in the range of the mean predicted values.
- however, the model overestimates the observation obtained in test area for the shoreline position. The 95% prediction interval in 2007 is of [85.04 m, 129.8 m], with a mean extrapolated value of 107.6 m. The observation displays a retreat of the shoreline. As the beach volume remains constant between 2006 and 2007 (Figure 5.8), this might suggest a cross-shore exchange in sediment between the lower intertidal zone and the upper intertidal zone, with a steepening of the profile.
- for the dune foot position in the test area, the 95% prediction interval in 2007 is of [-36.20 m, -24.82 m], with a mean predicted dune foot position of -30.51 m. Observation in 2007 is of -31.9 m.
- in 2007, the 95% prediction intervals for the beach volume is of [154.2 m^3/m, 193.7 m^3/m], whereas the mean predicted value is of 174.1 m^3/m. Observation in 2007 is of 168.5 m^3/m.

- on the dune dynamics

- with respect to the dunes, the analysed data show a large spatial and temporal variability of volume changes. Therefore, it is necessary to analyse the data over periods of at least 5 years, in order to get reliable results. On average, the dunes are increasing in volume. Focussing on the period 2006-2007, a decrease of the dune volume is obtained.
- a regression model has also been set-up for the dune volumes. In 2007, the prediction interval is of [1160 m^3/m, 1214 m^3/m], with a mean extrapolated value of 1187 m^3/m. Observation in 2007 is of 1193.4 m^3/m.

Shorter-term historical monthly dGPS- and Argus-based data enable to predict future coastal evolution of a selection of Coastal State Indicators. These predictions have been compared to observations obtained from November 2006:

- on the wave influence

- correlations between the average of the hourly wave height over [2 days; 7 days; number of days between two successive surveys] and the beach characteristics have been successively investigated.
- no clear relation between beach characteristics and wave parameters can be found. It appears of marginal importance to include any wave schematisation to force the statistical model in order to improve its representation of seasonal patterns.

- on the MiCL volume and position

- after the installation of the Ecobeach technique (November 2006), the model predictions and the observations are in the same order. 92% of the observed MiCL volumes (based on Argus images) remain within the prediction interval. A visual inspection of the data does not show any trend break in the medium-term behaviour of the MiCL volume.
- the general behaviour of the observed MiCL volumes (based on dGPS data) is well represented by the model. No trend break can be noticed in the dataset. Moreover, all observations carried out after the installation of the Ecobeach technique are included within the prediction interval.

- on the upper part of the beach

- in the period 2002-2004, observations of the dune foot position show a retreat of the dune foot position in the winter and an offshore migration in the summer, which is well reproduced by the model.
- in the period 2006-2007, the general behaviour of the observations is not well represented by the model. A trend break can be clearly seen in the dataset, as all observations since November 2006 are in a range out of the prediction interval.
- however, the measurement techniques (by walking or by motor-quad), the spatial covering, and the interval between successive surveys have changed in time. In particular, the spatial covering of the upper part of the beach (around the dune foot position) in the period 2006-2007 seems not as precise as it was when surveying a smaller area in the period 2002-2004. Such inaccuracies in the monitoring might have induced errors in the interpolation process from samples to grids and in the analysis.

- on the statistical method

- the small amount of available data (in a statistical point of view) prevents the statistical representation of the medium-term behaviour of all Coastal State Indicators for the period post-installation of the drainage system.

8 Recommendations

A statistical analysis requires sufficient information to describe trends, ideally including cyclic pattern of coastal bar migration and seasonal variations. In particular, the analysis has shown that the small amount of data available after the installation of the Ecobeach technique (in a statistical point of view) prevents the representation of the medium-term behaviour of all Coastal State Indicators. In this context, it is recommended to gather more data after the installation of the drainage system, potentially covering the test area and the reference area.

Since 1996, the Argus station provides images, enabling a monthly analysis of the evolution of Coastal State Indicators. So far, a 3-years dataset has been generated, and 1 year after the installation of the Ecobeach technique has been covered. ***It is recommended to continue the monitoring of data in order to extend the Argus dataset to a longer historical period of about minimum 2 years after the installation of the drainage system.***

Over the last 5 years, dGPS system has also been used to monitor the studied area. The monitoring project based on this measuring technique is covering the periods May 2002- June 2004 and March 2006 to present, with a monthly measuring frequency for the period May 2002- June 2004. Since spring 2007, the period between 2 surveys has increased. Moreover, the way of monitoring (either by walking, or by motor-quad) has changed, preventing the gathering of data of similar quality. In this context, ***it is recommended to collect data with a 50-m alongshore spacing, with capturing details of small rips by walking, from Beach Pole RSP 40.00 to RSP 43.00***. Ideally, ***such monitoring should also be done in the reference area***, in order to compare the behaviours of Coastal State Indicators in both areas.

With respect to the dune volume analysis, both temporal and spatial variability are large, and the expected changes due to the Ecobeach experiment are small. To be able to relate any change to the experiment, a long monitoring period will be necessary. Otherwise it will not be possible to detect any changes in current trends, unless of course the changes due to the Ecobeach experiment are much larger than expected. Because of the large temporal variability, and uncertainties with respect to Jarkus and laser altimetry data, ***we recommend to perform field measurements on dune erosion and accretion, by means of a regular measurement of a grid of erosion pins.*** These measurements are very cheap, easy and reliable, and will provide valuable calibration data for both Jarkus and laser altimetry data.

In a statistical point of view, it is recommended to increase the amount of data available, by adjusting the monitoring programme to provide as much as possible ***monthly-recorded information on the beach development. To that end, dGPS measurements and Argus images appear therefore particularly useful***.

9 References

Aarninkhof, S.G.J., and J.A. Roelvink, Argus-based monitoring of intertidal beach morphodynamics. Proc. of Coastal Sediments Conf., Long Island (NY), USA, pp. 2429– 2444, 1999.

Battjes, J.A., Janssen, J.P.F.M., 1978. Energy loss and set-up due to breaking in random waves. Proc. of 16th Int. Conf. on Coastal Eng. ASCE, New York, pp. 569– 587.

Boogaard van den, H.F.P., Uittenbogaard, R.E., Mynett, A.E., 2006, Generalised cross-covariance analysis for uncertainty estimation of shifts in time series, in *Proc. Hydroinformatics 2006, Vol.II,* pp. 1543-1550, Chennai, Research Publishing.

Brière C., A.B. Cohen, H.F.P. van den Boogaard and S.M. Arens, 2007. Ecobeach monitoring project, Half-year study. Report Z4398. WL | Delft Hydraulics. July 2007.

Cohen, A.B. en B.T. Grasmeijer, 2007. Ecobeach monitoring project Phase 1. Opdracht RKZ-1755. Rapport Z4213, januari 2007.

Davis, R. A. and M.O. Hayes, 1984. What is a wave-dominated coast? Marine Geology 60, 313-329.

Douglas, B.C. and Crowell, M., 2000. Long-term shoreline position prediction and error propagation. Journal of Coastal Research, 16(1) 145 – 152.

Efron B., and Tibshirani R., 1993, An introduction to the Bootstrap, Chapman & Hall, London.

Elias, E.P.L., Walstra, D.J.R., Roelvink, J.A., Stive, M.J.F., Klein, M.D., 2000. Hydrodynamic validation of Delft3D with field measurements at Egmond. In: Edge, B.L. (Ed.), Proc. 27th Int. Conf. on Coastal Engineering. ASCE, New York, pp. 2714–2727.

Janssen, P.C., 1997. Intertidal Beach Level Estimations from Video Images. Netherlands Centre for Coastal Research. MSc. thesis Delft University of Technology, Department of Civil Engineering.

Kendall, M.G. and Stuart A.S., 1961, The advanced theory of statistics. Volume 2, Inference and relationship, Charles Griffin & Company Ltd., London.

Knoester, D., 1990. De morfologie van de Hollandse kustzone (analyse van het JARKUS-bestand 1964-1986). Rijkswaterstaat, Rep., GWAO-90.010, 85 pp. [The morphology of the coastal zone of Holland (analysis of the JARKUS data base 1964-1986).]

Koningsveld van and Mulder, 2004, Sustainable Coastal Policy Developments in The Netherlands. A Systematic Approach Revealed, Journal of Coastal Research, DOI: 10.2112/1551-5036(2004)020[0375:SCPDIT]2.0.CO;2

Kroon, A., 1994. Sediment transport and morphodynamics of the beach and nearshore zone near Egmond, the Netherlands. Ph.D. Thesis, Fat. Geogr. Sci., Utrecht Univ., 275 pp.

Larson, M., Capobianco, M., Jansen, H., Różyński, G., Southgate, H.N., Stive, M., Wijnberg, K.M. and Hulscher, S., 2003. Analysis and modelling of field data on coastal morphological evolution over yearly and decadal time scales. Part 1: Background and linear techniques. Journal of Coastal Research, 19(4) 760 – 775.

Plant, N.G., and R.A. Holman, Intertidal beach profile estimation using video images, Marine Geology, 140, 1-24, 1997

Press, W.H., B.P. Flannery, S.A. Teukolsky, W.T. Vetterling: *Numerical Recipes. The Art of Scientific Computing.* Cambridge University Press, Cambridge, 1986.

Quartel, S. en Grasmeijer, B.T., 2006. Dynamiek van het strand bij Noordwijk aan Zee en Egmond aan Zee en het effect van suppleties. Opdracht RKZ-1667, Concept T1-Rapport, Rapport CR-2007-01, februari 2006.

Rijn, L.C. van,Walstra, D. J. R., Grasmeijer, B. T., Kleinhout, K. 2001. Hydrodynamics and morphodynamics in the surf zone of a dissipative beach. In: Proc. 4th Coastal Dynamics Conf. Lund, Sweden.

Rijn, L.C. van, Walstra, D.J.R., Grasmeijer, B., Sutherland, J., Pan, S., Sierra, J.P., 2003. The predictability of cross-shore bed evolution of sandy beaches at the time scale of storms and seasons using process-based profile models. Coast. Eng. 47, 295– 327.

Stolk, A., 1989. Zandsysteem kust – een morfologische karakerisering. Kustverdering na 1990, Report Geopro 1989-02, Department of Physical Geography, Utrecht University, 97 pp.

A Ecobeach system (United States Patent 6547486)

Patent information
Name: Method for Coastal Protection
Inventor: Poul Jakobsen
Assignee: SIC Skagen Innovationscenter
Patent no.: US 6,547,486 B1
Date of Patent: 15 April 2003

Abstract

In a method for coastal protection, where the coastal area has an underlying freshwater basin and below this a salt water tongue which extends obliquely down into the coastal area, the pressure is equalized in the groundwater basin at least along an area at the shore line completely or partly to the atmosphere through pressure equalization modules, preferably in the form of pipes with a filter at the bottom, which extend down into the groundwater basin. This causes sedimentation of material and thereby an increase in the width of the shore. The resulting sand drift may be utilized for additional building-up of the coastal area by further establishing fascines.

Claims

What is claimed is:

1. A method for protecting a coastal area which includes a beach area that meets salt water at a shoreline, and where a freshwater basin underlies the coastal area and a salt water tongue extends below the freshwater basin at an oblique angle, the method comprising extending at least one pipe downwardly in the beach area near the shoreline so as to reach the freshwater basin and communicate the freshwater basin with the atmosphere such that at least a partial equalization of a pressure in the freshwater basin with a pressure of the atmosphere is achieved in said beach area by means of said communication.

2. A method according to claim 1, wherein said at least one pipe includes a filter in a part thereof that extends into the freshwater basin.

3. A method according to claim 1, wherein a plurality of pipes are extended downwardly through the beach to the fresh water basin at a distance from the shoreline.

4. A method according to claim 3, wherein, said coastal area also defines a swash zone adjacent said shoreline, and including placing a plurality of additional said pipes in said swash zone to communicate with said freshwater basin.

5. A method according to claim 1 wherein fascines are provided on the coastal area.

6. A method according to claim 1, wherein said at least one pipe includes an anchoring element.

7. A method according to claim 6, wherein said at least one pipe has a pipe stub which protrudes upwardly from the coastal area and a downwardly bent extension attached to the stub which includes an aperture facing downwardly and which defines an upper free end of the pipe.

Description

BACKGROUND OF THE INVENTION

1. Field of the Invention

The present invention relates to a method for coastal protection where the coastal area has an underlying freshwater basin and below this a salt water tongue which extends obliquely down into the coastal profile.

2. The Prior Art

For coastal protection, it is generally known to build breakwaters of huge stones or concrete blocks which extend from the beach to a distance into the water. Breakwaters are effective, but the costs of construction and maintenance are relatively great. Another coastal protection method is coastal feeding where large amounts of sand are transported to the stretch of coast which is to be protected. This method also involves great costs of construction and maintenance, since large amounts of sand have to be transported. These two methods are still the most widely used coastal protection methods.

In connection with the establishment of intakes for the pumping of sea water for use in salt water aquarias, it was discovered in the early 1980s that sedimentation took place around the intake, which became clogged because of the deposits on top of the intake. This was the incentive for experimenting with a new method for coastal protection, as described in DK 152 301 B. The idea of the method is to pump water from drains established along the shore line, resulting in sedimentation at the drains. However, this method never found extensive use, as it requires a great pumping capacity and consequently high costs of construction and high pump operating costs.

U.S. Pat. No. 5,294,213 discloses a similar system likewise based on drainage pipes established in parallel with the coastal both on the beach and in the water. The operation of the system, which is likewise based on pumping of water, is adapted to the weather, i.e., whether ordinary water level, low water, high water or storm conditions. The system includes a water reservoir into which the water may be pumped through the drainage pipes, and water may be pumped through these into the sea, e.g., to remove sand banks formed by a storm.

A corresponding method is known from U.S. Pat. No. 4,898,495 to keep an inlet, which debouches into the sea, open. This method is likewise based on pumps. The system comprises various diffuser arrangements to remove deposits from the mouth of the inlet by fluidizing these and transporting the material further downstream of the inlet mouth by generating a flow. Sedimentation is carried out downstream of the inlet mouth by pumping water from drains to the diffuser arrangements.

An object of the present invention is to provide a method for coastal protection which is not vitiated by the drawbacks of the known coastal protections.

SUMMARY OF THE INVENTION

This is achieved according to the invention by a method which is characterized in that the pressure of the groundwater basin at least along an area at the shore line is equalized completely or partly through pressure equalization modules, preferably in the form of pipes with a filter at the bottom, which extend down into the groundwater basin.

It has surprisingly been found by the invention that positioning of pressure equalization modules in the beach results in sedimentation of material at the area where the modules are placed.

A possible explanation as to why coastal accretion takes place is that the very fine sand which is fed to the profile partly by the sea and partly by the wind and which is packed with silt and other clay particles, reduces the hydraulic conductivity. Deeper layers in the coastal profile, which have exclusively been built by the waves of the sea, are primarily coarse in the form of gravel and pebbles which have a greater hydraulic conductivity. The difference in hydraulic conductivity will be seen clearly when digging into a coastal profile, it being possible to dig a hole in the profile, and the groundwater will then rise up into the profile once the water table is reached. The reason is the very different hydraulic conductivity and that the freshwater is under pressure from the hinterland. Thus, the coastal profile may be compared to a downwardly open tank where the tank is opened at the top with the pressure equalization modules which extend through the compact layers of the profile so that the water runs more easily and thereby more quickly out of the profile in the period from flood to ebb. This means that a pressure equalized profile is better emptied of freshwater and salt water in the fall period of the tide. When the tide then rises from ebb to flood, a greater fluctuation occurs in the foreshore, as the salt water in the swash zone is drained in the swash zone so that materials settle in the foreshore during this period of time. Conversely, coastal erosion takes place if the freshwater is under pressure in the foreshore, as the salt water will then run back into the sea on top of the freshwater and thereby erode the foreshore. In reality, the pressure equalization modules start a process which spreads from the pressure equalization modules, as the silt and clay particles are flushed out of the foreshore when the fluctuation is increased because of the draining action of the modules. Further, a clear connection has been found between the amount of sediment transport on the coast and the rate of the coastal accretion. It has been found that the pressure equalization modules create a natural equilibrium profile with a system of about 1:20, so that the waves run up on the beach and leave material, as water in motion can carry large amounts of material which settle when the velocity of the water decreases. The profile must therefore have a given width with respect to the tide and a maximum water level in the area. Coastal profiles with pressure equalization modules naturally become very wide, which results in a very great sand drift on the foreshore. This great sand drift is utilized by establishing longitudinal fascines high up in the beach and transverse fascines with an increasing height toward the foot of the dune, the fascines forming the upper part of the beach profile.

The invention will be described more fully below with reference to the accompanying drawings.

BRIEF DESCRIPTION OF THE DRAWINGS

FIG. 1 shows a cross-section through a coastal profile,
FIG. 2 shows a pressure equalization module intended to be positioned on the beach,
FIG. 3 shows a pressure equalization module intended to be positioned in the swash zone,
FIG. 4 shows a stretch of coast seen from above with pressure equalization modules and fascines, and
FIG. 5 shows a coastal profile in the stretch of coast in FIG. 4.

DETAILED DESCRIPTION OF THE PREFERRED EMBODIMENTS

As shown in FIG. 1, a freshwater basin is present below a coastal profile 1, and this freshwater basin is defined at the bottom in a downwardly inclined plane by a tongue of salt water 3 which has a greater density than freshwater.

The reason for coastal erosion is thus that when the freshwater below the beach profile is under pressure, the salt water seeping down into the profile runs back into the sea on top of the freshwater 2, as shown in FIG. 1. When the pressure of the freshwater decreases, the salt water seeps down through the material in the coastal profile and is mixed with the freshwater and thus does not erode the coastal profile, but, instead, material settles on the beach.

As shown in FIG. 2, the pressure equalization modules may consist of a rigid filter pipe 6 which is connected to a pipe 7 having a sleeve 7a. The filter and the pipe may thus be pressed, flushed or dug into the freshwater basin 2. Preferably, the pipe 7 has a length such that it protrudes slightly above the surface of the coastal profile 1 when the filter is in position in the freshwater basin. The pipes with filters, as shown in FIG. 2, are arranged in a row in a line which is perpendicular or approximately perpendicular to the shore line. The pipe 7 is open at the top so as to create good hydraulic contact down to the freshwater basin.

When the pressure in the freshwater basin has been equalized by means of the pressure equalization modules 12, the sedimentation of material on the stretch of coast may be accelerated according to the invention by establishing further pressure equalization modules 13 in the swash zone 4. An expedient arrangement of a module to be positioned in this zone is shown in FIG. 3 and comprises a rigid pipe 7' connected with a horizontal filter pipe 6'.

In both cases, the modules are provided with an anchoring element 8 intended to be dug into the sand to prevent unauthorized removal of the modules. The anchoring element is in the form of two angled plate elements secured to the rigid pipe. Furthermore, the pipe end, which protrudes from the sand, is provided with a curved termination 9 to prevent unauthorized filling of the pipe with sand, stone, etc. Optionally, the pressure equalization modules may be connected with dug pipes which are run to the foot of the dune where free communication with the atmosphere is created, thereby avoiding protruding pipe stubs.

The use of such pressure equalization modules on a stretch of coast has resulted in a land reclamation of a width of 4-6 metres and an increase in the coastal profile of 60-70 cm in 40 days.

Coastal profiles with pressure equalization modules naturally become very wide, as mentioned, which results in a great sand drift on the foreshore. As will appear from FIGS. 4 and 5, this great sand drift is utilized by establishing longitudinal fascines 10 high up in the beach and transverse fascines 11 of an increasing height toward the foot of the dune. The upper part of the beach profile may be given the desired shape by adapting the length, orientation and height of the fascines. The fascines may, e.g., be formed by brushwood of pine and spruce or the like dug into the coastal profile or stacked between buried piles, which makes it easy to give the fascines the desired shape.

The invention is unique by low costs of construction and operation, the cost of operation involving merely ordinary inspection and maintenance of the systems.

New research in the field has documented that the groundwater pressure on a coastal profile is very decisive for its appearance. It has been demonstrated that coastal profiles having a high freshwater pressure become narrow and concave (also called winter profile), while coastal profiles without noticeable freshwater pressure become wide and convex (also called summer profile). Narrow, concave coastal profiles having a high freshwater pressure are seen in Denmark typically at Vejby Strand on the north coast of Zealand and south of Lønstrup at Mårup Kirke.

Narrow, concave coastal profiles are greatly exposed to erosion, while wide, convex coastal profiles have beach accretion. With the invention, as described, it is possible to convert a narrow, concave coastal profile into a wide, convex coastal profile and thereby to protect the coast.

Schematic placing in coastal profile

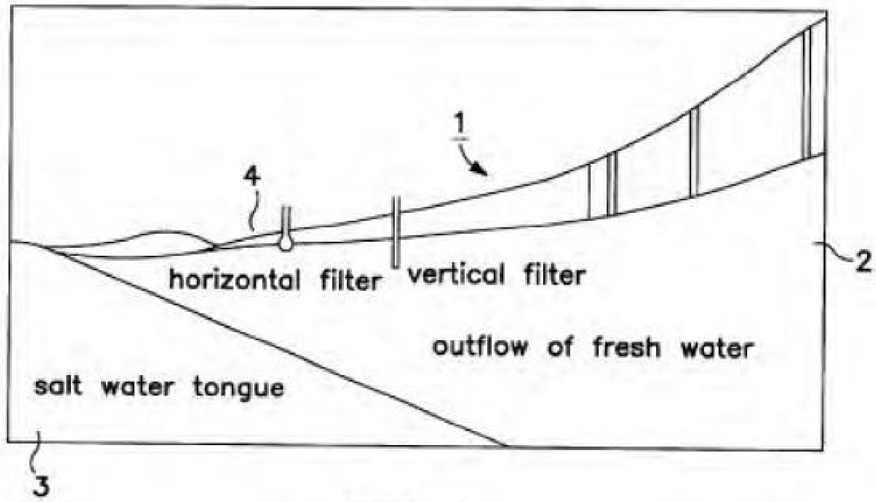

FIG. 1

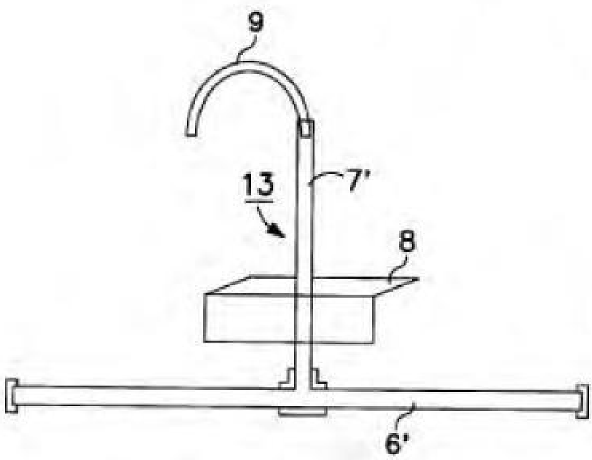

FIG. 3

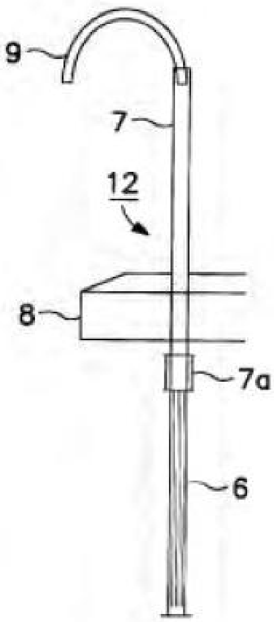

FIG. 2

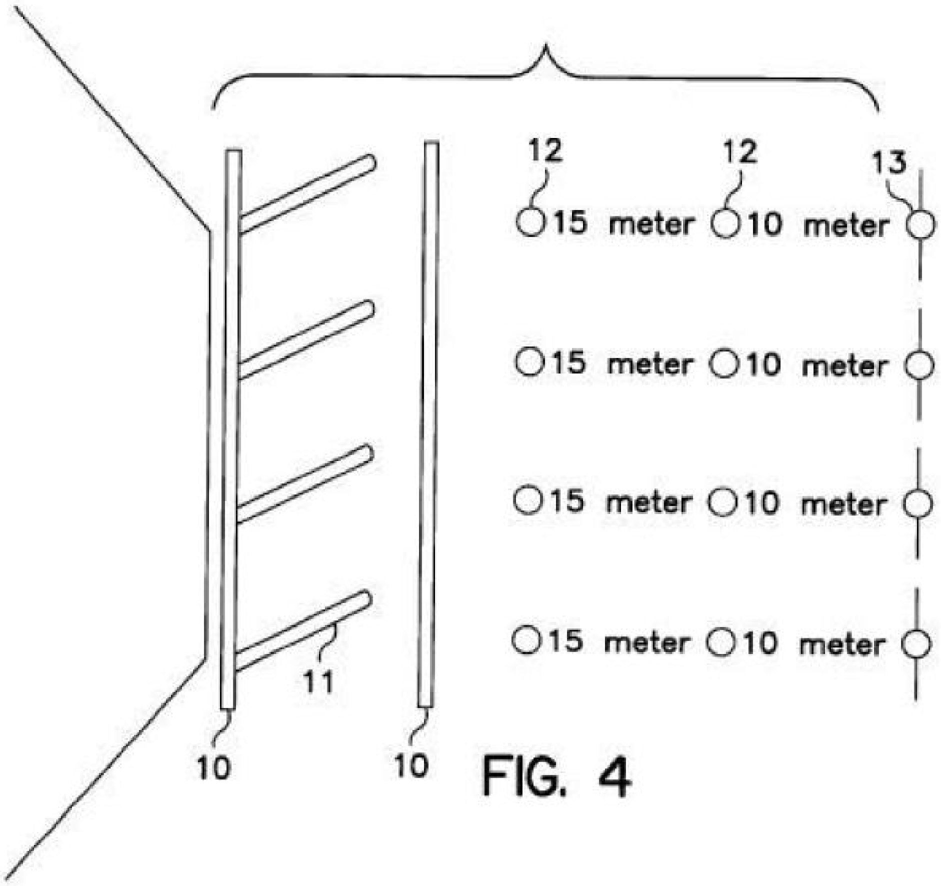
12
12
13
15 meter
10 meter
15 meter
10 meter
15 meter
10 meter
15 meter
10 meter
11
10
10

FIG. 4

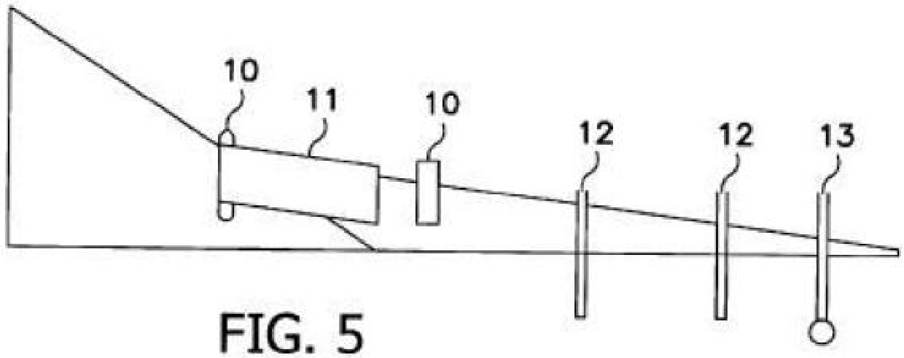
10
11
10
12
12
13

FIG. 5

B Statistical model

B.1 Introduction

Historical trend analysis relies on the extrapolation of historic data to predict future coastal evolution. A statistical model can only predict behaviour under conditions that are similar to those in the historic record and cannot cope with changes in forcing conditions, beach management or geological controls. Under this condition, such a model is able to predict changes which would have occurred if the Ecobeach system would not have been installed. Comparison between model outputs and observations, obtained after installation of the drainage system, enables therefore the identification of potential effects of the drains.

Which data to use?
Statistical methods can use long-term data sets which are available for the coastline at a number of times. The use of long-term datasets may allow extrapolation further into the future than from using shorter datasets. Shorter-term, often more detailed datasets, can be used to try and confirm the long-term behaviour and can be used for analysis at shorter timeframes.

Which model to set-up?
The majority of statistical modelling performed for coastal management appears to have been carried out using simple linear analysis methods. More complicated linear analysis techniques (e.g. wavelet analysis, Empirical Orthogonal Function analysis, Canonical Correlation Analysis, Principal Interaction Pattern analysis, etc ….) and the non-linear analyses (e.g. Singular Spectrum Analysis, fractal analysis, neural networks, etc …) have only recently been applied to beaches. Larson et al. (2003) noted that the choice of method for data analysis depends crucially on the quality and the quantity of data. The more sophisticated methods require more data of good quality and may pose additional constraints on the data, such as the need for data to be equally spaced in time and position.

Which confidence in the predictions?
Confidence limits can be calculated to provide a measure of the reliability of the predictions. They provide a range for the calculated erosion or accretion rate and depend on the variance of the data, the number of samples and the desired level of confidence. They strictly apply only to the time period the data weres collected in. The extrapolation of trends and confidence limits into predictions assumes that the future hydrodynamic climate will be statistically similar to the climate during the period the measurements are made. This restriction is important to take into account when short-term datasets are used. In case of long-term datasets (yearly Jarkus CSI) the morphology and the wave forcing are not strongly correlated (small seasonal bias). The forecasting of morphological changes can be therefore considered.

B.2 Modelling of the CSI and uncertainty assessments

For the modelling and forecasting of a time series of a CSI linear or non-linear parameterised regression models have been used. Uncertainties in the model and observations are represented by a random noise. As a consequence *stochastic* rather than deterministic models are used for the description of the temporal evolution of a CSI.
Observed CSI data of the past are used for the estimation of the model parameters. This identification of the parameters actually represents the model's calibration.
The embedding of the regression models in a stochastic environment has the important advantage that apart from estimates for the parameters also (and in a statistically sound way) uncertainties can be derived for these model parameters. Similarly the uncertainty can be derived in the model's predictions of future CSI. These forecasts of a CSI and associated *prediction intervals* can e.g. be compared with future measurements to assess whether or not the installation of Pressure Equilibrium Modules has induced a statistically significant effect.

B.2.1 Description of the stochastic model for CSI time series

In continuous time, the mathematical formulation of the model reads:

$$Z_t = \Phi\left(t \mid \vec{\Theta} \right) + V_t \tag{B.1}$$

The Z_t in this equation represents the model's prediction of a CSI at a time *t*. The model's prediction is built up of two components, $\Phi\left(\cdot \mid \vec{\Theta} \right)$ and V_t. The $\Phi\left(\cdot \mid \vec{\Theta} \right)$ is a parameterised function of time. It represents the deterministic, long term "systematic" variations in the temporal evolution of a CSI. These systematic variations may consist of trends in the series, and/or seasonal or even longer term cyclic behaviour. The vector $\vec{\Theta} := \left(\Theta_1, \Theta_2, \Theta_3, \cdots, \Theta_N \right)$ in Equation B.1 denotes a set of (uncertain) model parameters that are used in the mathematical description of the long term trends or formulation of cyclic components in the CSI. Below the deterministic model $\Phi\left(\cdot \mid \vec{\Theta} \right)$ and parameters $\vec{\Theta}$ will be worked out in a more concrete form, when describing the models that are used in the actual applications.

The V_t in Equation B.1 is a zero mean random noise. It represents the uncertainties in the modelling of the CSI and/or the uncertainties in the observations. In the present case it is assumed that V_t is a *Gaussian white* noise. This assumption is justified (though not reported here) by the results of preliminary analyses of the present CSI time series. "V_t is a *Gaussian white* noise" means that for each time *t* the noise V_t is a Gaussian random variable, and V_s and V_t are independent for times *s* and *t* when $s \neq t$. The spread of V_t is denoted by σ_V and is assumed to be independent of time, so that V_t is actually a *stationary* noise. The spread σ_V is not known beforehand and is considered as an uncertain model parameter as well. The value of σ_V must thus be estimated from observed data, just as the parameters $\vec{\Theta}$ in the deterministic part of the model.

Summarising, while $\Phi\left(\cdot \mid \vec{\Theta} \right)$ represents the deterministic component of the model of Equation B.1 dealing with the long(er) term systematic variations, the V_t provides a stochastic component representing the random short term variations. The right hand side of Equation B.1 thus consists of a stochastic model of a CSI. This embedding of the modelling in a stochastic environment is essential for a statistically consistent and well defined assessment of the uncertainties in (estimates of) the model parameters and model predictions.

B.2.2 Models for the deterministic long term variations

A visual inspection of plots of the time series of the several (aggregated, Jarkus based yearly samples) CSI over the period 1965 to 2006 suggest a temporal evolution that often contains a long term, gradually increasing (or decreasing) trend. In the present case such long term trends are described by a polynomial function of time *t*, leading to:

$$\Phi\left(t \mid \vec{\Theta} \right) = \alpha_0 + \alpha_1 \cdot t + \alpha_2 \cdot t^2 + \cdots\cdots + \alpha_N \cdot t^N \qquad \text{(B.2a)}$$

with the model parameters $\vec{\Theta}$ then consisting of:

$$\vec{\Theta} := \left(\alpha_0 \,, \alpha_1 \,, \alpha_2 \,, \cdots\cdots, \alpha_N \right) \qquad \text{(B.2b)}$$

For the (maximal) order *N* of the polynomial a proper guess must be made. On one hand the value of *N* should be large enough to represent sufficiently accurate the shape of a trend. On the other hand, however, *N* must be small compared to the number of data points to prevent overfitting of the model. Overfitting means that the complexity of the model is too large compared to the amount of – and variation in the data. In that case estimates of the parameters can be highly sensitive to noise, and an absurd and false model is fit to the data. Such an overfitted model may produce meaningless predictions for novel data.
In the present case, when dealing with 42 yearly Jarkus samples, preliminary experiments showed that the order of the polynomial should be restricted to *N*=1 (linear trend in time).

In many cases the visual inspection of the CSI time series also suggested the presence of a cyclic component, potentially representing the cyclic coastal bar behaviour. Such a component was modelled by a harmonic time series. This harmonic function was added to the polynomial function described above, leading to the following extension of the model:

$$\begin{aligned} \Phi\left(t \mid \vec{\Theta} \right) = {} & \alpha_0 + \alpha_1 \cdot t + \alpha_2 \cdot t^2 + \cdots\cdots + \alpha_N \cdot t^N + \\ & A_1 \cdot \cos\left(\tfrac{2\cdot\pi}{P_1} \cdot t \right) + B_1 \cdot \sin\left(\tfrac{2\cdot\pi}{P_1} \cdot t \right) \end{aligned} \qquad \text{(B.3a)}$$

More generally, more than one harmonic component may be present, or necessary to represent or approximate a period function, so that Equation B.3 can be generalised to:

$$\Phi\left(t \mid \vec{\Theta} \right) = \alpha_0 + \alpha_1 \cdot t + \alpha_2 \cdot t^2 + \cdots\cdots + \alpha_N \cdot t^N \quad + \sum_{\ell=1}^{L} \left(A_\ell \cdot \cos\left(\tfrac{2\cdot\pi}{P_\ell} \cdot t \right) + B_\ell \cdot \sin\left(\tfrac{2\cdot\pi}{P_\ell} \cdot t \right) \right) \tag{B.3b}$$

In that case the vector of model parameters $\vec{\Theta}$ consists of:

$$\vec{\Theta} := \left(\alpha_0 , \alpha_1 , \alpha_2 , \cdots\cdot, \alpha_N \; ; P_1, A_1, B_1, \; P_2, A_2, B_2, \cdots\cdots , P_L, A_L, B_L \right) \tag{B.3b}$$

Parameter P_ℓ denotes the period (here in years) of the $\ell - th$ harmonic component, while A_ℓ and B_ℓ denote the amplitudes of the cosine and sine functions.

It must be realised that through $r_\ell := \sqrt{A_\ell^2 + B_\ell^2}$ and $\varphi_\ell := \mathrm{atan2}\left(B_\ell , A_\ell \right)$ the harmonic function $H_\ell(t) := A_\ell \cdot \cos\left(\tfrac{2\cdot\pi}{P_\ell} \cdot t \right) + B_\ell \cdot \sin\left(\tfrac{2\cdot\pi}{P_\ell} \cdot t \right)$ can equivalently be written as a cosine function according to $H_\ell(t) = r_\ell \cdot \cos\left(\tfrac{2\cdot\pi}{P_\ell} \cdot t - \varphi_\ell \right)$. Presently the first expression is preferred, however, because of the linear form with respect to A_ℓ and B_ℓ. This linearity in A_ℓ and B_ℓ provides advantages in the estimation of the parameters.

It must also be remarked that the period P_ℓ of the $\ell - th$ cyclic component is not fixed or chosen manually but is considered as an unknown model parameter and the derivation of a best estimate of this period is a part of the calibration procedure (see below).

For every harmonic/cyclic component three unknown model parameters are involved and for the same reasons as mentioned above for the maximal degree of the polynomial, the number L of harmonic components that is included in the model must be limited to avoid overfitting. In most of the present applications this L was restricted to $L=1$.

With the $\Phi\left(\cdot \mid \vec{\Theta} \right)$ of Equation B.3b the model for the observations Z_t of a CSI is then finally:

$$Z_t = \alpha_0 + \alpha_1 \cdot t + \alpha_2 \cdot t^2 + \cdots\cdots + \alpha_N \cdot t^N \quad + \sum_{\ell=1}^{L} \left(A_\ell \cdot \cos\left(\tfrac{2\cdot\pi}{P_\ell} \cdot t \right) + B_\ell \cdot \sin\left(\tfrac{2\cdot\pi}{P_\ell} \cdot t \right) \right) + V_t \tag{B.4a}$$

It was already mentioned that also the spread σ_V of the noise V_t was considered as an unknown model parameter, although for the stochastic rather than the deterministic part of the model. For convenience the σ_V is augmented to the model parameters $\vec{\Theta}$ of Equation B.3b leading to:

$$\vec{\Theta} := \left(\alpha_0 , \alpha_1 , \alpha_2 , \cdots , \alpha_N \; ; P_1, A_1, B_1, P_2, A_2, B_2, \cdots , P_L, A_L, B_L \, ; \sigma_V \right) \tag{B.4b}$$

The total number of unknown parameters in the modelling is thus $N + 3 \cdot L + 2$. In the next section it is explained how observations $\left\{ \hat{Z}_{t_k} \right\}_{k=1}^{K}$ are used to find estimates for the parameters.

B.2.3 Calibration of the CSI models

For the calibration of the model of Equation B.1 (or A.4 in a more explicit form) a set of CSI observations $\left\{ t_k , \hat{Z}_{t_k} \right\}_{k=1}^{K}$ must be available and the parameters $\vec{\Theta}$ must be identified such that in an "appropriate sense" the model's predictions agree optimally with the 'targets' $\left\{ \hat{Z}_{t_k} \right\}_{k=1}^{K}$. In the present case we are dealing with a stochastic model, and therefore the calibration must be carried out in a statistically consistent and meaningful way. Here we will follow closely the approach described by Van den Boogaard et al. (2006). The main issues of the calibration and uncertainty assessment are conveniently summarised in the remainder of this section.

The t_k and $\hat{Z}_{t_k}$ in $\left\{ t_k , \hat{Z}_{t_k} \right\}_{k=1}^{K}$ denote the time and CSI value of the k^{th} measurement. Because the model is formulated in continuous time, the times t_k can actually be arbitrary (but must be mutually different) and need not to be on an equidistant temporal grid.

For a set of CSI "observations" $\left\{ t_k , \hat{Z}_{t_k} \right\}_{k=1}^{K}$ the model of Equation B.1 "reduces" to a set of K stochastic equations:

$$\hat{Z}_{t_k} = \Phi\left(t_k \mid \vec{\Theta} \right) + V_{t_k} \tag{B.5a}$$

Fully equivalently, Equation B.5 can be interpreted as a set of K observations for the noise V_t according to:

$$\hat{V}_{t_k} = \hat{Z}_{t_k} - \Phi\left(t_k \mid \vec{\Theta} \right) \tag{B.5b}$$

For the model's uncertainty it is assumed that V_t is a zero mean Gaussian white random process. Therefore the K "observations" $\hat{V}_{t_k}$ should satisfy a K-variate zero mean Gaussian probability density distribution $f_K(\cdot)$ with a $K \times K$ auto-covariance matrix Γ with entries $\Gamma_{k,k} = \sigma_V^2$ and $\Gamma_{k,\ell} = 0$ for $k \neq \ell$. On this basis, a Maximum Likelihood criterion (Kendall and Stuart, 1961) can be applied to derive an estimate for the parameters $\vec{\Theta}$. In fact, this estimate $\hat{\Theta}$ is the value of $\vec{\Theta}$ that minimises the minus Log-Likelihood function $J(\Theta) := -\ell n\left(f_K\left(\hat{V}_{t_1}, \hat{V}_{t_2}, \cdots, \hat{V}_{t_K}\right)\right)$. In the present case this function $J(\cdot)$ is:

$$J(\Theta) = \tfrac{1}{2} \cdot K \cdot \ell n\left(2 \cdot \pi \cdot \sigma_V^2\right) + \tfrac{1}{2} \cdot \sum_{k=1}^{K} \left(\frac{\hat{Z}_{t_k} - \Phi\left(t_k | \vec{\Theta}\right)}{\sigma_V^2} \right)^2 \tag{B.6}$$

Due to the non-linear dependence of $\Phi\left(\cdot \,|\, \vec{\Theta}\right)$ on $\vec{\Theta}$ the cost function of Equation B.6 cannot be minimised analytically, and one must rely on numerical methods. In the present applications a Quasi-Newton gradient descent technique (see e.g. Press et al., 1986) was applied for the minimisation of the minus LogLikelihood function.

B.2.4 Analytical covariance matrix and spreads for the estimates of the model parameters

Apart from the estimate for $\hat{\Theta}$, the Maximum Likelihood (MLH) formalism also provides an estimate for its covariance matrix $\Gamma^{(\Theta)}$. This covariance matrix is the inverse H^{-1} of the Hessian matrix H of the minus Log Likelihood function evaluated at its minimum. The Hessian matrix is the matrix of second order derivatives and thus the entries of H are $H_{n,m} := \left.\frac{\partial^2 J}{\partial \Theta_n \, \partial \Theta_m}\right|_{\Theta = \hat{\Theta}}$. From a so determined $\Gamma^{(\Theta)} := H^{-1}$ the spreads and correlation coefficients of the estimate $\hat{\Theta}$ can be computed which provide a quantitative measure for the uncertainties in $\hat{\Theta}$.

B.2.5 Uncertainty assessment by means of resampling

It was noted above that the spread of the estimates $\hat{\Theta}$ can be evaluated through the Hessian of the Minus Log Likelihood function. It must be mentioned, however, that theoretically this recipe is valid under the asymptotic condition of a sufficiently large data set of observations. It is then allowed to assume a Gaussian distribution for the identified parameters $\hat{\Theta}$. For small data sets this need not to be true, however, and in such cases *skewness* properties can be highly important in the representation of the uncertainties, especially when constructing non-symmetric (skew) confidence and/or prediction intervals. Resampling techniques may then serve as an attractive alternative method for uncertainty assessment. In effect, resampling creates a large *ensemble* of data sets, each of which is replicated from the original data sample. For each resample the actual statistic $\hat{\Theta}$ is recomputed. The most commonly applied resampling techniques are the JackKnife and Bootstrap, see e.g. Efron and Tibshirani (1993).

Now it is briefly outlined how for the present modelling a *Bootstrap resampling of residuals* can be applied to obtain spreads, quantiles, confidence intervals, or any other desired uncertainty measure.
A *bootstrap* resample is a random selection *with replacement* of K data out of the K original data. In such a resample an original data point may be absent, it may be present once, or it may be present more than once. Care must be taken that the resampling is applied to a data set of independent and identically distributed (IID) data points. In the present case it is then most convenient to base the resampling on the *residuals* $\hat{V}_{t_k} := \hat{Z}_{t_k} - \Phi\left(t_k \mid \hat{\Theta} \right)$ of the calibrated model, rather than using the original CSI observations $\hat{Z}_{t_k}$. Fortunately, as verified beforehand, the residuals were found to be highly mutually independent. This property was already conveniently used in the formulation of the present model through the assumption that V_t is a white and stationary Gaussian random noise. For completeness it is mentioned that in case the residuals $\hat{V} := (\hat{V}_{t_1}, \hat{V}_{t_2}, \cdots, \hat{V}_{t_K})^{\mathrm{T}}$ are not IID a suitable pre-whitening procedure must be applied, see e.g. (Van den Boogaard et al., 2006).
In the present case with the residuals satisfying the IID-property, an ensemble of L standard Bootstrap resamples $\hat{V}^{*(\ell)} := (\hat{V}^{*(\ell)}_{t_1}, \hat{V}^{*(\ell)}_{t_2}, \cdots, \hat{V}^{*(\ell)}_{t_K})^{\mathrm{T}}$ $(1 \le \ell \le L)$ are generated from the identified residuals $\hat{V} = (\hat{V}_{t_1}, \hat{V}_{t_2}, \cdots, \hat{V}_{t_K})^{\mathrm{T}}$. For each resample $\hat{V}^{*(\ell)}$ of $\hat{V}$ a new series of K "resampled observations" $\left\{ \hat{Z}^{*(\ell)}_{t_k} \right\}_{k=1}^{K}$ of the target series is constructed according to the calibrated model:

$$\hat{Z}^{*(\ell)}_{t_k} = \Phi\left(t_k \mid \hat{\Theta} \right) + \hat{V}^{*(\ell)}_{t_k} \tag{B.7}$$

Next, the Log Likelihood function of Equation B.6 (but with the original targets $\left\{ \hat{Z}_{t_k} \right\}_{k=1}^{K}$ replaced by their resamples $\left\{ \hat{Z}^{*(\ell)}_{t_k} \right\}_{k=1}^{K}$) is again minimised to find a resampled estimate $\hat{\Theta}^{(\ell)}$ for the model's parameters. This procedure is repeated many (L) times, to achieve an *ensemble* of estimates $\left\{ \hat{\Theta}^{(\ell)} \right\}_{\ell=1}^{L}$ for the model parameters Θ.

The ensemble $\left\{ \hat{\Theta}^{(\ell)} \right\}_{\ell=1}^{L}$ provides an *empirical probability distribution* of the model parameters $\hat{\Theta}$ and apart from the mean, spread or covariance/correlation matrix, it allows a convenient assessment of other distribution properties such as skewness, quantiles, and/or confidence intervals. For example, for the 95%-level (skew) confidence interval of a model parameter (as for example the α_1 in $\vec{\Theta} := \left(\alpha_0, \alpha_1, \alpha_2, \cdots, \alpha_N ; P_1, A_1, B_1, P_2, A_2, B_2, \cdots, P_L, A_L, B_L ; \sigma_V \right)$, see Equation B.5b) the L estimates $\left\{ \hat{\alpha}_1^{(\ell)} \right\}_{\ell=1}^{L}$ must be ranked in ascending order of magnitude. The lower and upper limits of the confidence interval are then simply set equal to the 2.5% and 97.5% quantile of the ranked estimates (*percentile method*). Similarly as explicitly done here for

parameter α_1, it is possible to quantify in this way the uncertainties in all the other model parameters. In particular a confidence interval can thus be computed for the (estimate $\hat{\sigma}_V$ of the) spread of the random noise V_t.
Clearly the present approach is not restricted to 95% confidence intervals but can also be applied for another arbitrary confidence level γ.

B.2.6 Confidence intervals for model outputs

In the preceding sections it was outlined how to derive in quantitative form the uncertainties (spreads, confidence intervals, etc.) in the estimate $\hat{\Theta}$ of the *model parameters* $\vec{\Theta} := \left(\alpha_0 , \alpha_1 , \alpha_2 , \cdots, \alpha_N ; P_1, A_1, B_1, P_2, A_2, B_2, \cdots , P_L, A_L, B_L ; \sigma_V \right)$ In this and the next section it is shown how to obtain a quantitative measure for the *uncertainty in model outcomes*, i.e. a CSI as predicted by the calibrated model for some time *t*. This time *t* can be quite general and is not necessarily restricted to the observation times $\left\{ t_k \right\}_{k=1}^{K}$ of the data $\left\{ \hat{Z}_{t_k} \right\}_{k=1}^{K}$ used in the model's calibration. In particular the time *t* can now also refer to times out of the range covered by the $\left\{ t_k \right\}_{k=1}^{K}$ and for such times the model is actually used for extrapolation, or forecasting.

In this section we will deal with *confidence intervals* while in the next section *prediction intervals* will be considered.

The set $\left\{ \hat{\Theta}^{(\ell)} \right\}_{\ell=1}^{L}$ of parameter estimates found in a resampling based calibration procedure forms a convenient foundation for a quantitative and statistically well based assessment of confidence and prediction intervals for model outcomes. Actually, through the set of resamples $\left\{ \hat{\Theta}^{(\ell)} \right\}_{\ell=1}^{L}$ an ensemble of *L* (deterministic) models $\Phi\left(\cdot \mid \hat{\Theta}^{(\ell)} \right)$ is available. In fact, for any time *t* this provides *L* estimates $\left\{ \Phi\left(t \mid \hat{\Theta}^{(\ell)} \right) \right\}_{\ell=1}^{L}$ (see Equation B.1) for the "output" of the *deterministic part* of the model. In the same way as sketched above, this ensemble $\left\{ \Phi\left(t \mid \hat{\Theta}^{(\ell)} \right) \right\}_{\ell=1}^{L}$ can conveniently be used for the construction of spreads or (*skew*) confidence intervals. It must be realised, however, that a so constructed skew 95% (or other confidence level γ) confidence interval $\left[\Phi_{2.5\%}(t), \Phi_{97.5\%}(t) \right]$ represents the uncertainty in the output of the deterministic part of the model. Therefore this confidence interval reflects the uncertainty in the identified long term systematic variations in the CSI, such as trends and/or cyclic components. In the construction of the confidence interval $\left[\Phi_{2.5\%}(t), \Phi_{97.5\%}(t) \right]$ no effects of the short term *random* variations ("the noise in model and observations) have yet been included. This will be the issue of the next section, and will lead to a procedure for the estimation of so called *prediction* intervals.

B.2.7 Prediction intervals

The *confidence* intervals $\left[\Phi_{2.5\%}(t), \Phi_{97.5\%}(t)\right]$ considered in the preceding section essentially describe the accuracy of (or uncertainty in) the response, $\Phi\left(t \mid \hat{\Theta}\right)$, of the deterministic model component $\Phi\left(\cdot \mid \hat{\Theta}\right)$. In case of a perfect model, and when an infinitely large data set $\left\{ \hat{Z}_{t_k} \right\}_{k=1}^{K}$ is available for calibration, the uncertainty in $\Phi\left(t \mid \hat{\Theta}\right)$ can be made arbitrary small. This does not mean, however, that new observations can be predicted with arbitrary precision as well. This is due to the remaining observation (and/or non-resolved model) errors, which are represented here by the random noise V_t in the model of Equation B.1: $Z_t = \Phi\left(t \mid \vec{\Theta}\right) + V_t$. This equation shows that the uncertainty in the prediction of an observation Z_t is at least as large as the "magnitude" of the noise. In practice when because of small data sets the deterministic component $\Phi\left(t \mid \hat{\Theta}\right)$ is 'merely' known with limited accuracy, the uncertainty in a prediction Z_t of an observation will inevitably be larger.
Prediction intervals (of some confidence level γ, e.g. $\gamma = 95\%$) are a means to quantify the accuracy with which such an observation Z_t can be predicted. In the construction of prediction intervals the uncertainty in both the calibrated model $\Phi\left(t \mid \hat{\Theta}\right)$ (represented by e.g. a confidence interval, see Section B.2.6) and spread of the observation noise V_t (here assumed to be a zero mean white Gaussian random process) must appropriately be accounted. The set $\left\{\hat{\Theta}^{(\ell)}\right\}_{\ell=1}^{L}$ of parameter estimates found in a resampling based calibration procedure forms again a highly convenient foundation for a quantitative and statistically well based assessment of (skew !) prediction intervals. Actually, for the 95% prediction interval $\left[Z_{2.5\%}(t),\, Z_{97.5\%}(t)\right]$ the cumulative distribution function $F_{Z_t}(\cdot)$ of Z_t is computed from the resampled models $\Phi\left(t \mid \hat{\Theta}^{(\ell)}\right)$ and corresponding resampled spreads $\hat{\sigma}_V^{(\ell)}$ of the noise V_t. The lower bound $Z_{2.5\%}(t)$ of the 95% (*skew*) prediction interval is then the z that satisfies $F_{Z_t}(z) = 0.025$ (i.e. the 2.5% quantile of the distribution) while similarly the upper bound corresponds to the 97.5% quantile.
For the interpretation of the 95% prediction interval $\left[Z_{2.5\%}(t),\, Z_{97.5\%}(t)\right]$ it must be realised that in a model hindcast or forecast (on the average) 95% of the available observations $\hat{Z}_{t_k}$ are expected to be within the prediction interval.

C Density probability functions

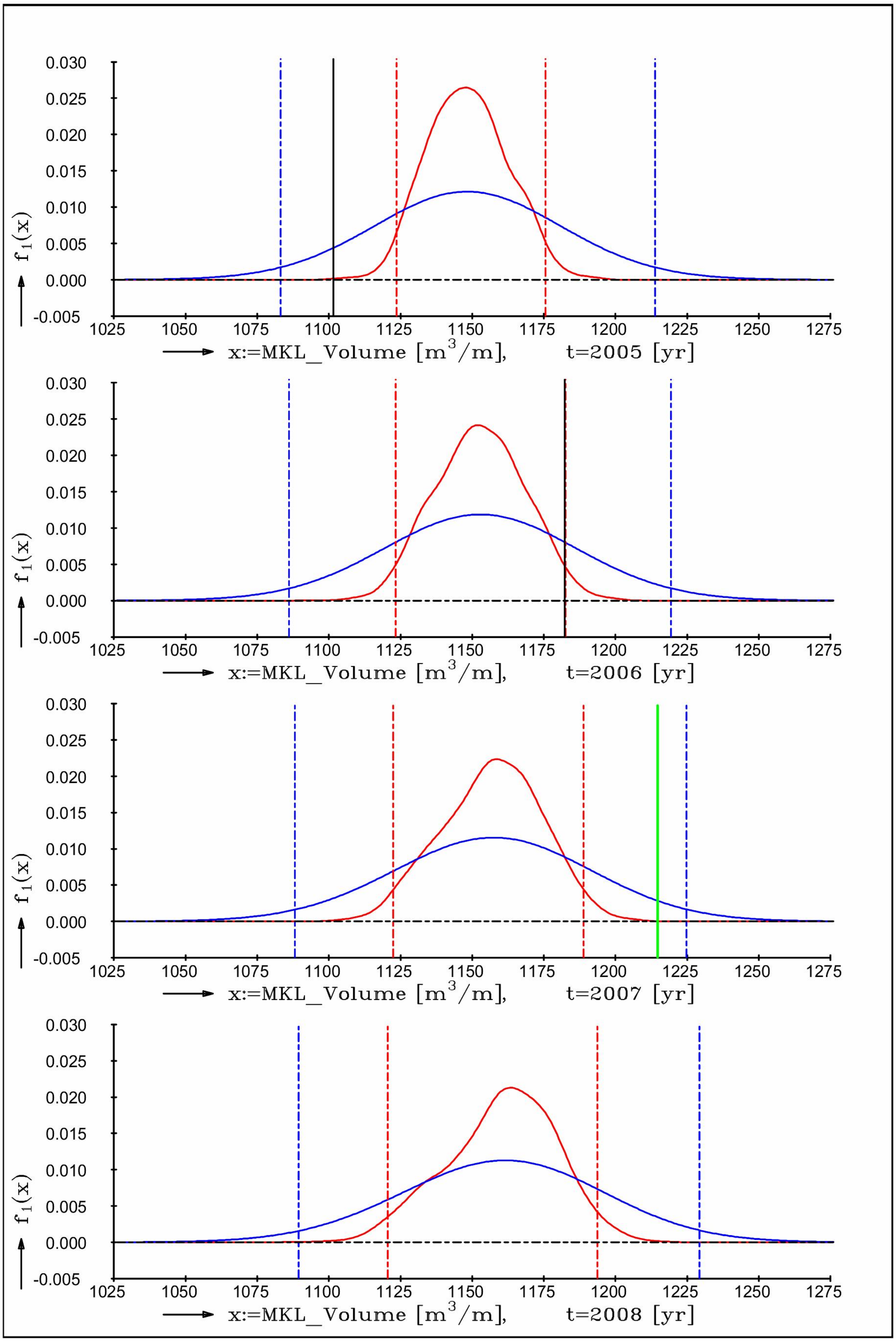

Figure C.1 MCL volume: Density probability functions of the predictions (solid red line for the deterministic part, and solid blue line when including stochastic part), for years 2005, 2006 (hindcasting), and 2007 and 2008 (forecasting); red and blue dashed lines display the limits of the confidence and prediction intervals, respectively; solid black and green lines define the observations.

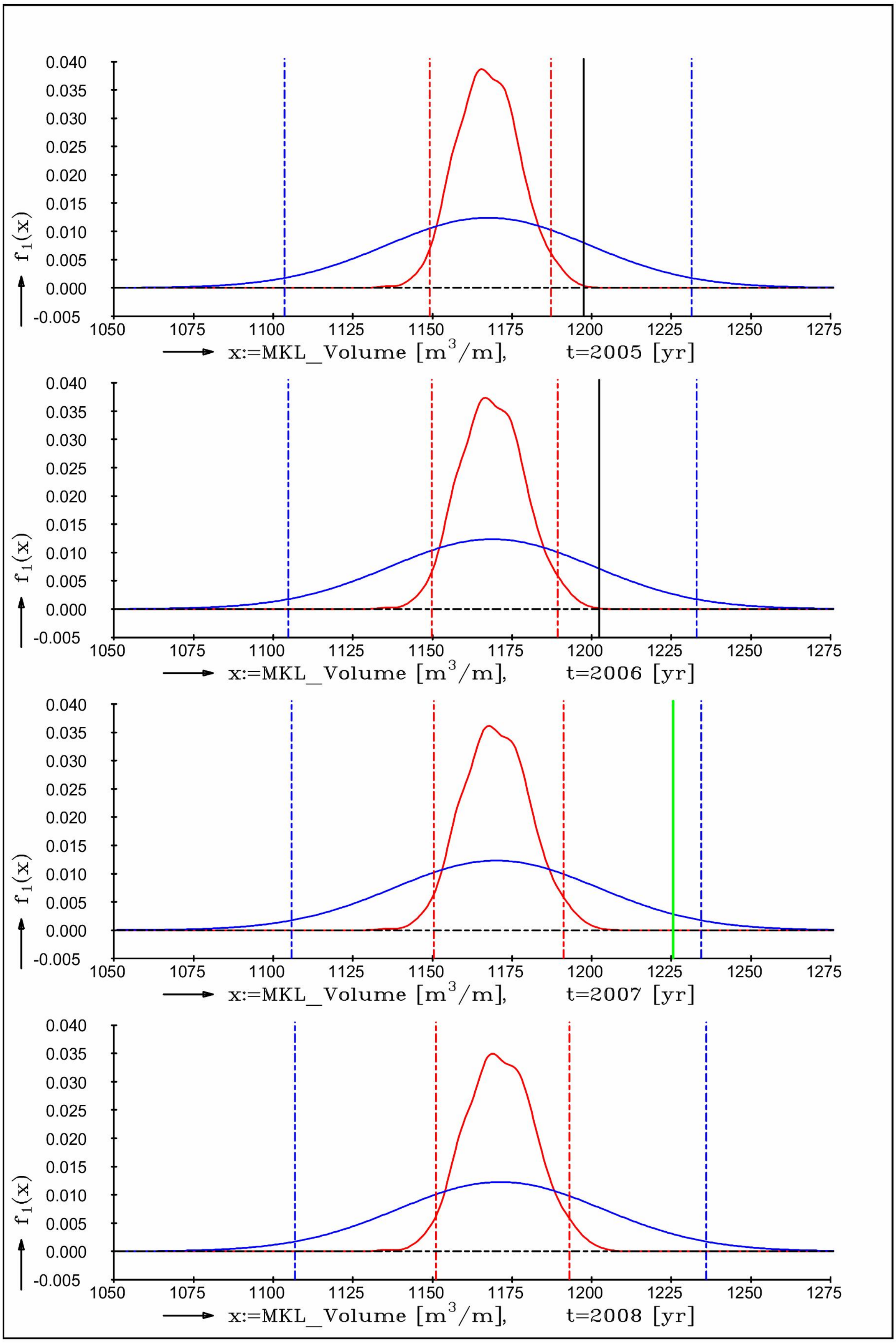

Figure C.2 MCL volume: Density probability functions of the predictions (solid red line for the deterministic part, and solid blue line when including stochastic part), for years 2005, 2006 (hindcasting), and 2007 and 2008 (forecasting); red and blue dashed lines display the limits of the confidence and prediction intervals, respectively; solid black and green lines define the observations.

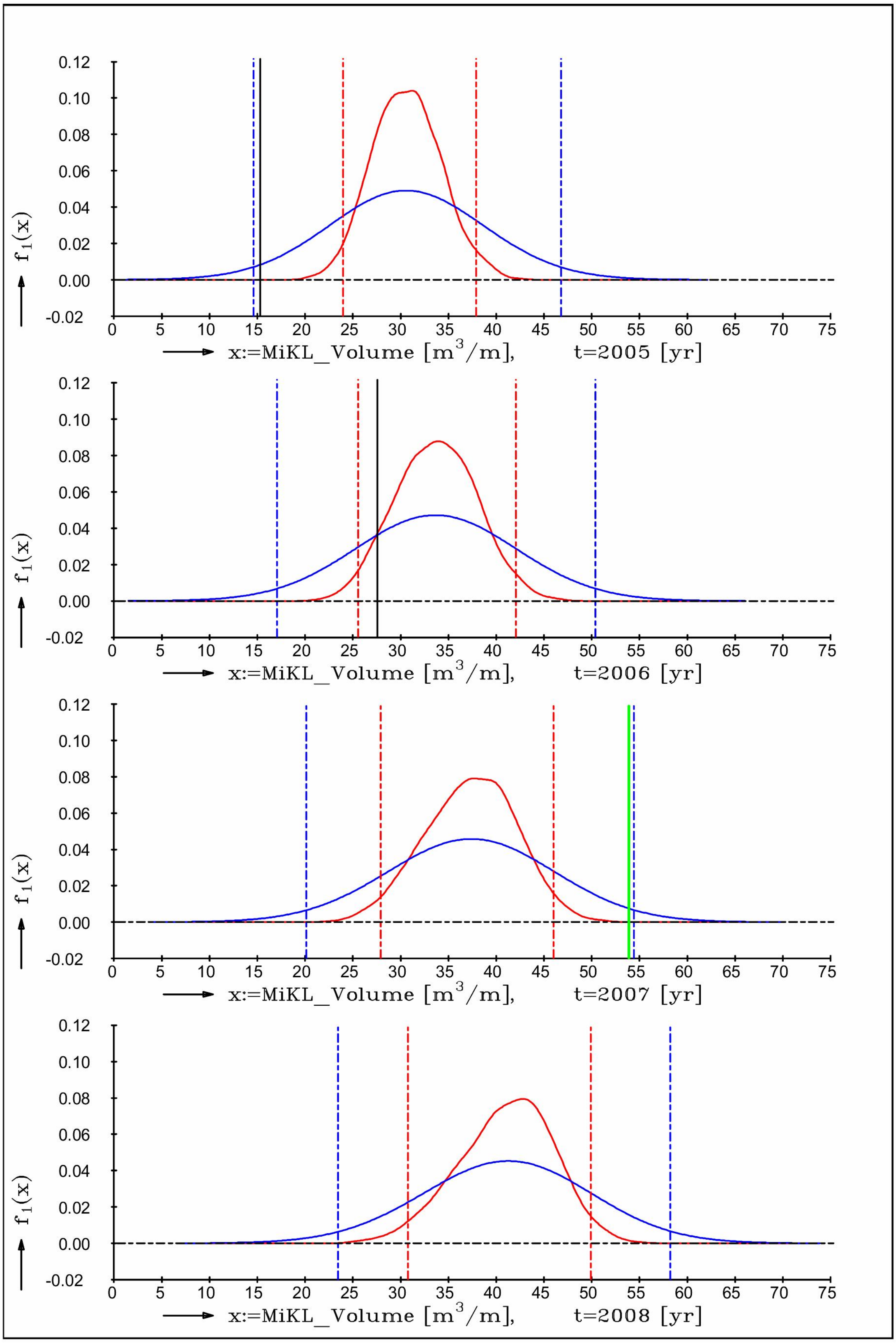

Figure C.3 MiCL volume: Density probability functions of the predictions (solid red line for the deterministic part, and solid blue line when including stochastic part), for years 2005, 2006 (hindcasting), and 2007 and 2008 (forecasting); red and blue dashed lines display the limits of the confidence and prediction intervals, respectively; solid black and green lines define the observations.

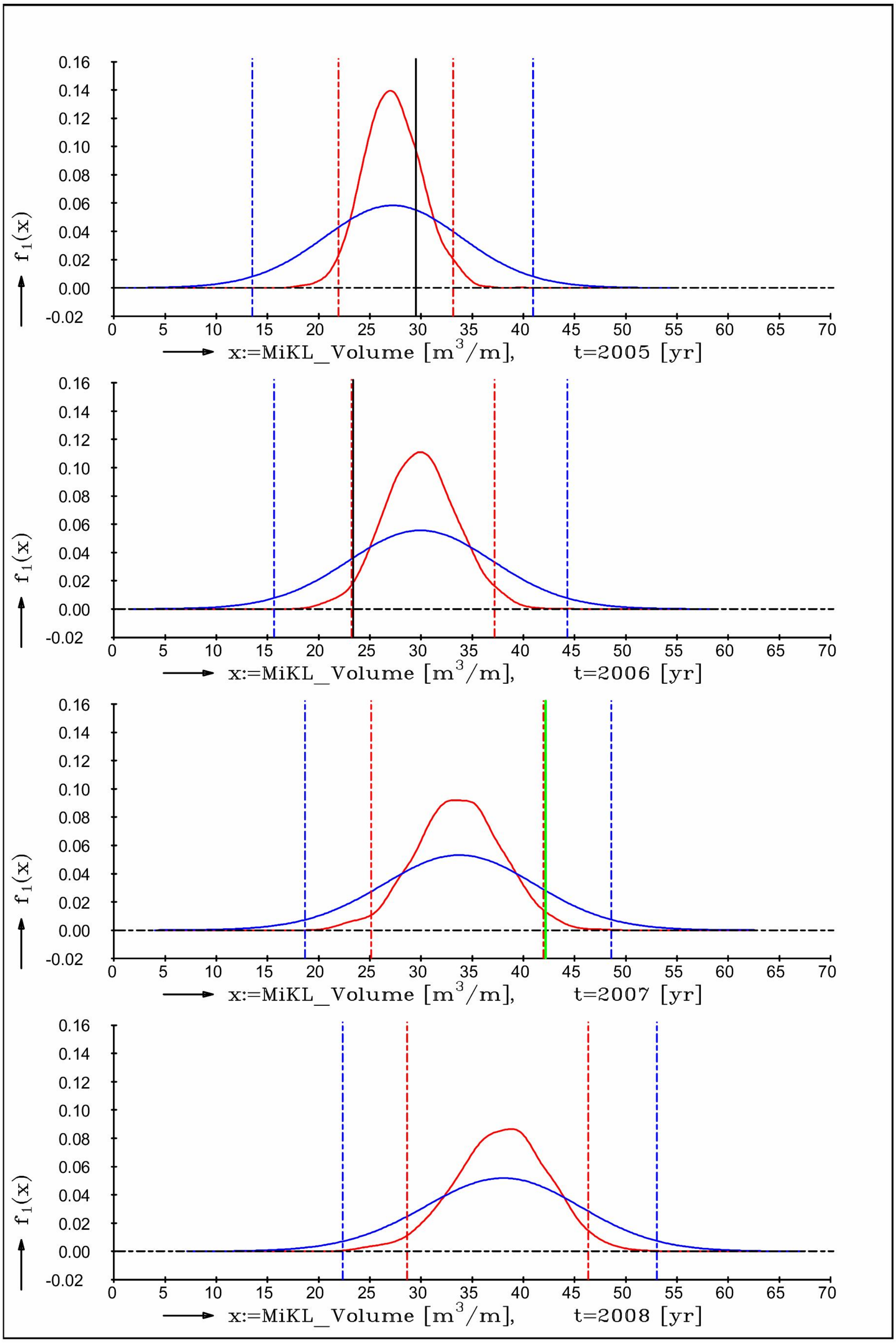

Figure C.4 MiCL volume: Density probability functions of the predictions (solid red line for the deterministic part, and solid blue line when including stochastic part), for years 2005, 2006 (hindcasting), and 2007 and 2008 (forecasting); red and blue dashed lines display the limits of the confidence and prediction intervals, respectively; solid black and green lines define the observations before and after the installation of the Ecobeach technique, respectively.

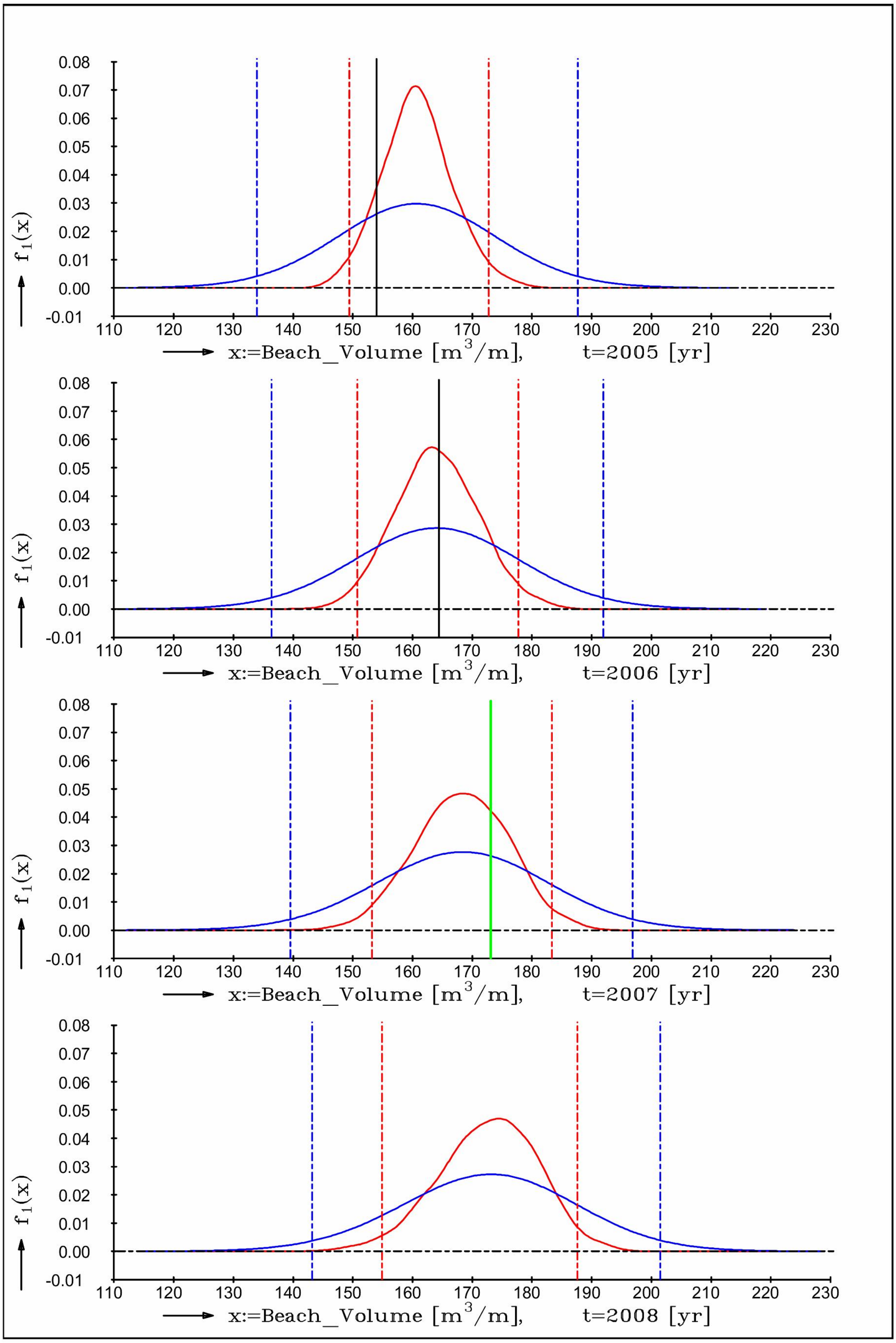

Figure C.5 Beach volume: Density probability functions of the predictions (solid red line for the deterministic part, and solid blue line when including stochastic part), for years 2005, 2006 (hindcasting), and 2007 and 2008 (forecasting); red and blue dashed lines display the limits of the confidence and prediction intervals, respectively; solid black and green lines define the observations.

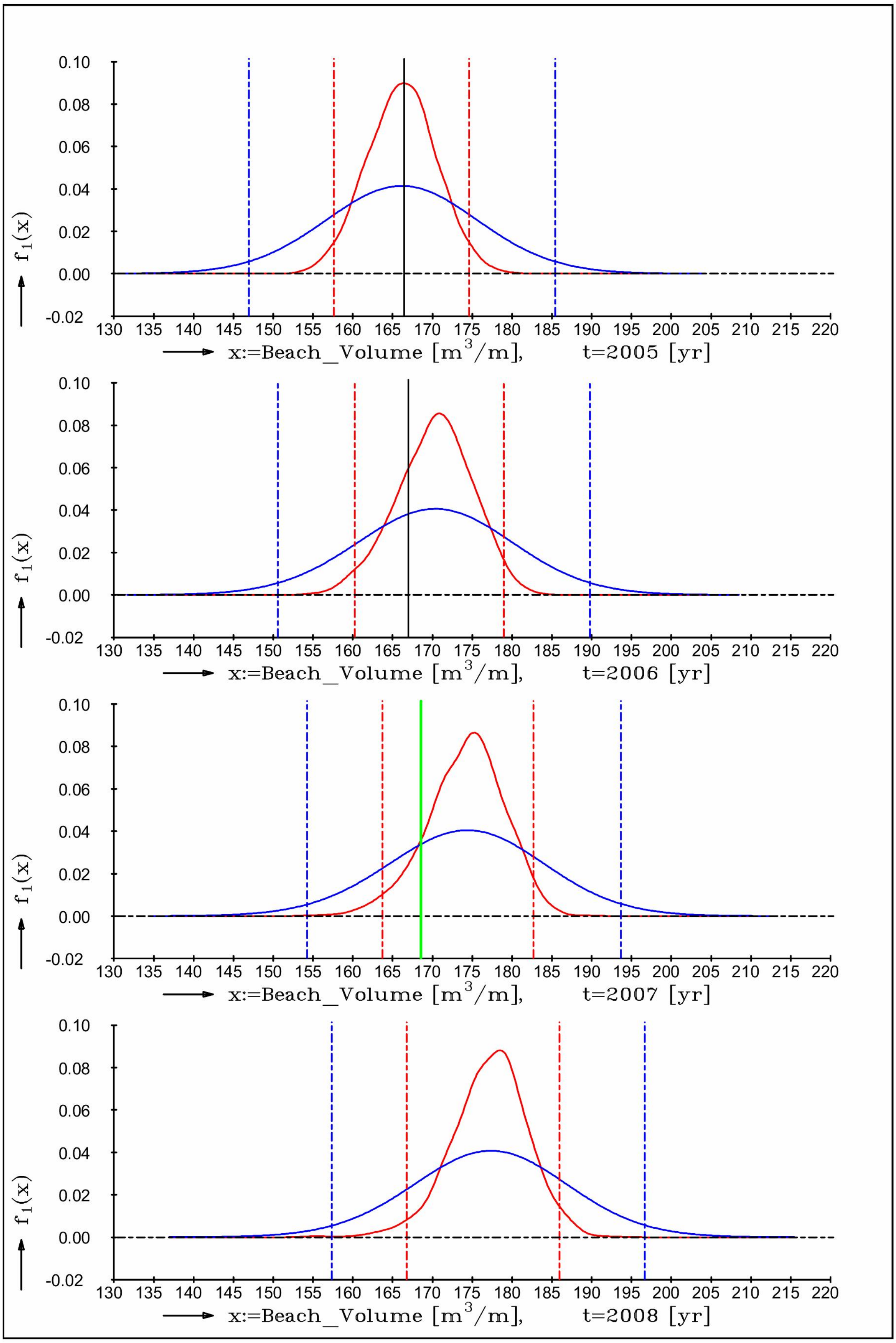

Figure C.6 Beach volume: Density probability functions of the predictions (solid red line for the deterministic part, and solid blue line when including stochastic part), for years 2005, 2006 (hindcasting), and 2007 and 2008 (forecasting); red and blue dashed lines display the limits of the confidence and prediction intervals, respectively; solid black and green lines define the observations.

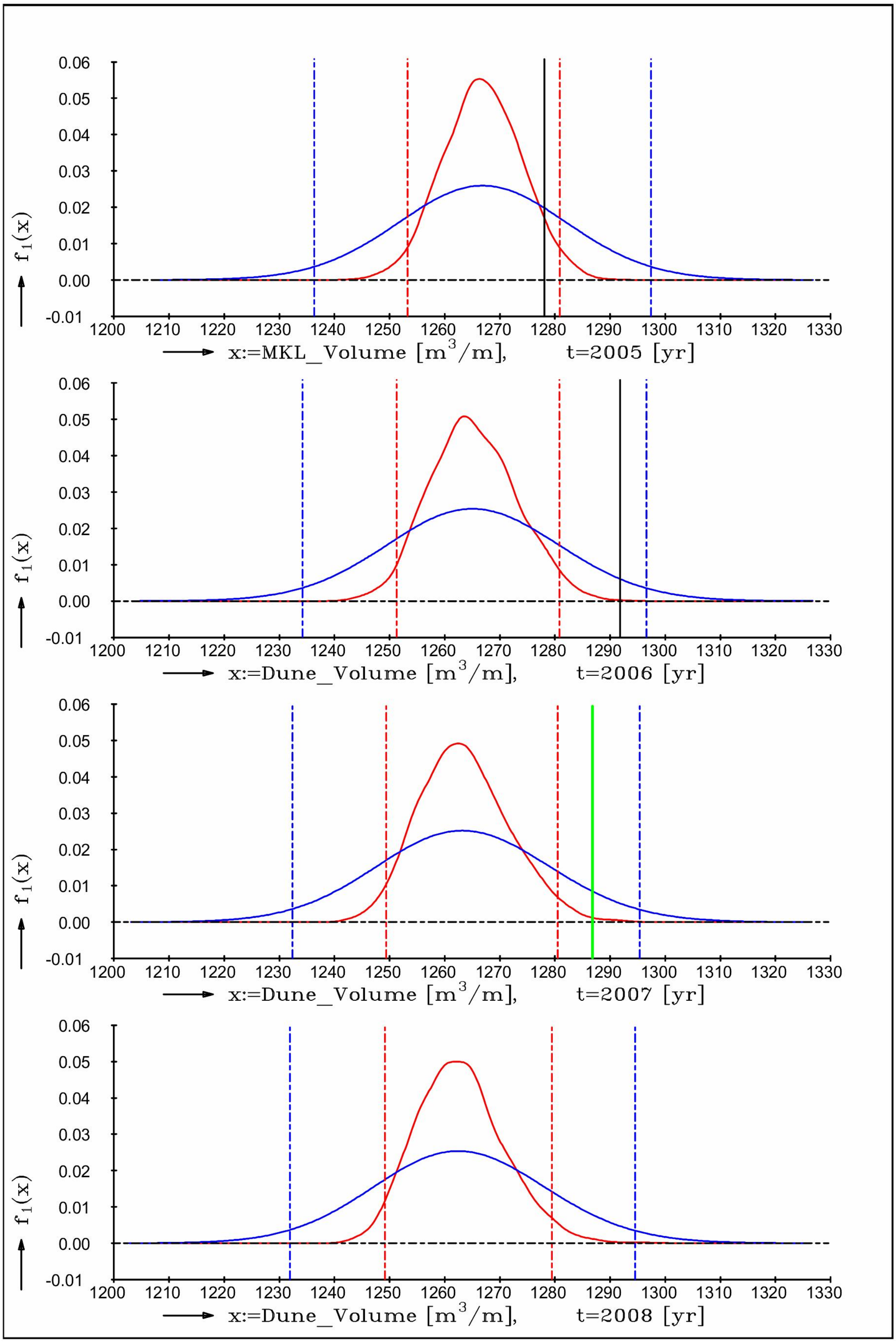

Figure C.7 Dune volume: Density probability functions of the predictions (solid red line for the deterministic part, and solid blue line when including stochastic part), for years 2005, 2006 (hindcasting), and 2007 and 2008 (forecasting); red and blue dashed lines display the limits of the confidence and prediction intervals, respectively; solid black and green lines define the observations before.and after the installation of the Ecobeach modules, respectively.

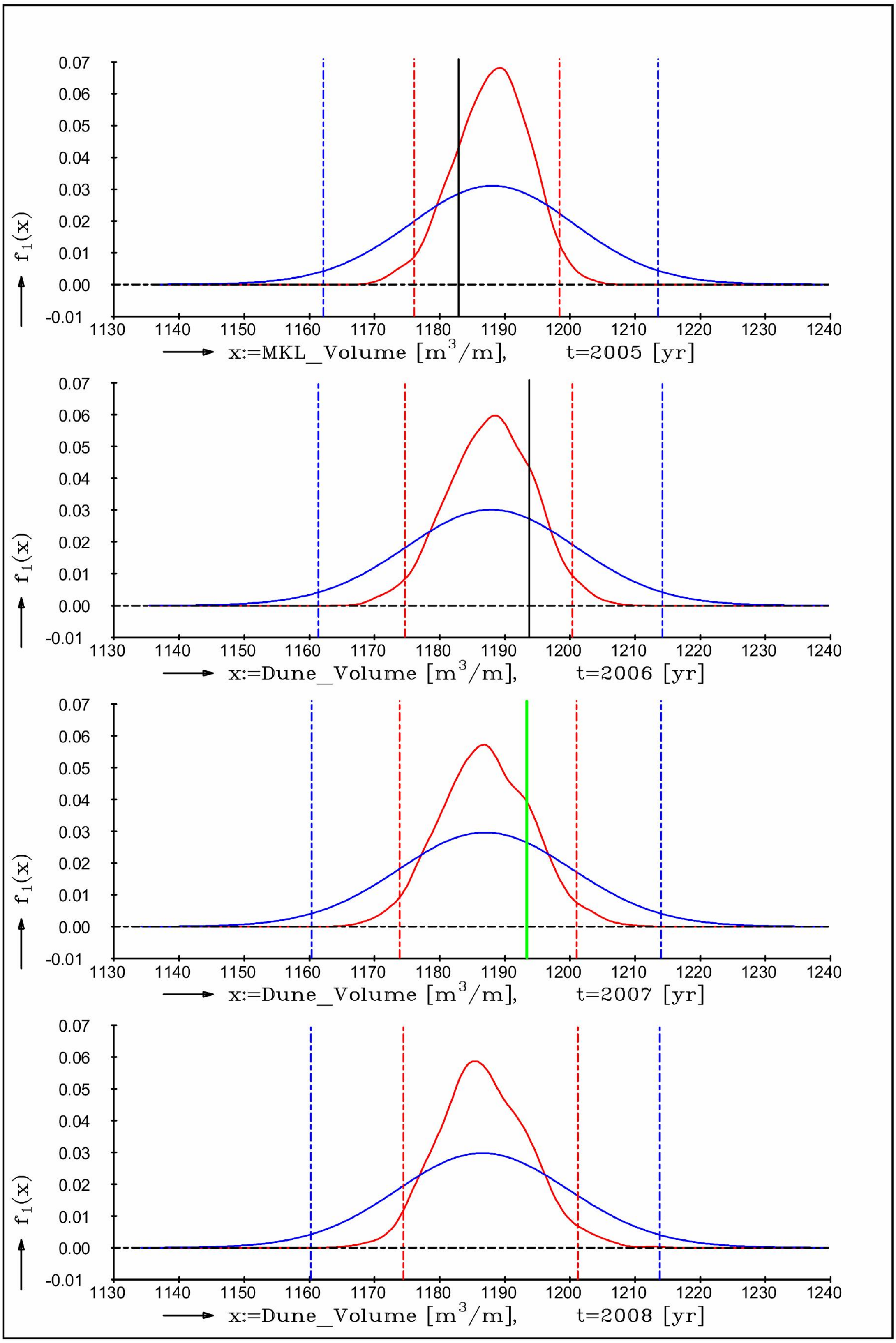

Figure C.8 Dune volume: Density probability functions of the predictions (solid red line for the deterministic part, and solid blue line when including stochastic part), for years 2005, 2006 (hindcasting), and 2007 and 2008 (forecasting); red and blue dashed lines display the limits of the confidence and prediction intervals, respectively; solid black and green lines define the observations before.and after the installation of the Ecobeach modules, respectively.

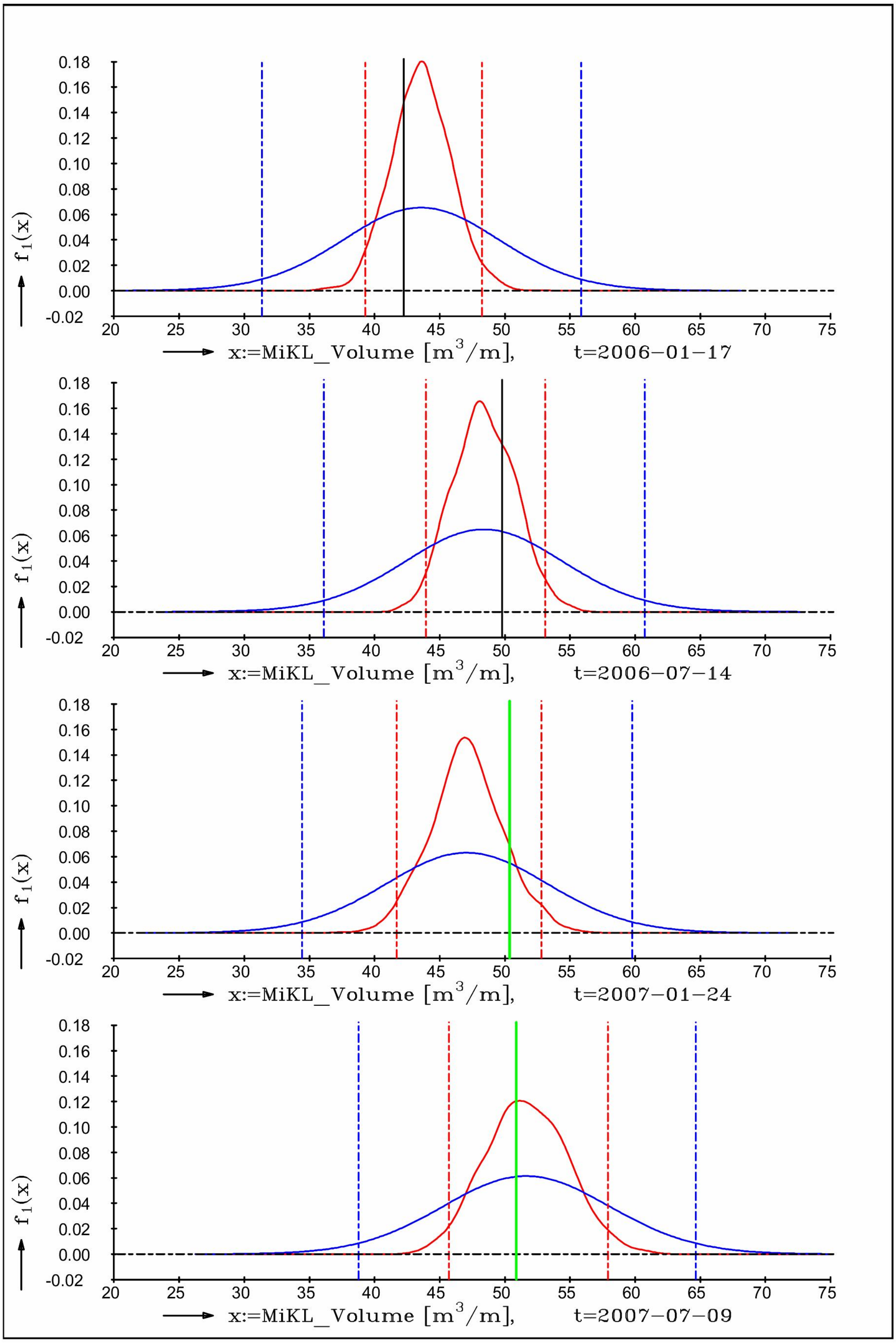

Figure C.9 MiCL volume: Density probability functions of the predictions (solid red line for the deterministic part, and solid blue line when including stochastic part), for year 2006 (including data in the model), and 2007 (excluding data in the model); red and blue dashed lines display the limits of the confidence and prediction intervals, respectively; solid black and green lines define the observations.

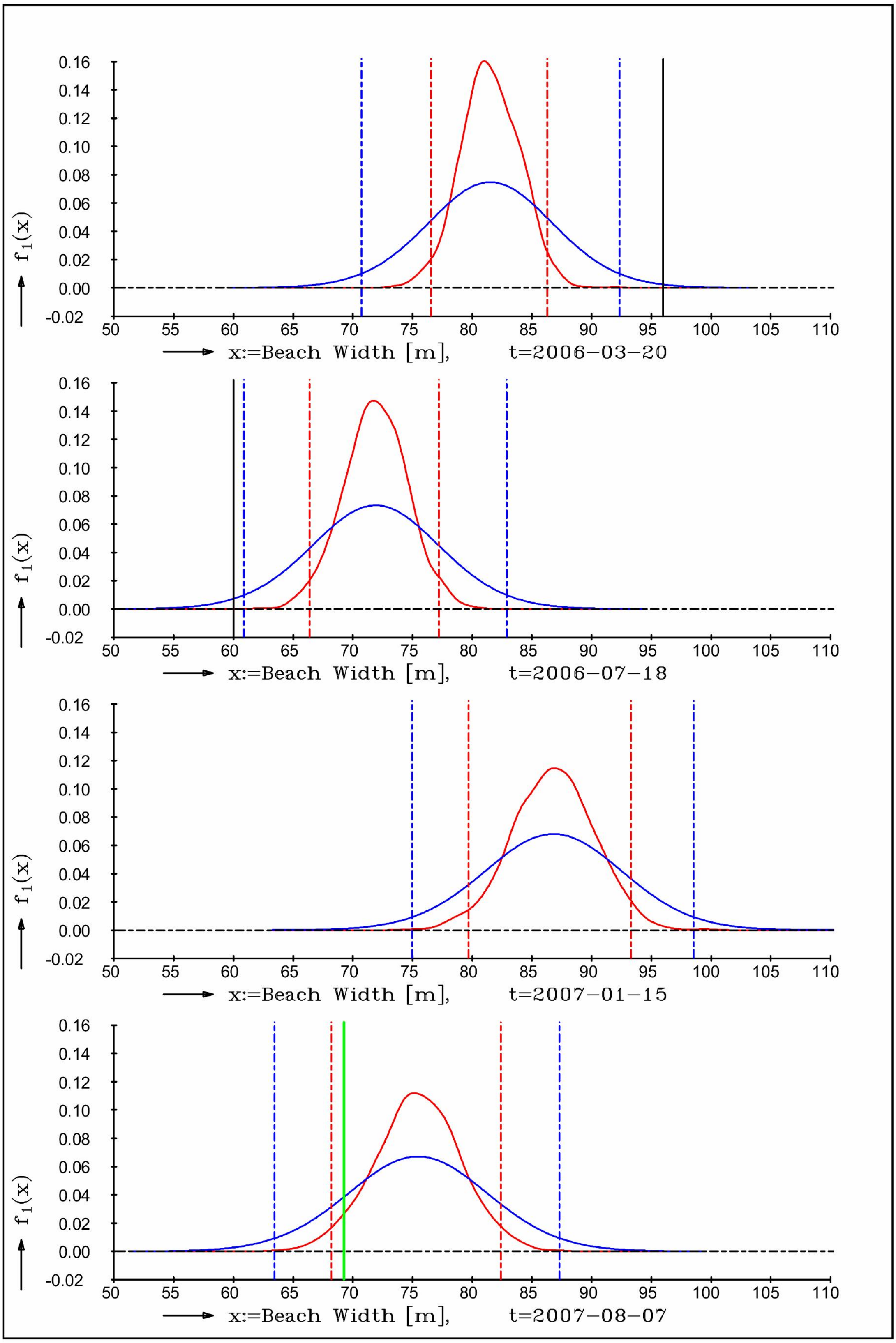

Figure C.10 Beach width: Density probability functions of the predictions (solid red line for the deterministic part, and solid blue line when including stochastic part), for year 2006 (including data in the model), and 2007 (excluding data in the model); red and blue dashed lines display the limits of the confidence and prediction intervals, respectively; solid black and green lines define the observations.

D Dunes dynamics

Visual description of the test and reference areas

profile	visual description of the area
40.00	former cliff; lower part bare; embryonic dunes
40.25	former cliff; lower part bare; embryonic dunes just to the north
40.50	lower cliff; just north active blowout in foredunes; beach houses
40.75	former cliff with slumping features
41.00	former cliff
41.25	former (small) cliff; active aeolian deposition at crest
41.50	established embryonic dunes; in slope active aeolian processes
41.75	vegetated slope, front part bare; embryonic dunes, in 2006 eroded
42.00	vegeated slope, front part bare; embryonic dunes
42.25	vegetated slope; front part bare; scattered embryonic dunes (closed in 2006)
42.50	former cliff, mostly vegetated; embryonic dunes in 2006
42.75	former cliff, just south from beach acces; recreation
43.00	former cliff, vegetated
43.25	former cliff, vegetated; at front bare zone and large, active, embryonic dunes, in 2006 eroded
43.50	former cliff, vegetated; at front wide zone with active embryonic dunes
43.75	just norht of beach access and restaurant; former cliff, vegetetad; front zone with embryonic dunes; in 2006 beach houses
44.00	former cliff, mostly vegetated; scattered embryonic dunes; recreation
44.25	former cliff, mostly vegetated; at front beach houses
44.50	fomer small cliff; at front beach houses
44.75	former small cliff; at front beach houses; large beach access in south
45.00	former cliff, vegetated; at front beach houses
45.25	former cliff, mostly vegetated; recreation; aeolian activiy, small embryonic dunes; at front beach houses
45.50	former cliff, vegetated; at front wide zone with embryonic dunes
45.75	former cliff, mostly vegetated; at front wide zone with embryonic dunes
46.00	former cliff, vegetated; at front wide bare zone and embryonic dunes

datasets

40.00 – 43.00
- AHN 2007
- Jarkus data 2007

43.00 – 46.00
- AHN 1997-2007
- Jarkus data 1965-2007

Volume calculations (method)

Jarkus

Jarkus data are derived from interpolation of the AHN data. The data consist of heights versus distance from RSP, with steps of 5m). The jarkus profile data are used for volume calculations of cross sections through the foredunes. The method of calculation is illustrated by Figure D.1. For each year the same length of transect is used. If data were missing (mostly in the landward part of the transect) they were supplemented with data from the closest year. For each transect and year the total volume above 3m NAP is calculated. For consecutive years, differences in volumes are calculated. There was an error in the calculations presented in the previous report. The data are corrected for all profiles.

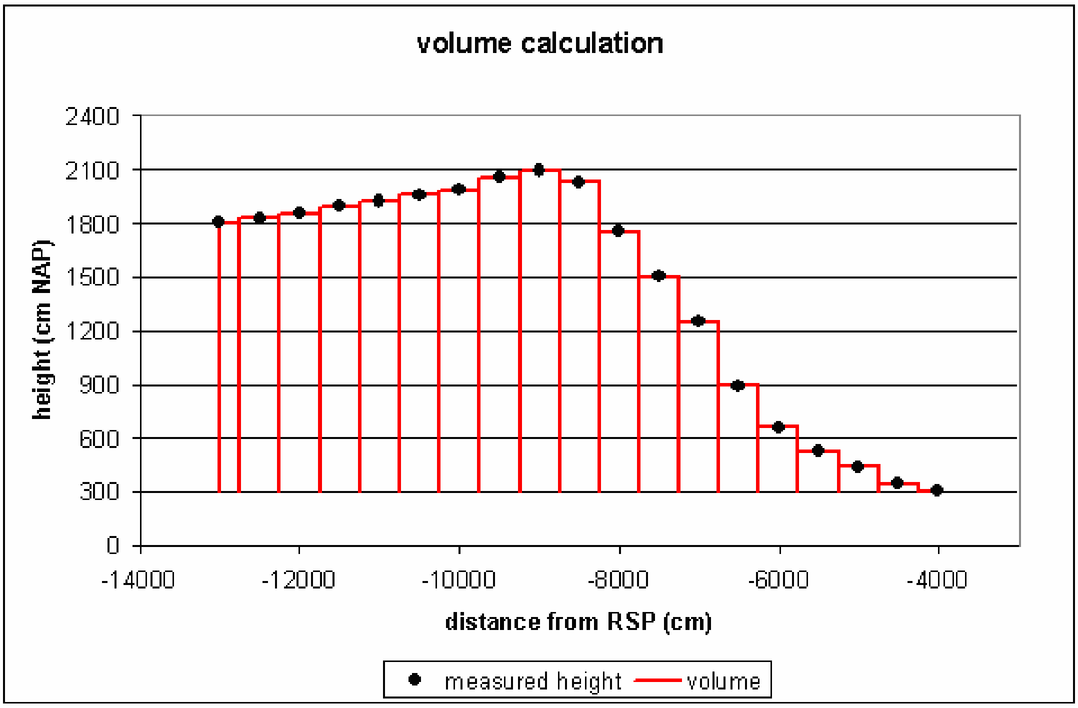

Figure D.1 Volume calculation

AHN

With the AHN data volumes are calculated (with 3D Analyst in ArcView) for areas in between the Jarkus profiles.

Comparison AHN and Jarkus data

The volumes calculated from AHN data for the areas in between Jarkus profiles are compared with the average values of the two profiles that border an area. In Figure D.2 and Figure D.3, 40.000 represents the area between 40.000 and 40.250 etc. Two Jarkus profiles represent 4% of the total AHN data for an area (250m wide, 5x5m^2 pixels).

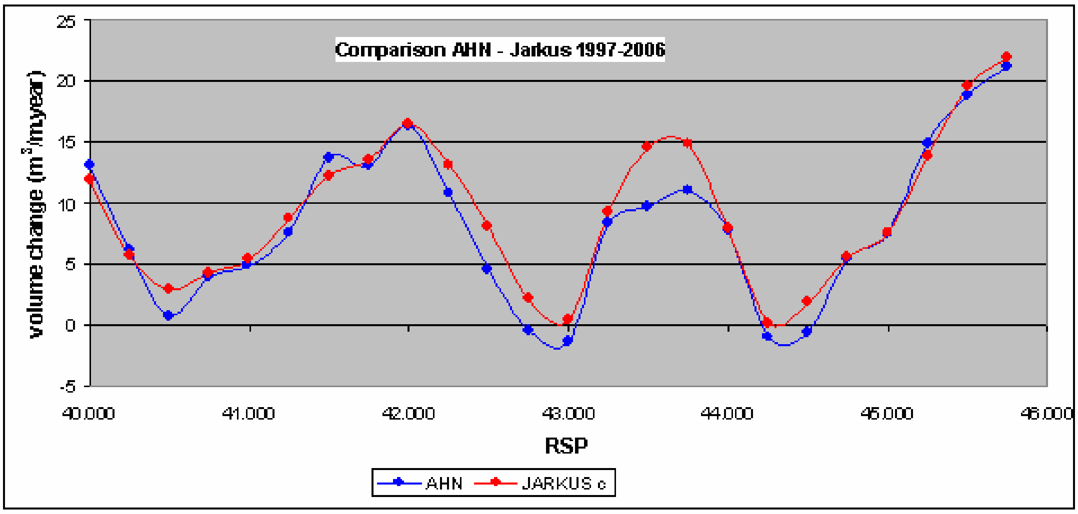

Figure D.2 Comparison AHN-Jarkus 1997-2006

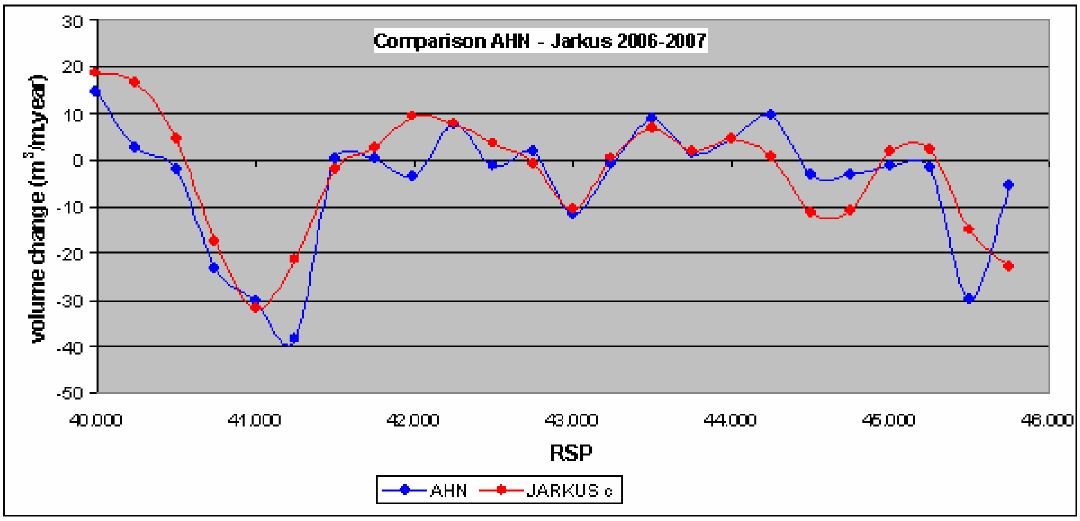

Figure D.3 Comparison AHN-Jarkus 2006-2007

As expected, the representativity of the Jarkus profiles for a larger area increases when the length of the study period extends. The source of information for both Jarkus and AHN is the same, so with perfect representativity the volumes for Jarkus and AHN would be exactly the same. Figure D.4 points out that over the period 1997-2006 the differences between Jarkus and AHN based volumes are much less than over the period 2006-2007.

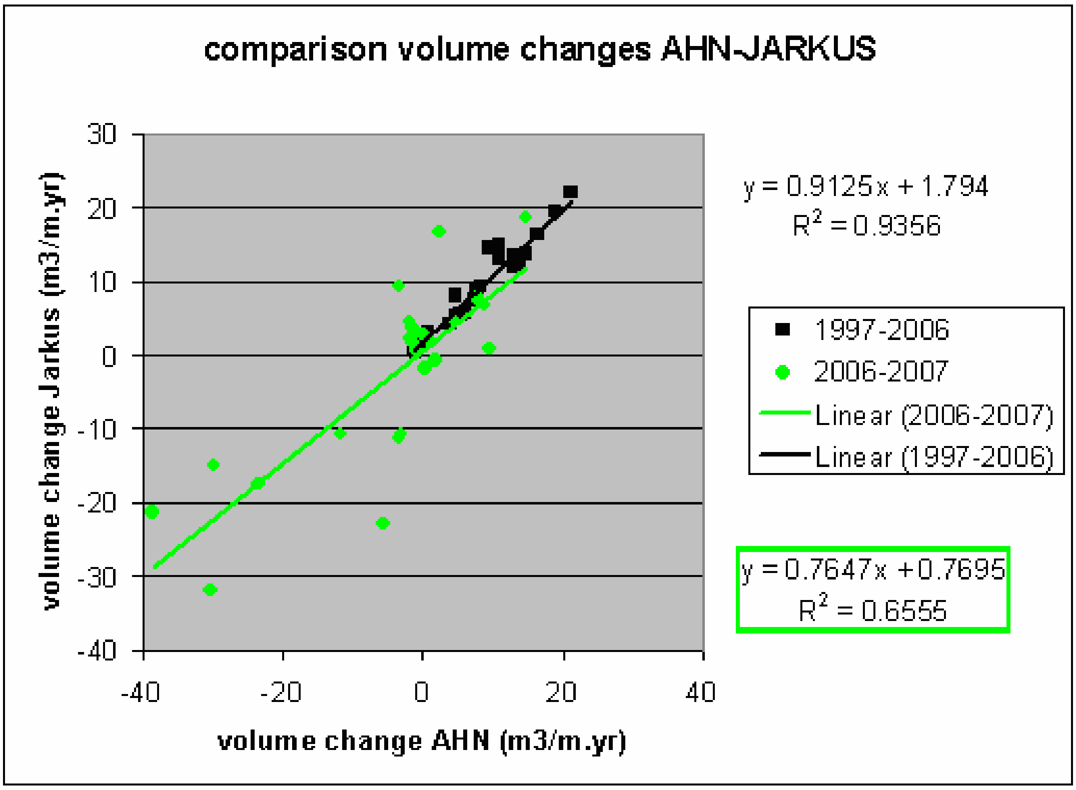

Figure D.4 Comparison of volume changes AHN-Jarkus

Long-term description

On the long term, there is a trend of accretion in the dunes. With the inclusion of the 2007 data, all profiles in both the study area (above) and the reference area (below), except 40.25 in the northern part of the study area, show increasing volumes. This does not necessarily correlate to long term dunefoot migration. Profile 40.25 is the only profile where dunefoot retreat coincides with a volume loss. Profiles 40.50, 40.75, 43.00, 43.25, 43.50, 43.75 and 44.00 all show dunefoot retreat and a gain in volume, which implies that the height of the foredune is changing, probably as a result of aeolian erosion of the dune front after scarping. A large gain in volume occurs between profiles 42.00 and 42.75 and in profile 46.00. In the study area, this coincides with the largest progression of the dunefoot, in the reference area it does not.

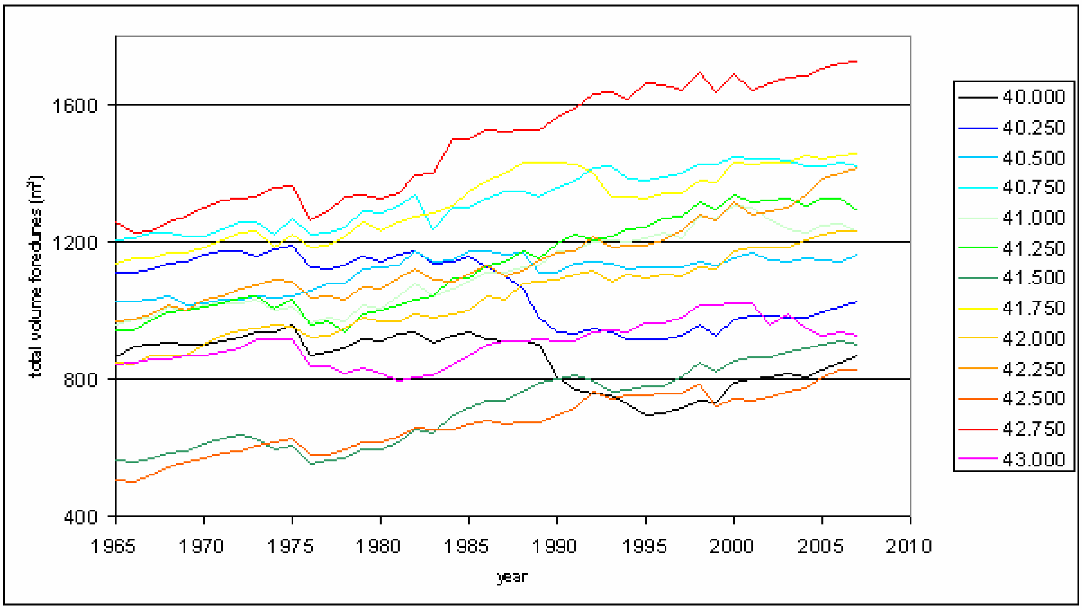

Figure D.5 Total volume of the foredunes in the test area

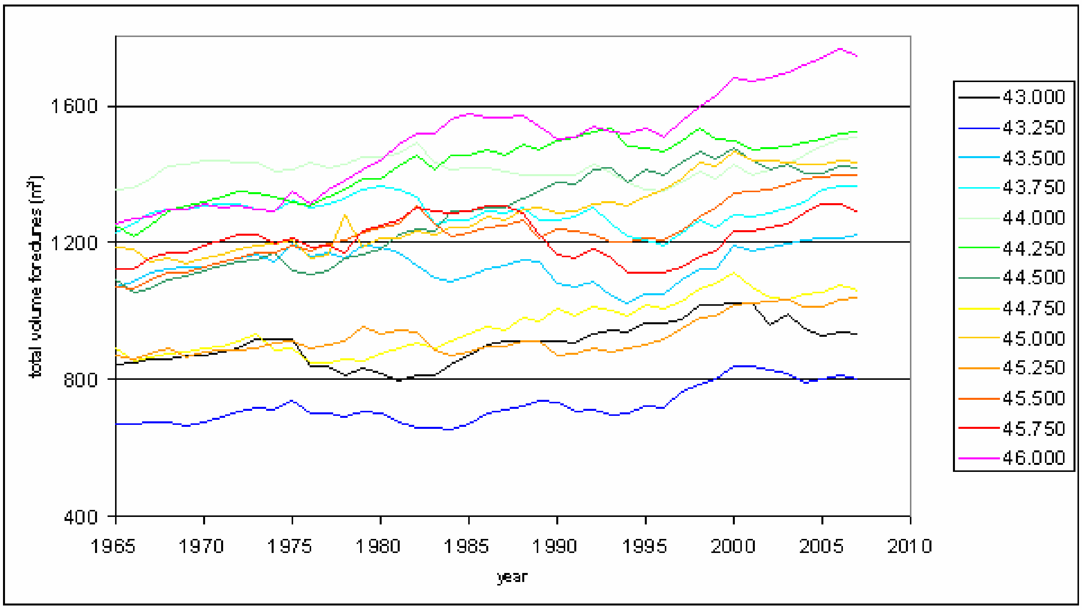

Figure D.6 Total volume of the foredunes in the reference area

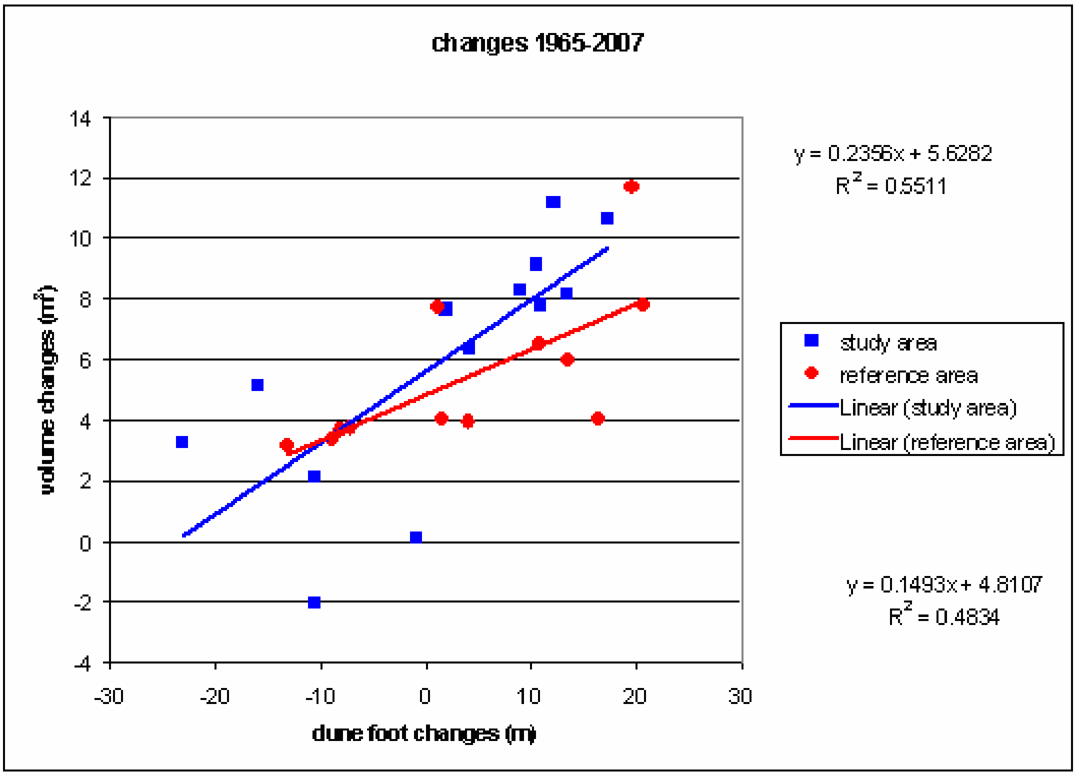

Figure D.7 Volume changes versus dune foot position changes between 1965 and 2007

Short-term-description

The laseraltimetry data of 1997, 1998, 1999, 2001, 2003 cover a large area, including foredunes and part of the inner dunes. The data of 2004, 2006 and 2007 only cover the foredunes up to crest. All laseraltimetry data show some errors due to spatial inaccuracy.

When looking at short term changes, over the period 1997-2006 and 2007 a different picture emerges. The northern profiles now show strong accretion for this period. The spatial variation in the short term is much larger, and also the absolute volume changes are larger. It is clear that, although general trends are clearly visible in the data, the yearly variation is huge. Yearly changes may vary between -100 and +120 m^3/m.year. The large negative numbers are possibly due to years with strong dune erosion. It is very likely that the large positive numbers are somehow related to measurement errors, especially when a year with a very large gain is preceded or succeeded by a large loss. Certainly this is true for profile 45.00 where a huge gain in 1978 is succeeded by a huge loss in 1979. It is very unlikely that volume changes larger than 50-70 m^3/m.year are due to natural aeolian processes, but also these quantities are very large although not impossible. Parts of the process of beach-foredune interaction are still not well understood, and it might be possible that our general concept of aeolian transport underestimates the extremes that may occur. After years with severe dune erosion, often a huge gain of sand at and above the dunefoot is observed (for example in profile 41, 2004-2005; profile 42.50, 1999-2000). This must be related to aeolian transport over the beach, leading to very strong deposition in front of the cliff.

Given the uncertainty in yearly volume changes, it is clear that for purposes of volume change analyses only trends over several years (at least 5) should be studied. Another possibility might be to put serious efforts in error analysis, and filter out any suspicious data.

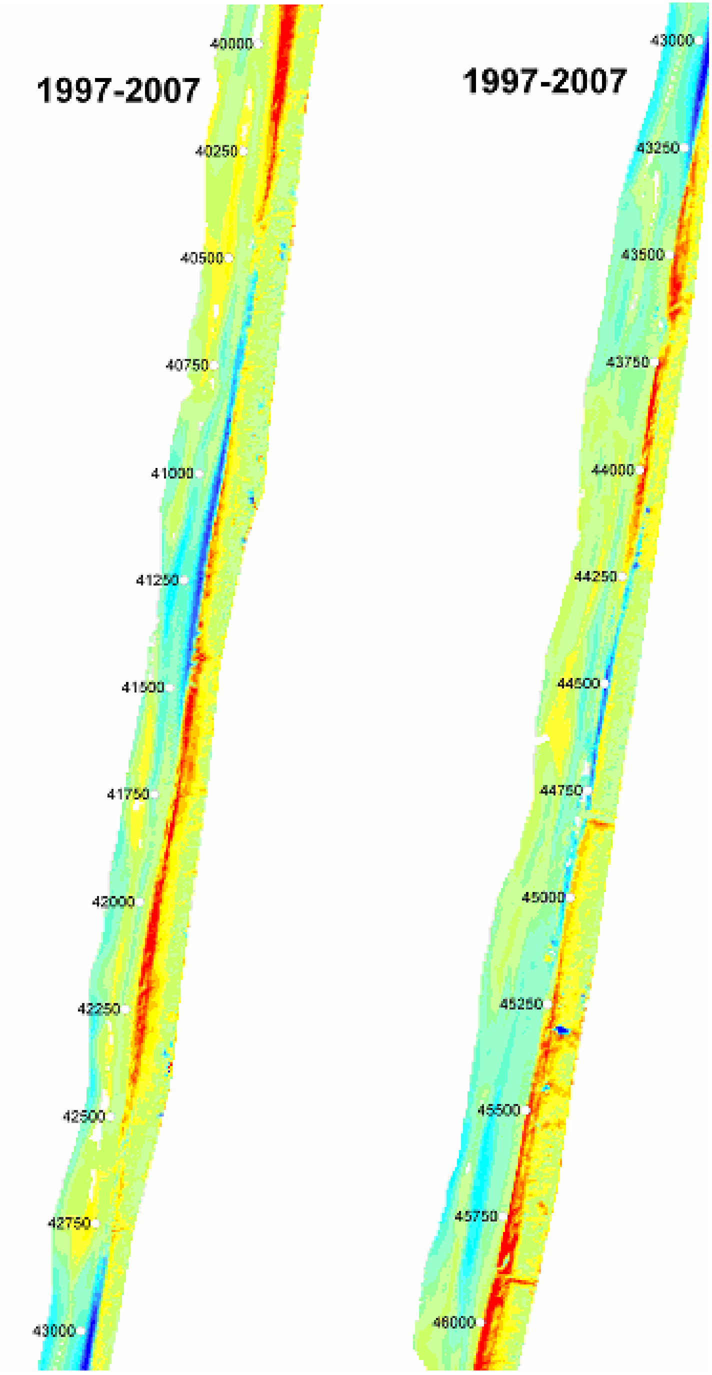

Figure D.8 Volume changes between 1997 and 2007. Scale: - 4 m (blue) to + 4 m (red). Left: test area, right: reference area.

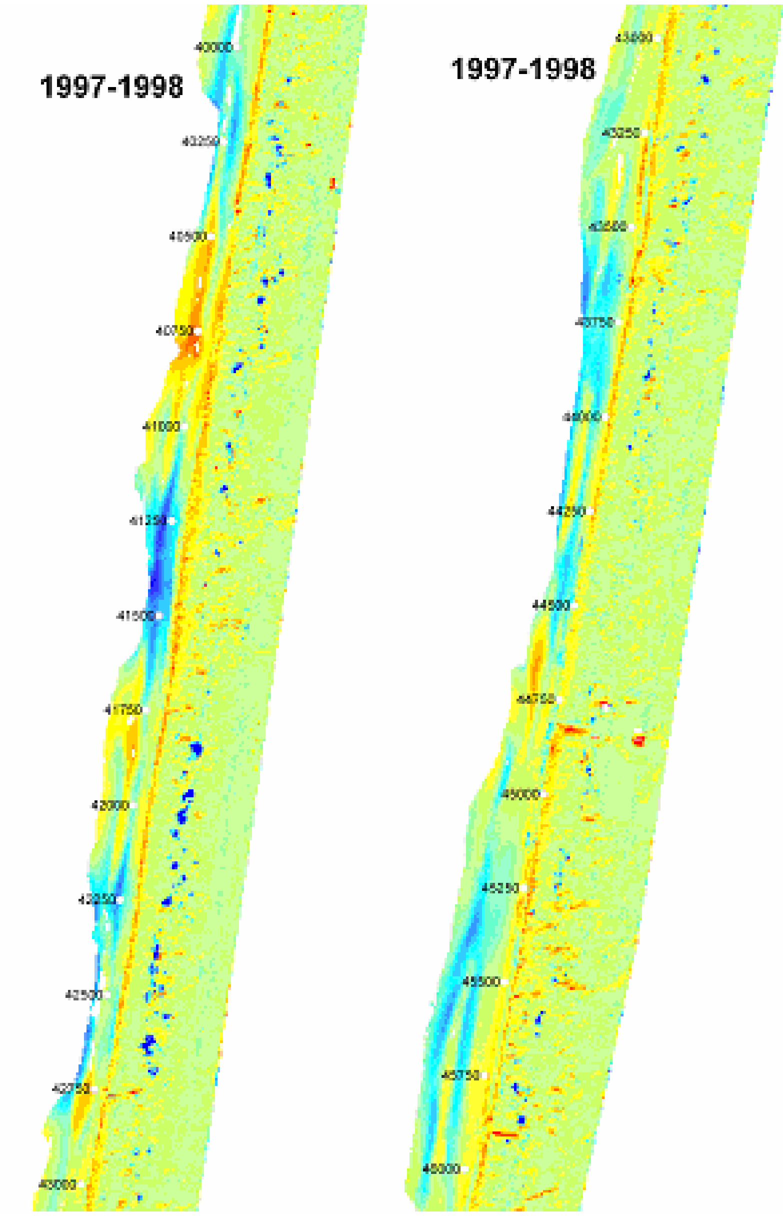

Figure D.9 Volume changes between 1997 and 1998. Scale: -2 m (blue) to + 2 m (red). Left: test area, right: reference area.

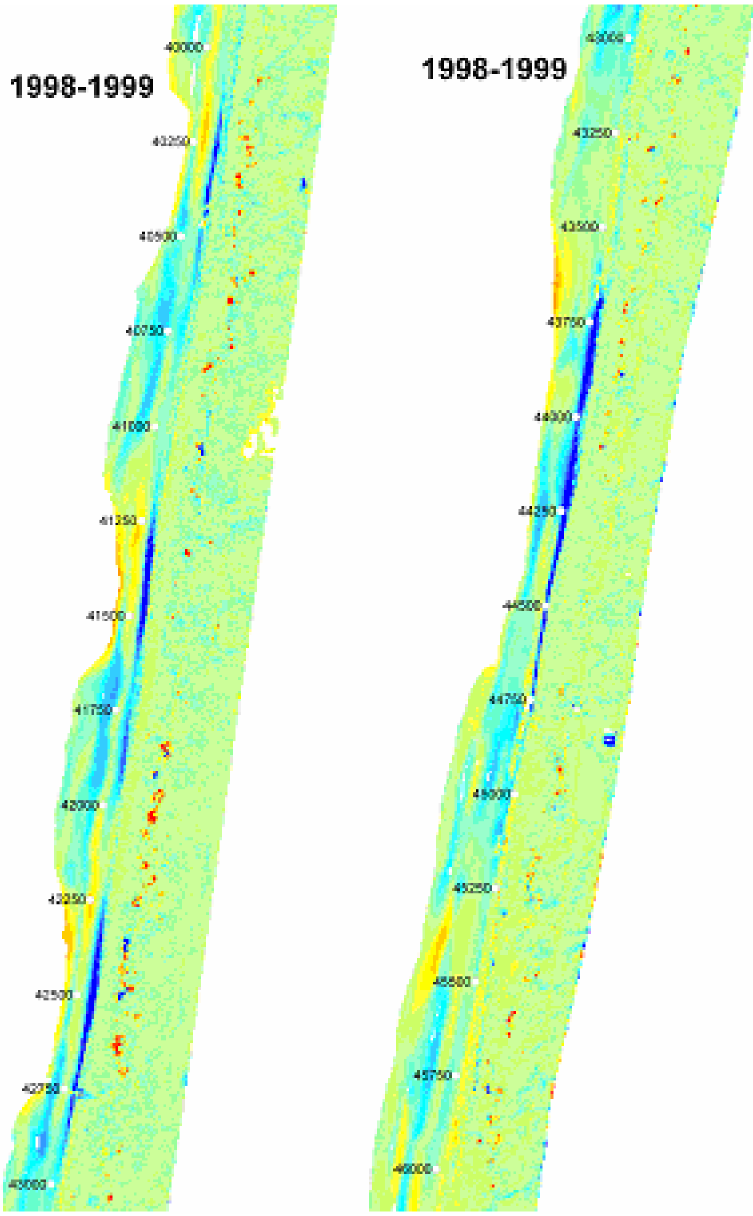

Figure D.10 Volume changes between 1998 and 1999. Scale: -2 m (blue) to + 2 m (red). Left: test area, right: reference area.

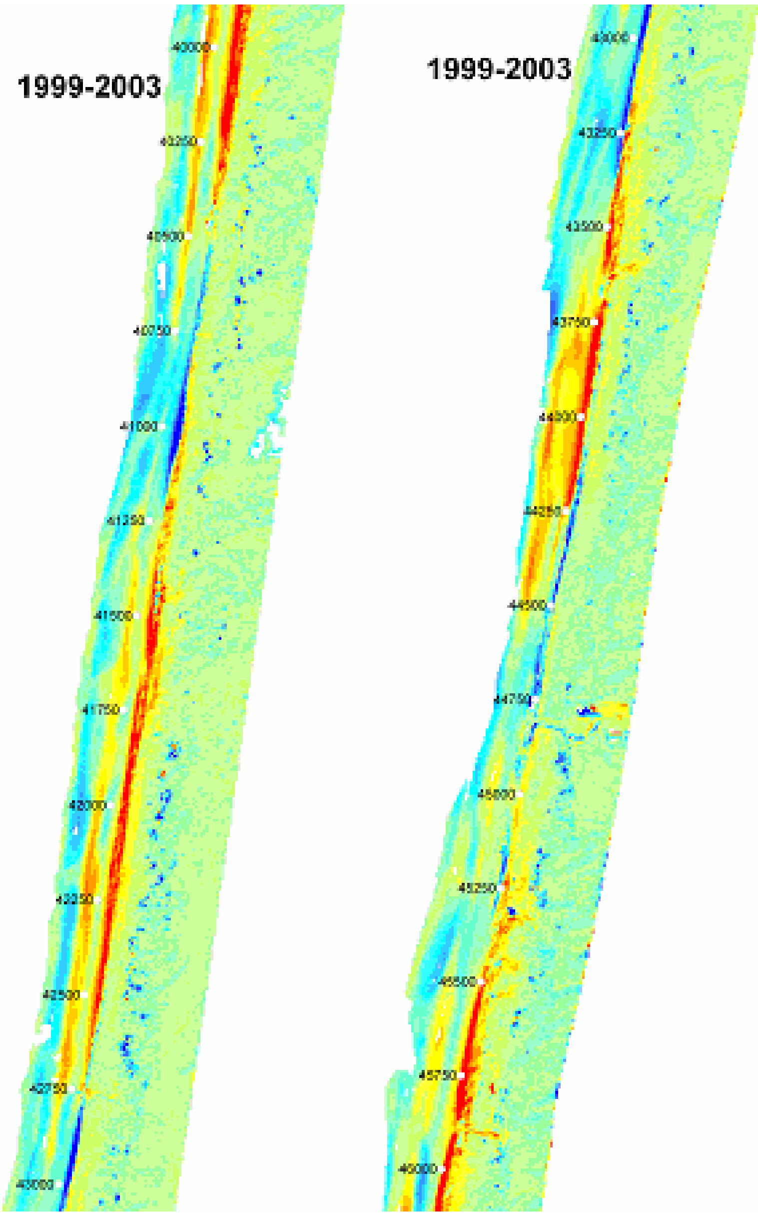

Figure D.11 Volume changes between 1999 and 2003. Scale: -2 m (blue) to + 2 m (red). Left: test area, right: reference area.

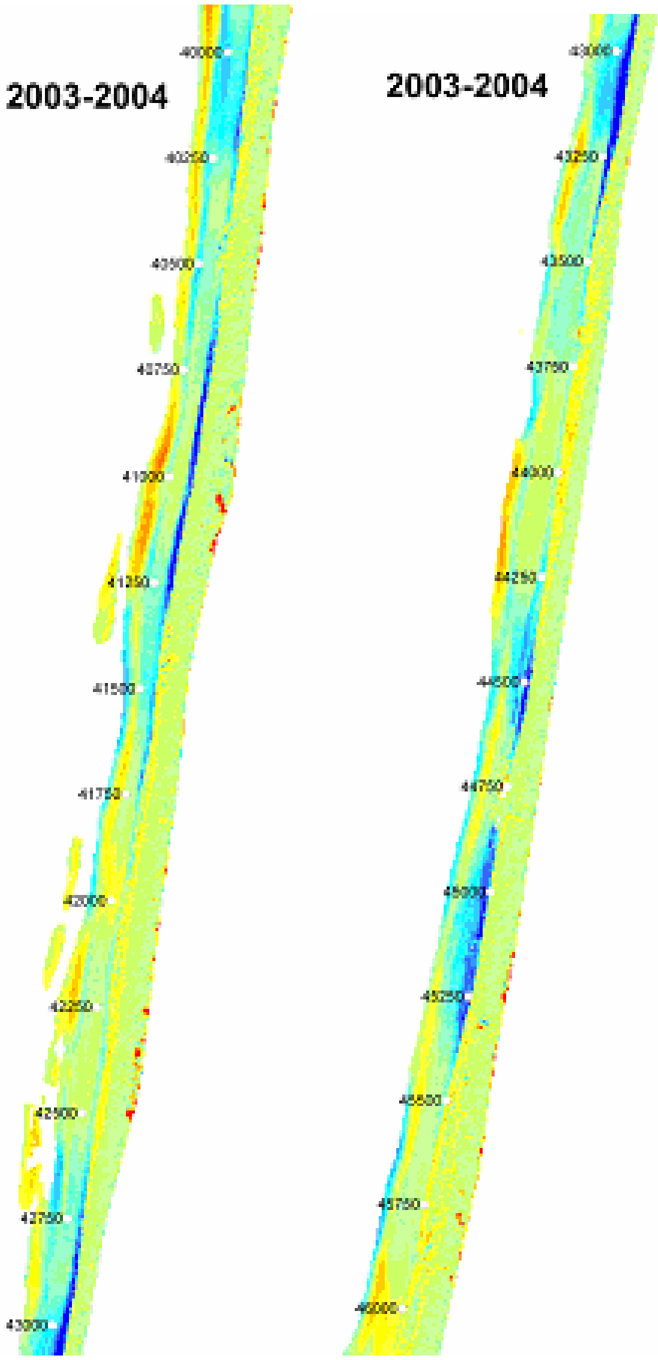

Figure D.12 Volume changes between 2003 and 2004. Scale: -2 m (blue) to + 2 m (red). Left: test area, right: reference area.

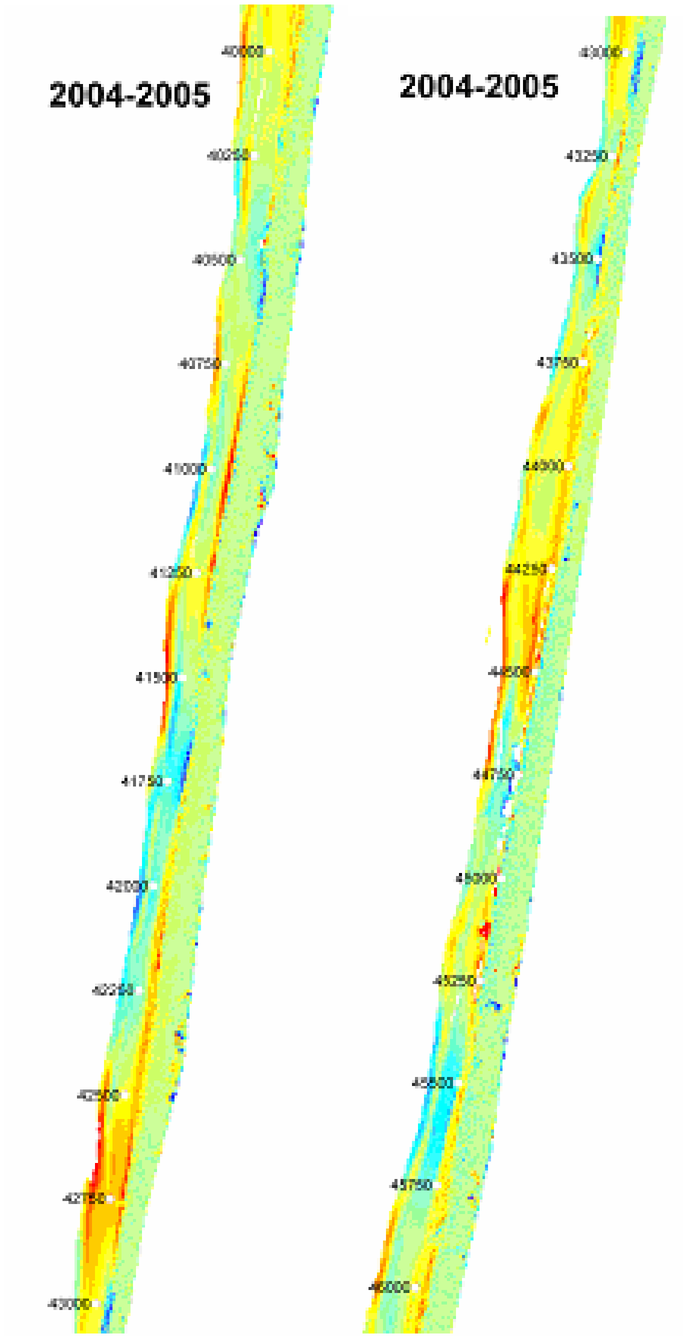

Figure D.13 Volume changes between 2004 and 2005. Scale: -2 m (blue) to + 2 m (red). Left: test area, right: reference area.

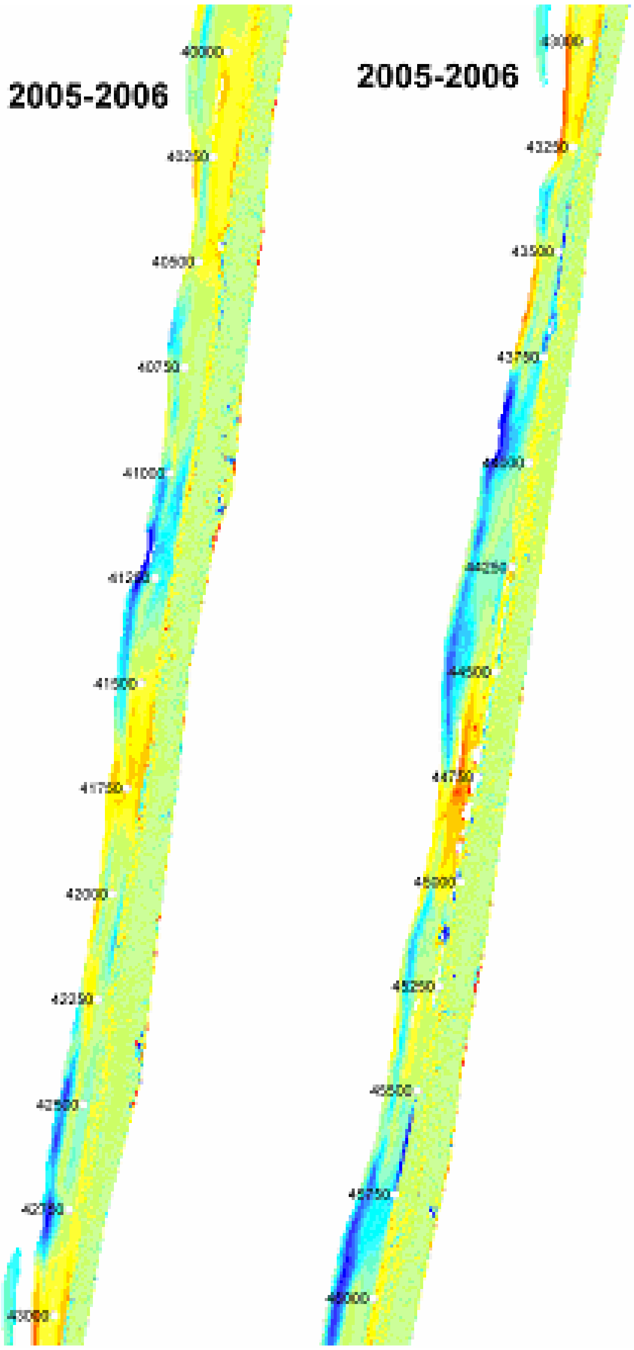

Figure D.14 Volume changes between 2005 and 2006. Scale: -2 m (blue) to + 2 m (red). Left: test area, right: reference area.

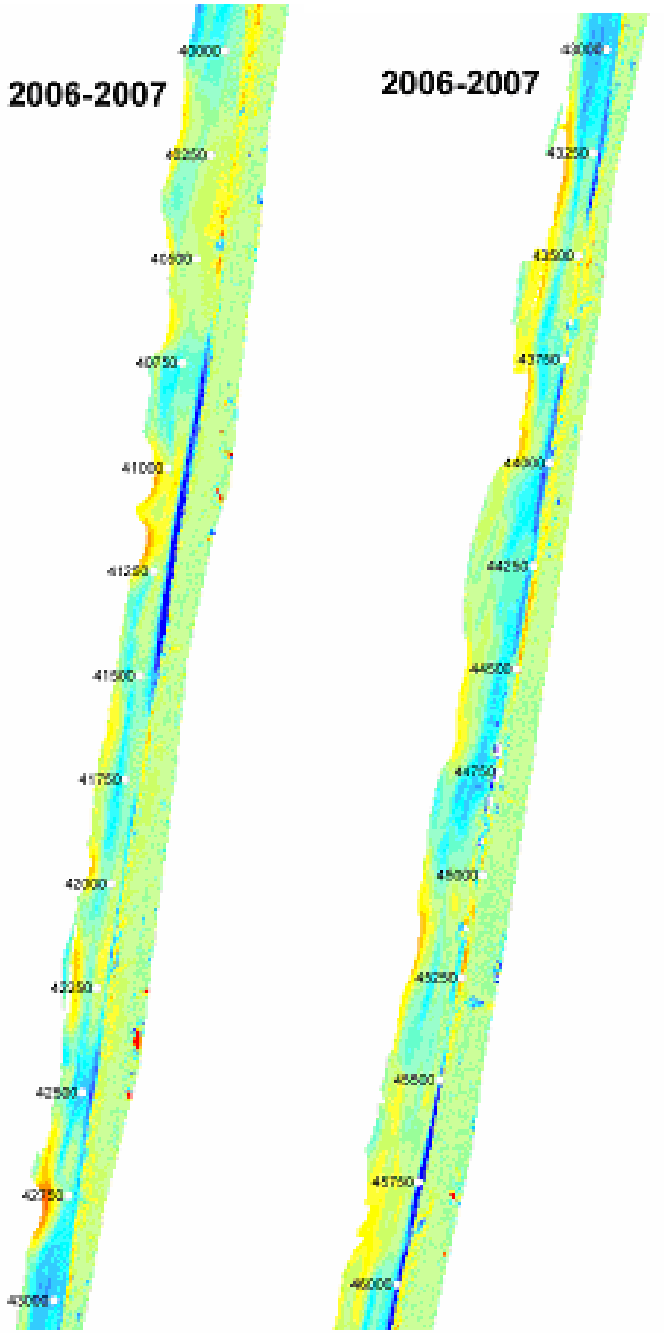

Figure D.15 Volume changes between 2006 and 2007. Scale: -2 m (blue) to + 2 m (red). Left: test area, right: reference area.

Description of dune dynamics per transect

profile	1965-2006	∆V	1997-2006	∆V
40.00	Dunefoot erosion, changing in accretion in 1995; slight increase in Aeolian deposits on the crest	-0.37	Strong aeolian accretion at front with occasional slight dunefoot erosion; very slight deposition on crest	14.40
40.25	Dunefoot erosion, changing in accretion in 1995; slight increase in Aeolian deposits on the crest	-2.50	Slight aeolian accretion of seaward slope with occasional slight dune erosion; very slight deposition on crest	9.34
40.50	Gradual dunefoot erosion changing into stability in 1990; initially strong Aeolian deposition on seaward slope; very slight deposition on crest	2.90	Stable strandslag direct ten n van 40.50	2.20
40.75	Slight dunefoot erosion; strong Aeolian accretion on seaward slope; slight deposition on crest	5.43	Slight dunefoot erosion or accretion; deposition on seaward slope	3.56
41.00	Strong accretion of dunefoot and seaward slope; deposition on top; dunefoot erosion and scarping since 2000	7.16	Occasional dunefoot erosion and scarping, very slight Aeolian deposition on seaward slope	5.03
41.25	Strong accretion of dunefoot and seaward slope; deposition on top; dunefoot erosion and scarping since 1998	9.35	Occasional dunefoot erosion and scarping, continuing Aeolian deposition on seaward slope	5.73
41.50	Strong accretion of dunefoot and seaward slope; deposition on top; dunefoot erosion and scarping since 1995	8.51	Occasional dunefoot erosion and scarping, continuing strong Aeolian deposition on seaward slope	11.74
41.75	Strong accretion of seaward slope and dunefoot; embryonic dune development 1985-1988, dunefoot erosion since 1988	7.74	Occasional dunefoot erosion and deposition; continuing gradual deposition on seaward slope	12.62
42.00	Strong accretion; occasional dunefoot erosion	9.27	Strong accretion; occasional dunefoot erosion	14.38
42.25	Strong accretion; occasional dunefoot erosion	10.50	Strong accretion; occasional dunefoot erosion	18.50
42.50	Strong accretion; occasional dunefoot erosion	7.94	Strong accretion; occasional dunefoot erosion	7.72
42.75	Very strong accretion on crest; moderate accretion on seaward slope; occasional dunefoot erosion and scarping	11.28	Slight accretion of seaward slope; occasional dunefoot erosion and scarping strandslag direct ten z van 42.75	8.51
43.00	Strong accretion of crest but occasional severe dune erosion	2.38	Accretion of crest but occasional severe dune erosion	-4.20
43.25	Strong accretion crest; limited deposition on seaward slope; variable dunefoot	3.52	slight extension of crest; variable dunefoot	5.14
43.50	Before 1995 dune erosion, afterwards increase of height and width	3.47	limited growth; accretion near dunefoot, after 2001 erosion and deposition behind scarp	13.41
43.75	slight increase in height; variable dunefoot	3.45	slight increase in height and progression of crest and seaward slope	15.61
44.00	slight increase inheigt at front of crest; variable dunefoot; very	3.76	gradual growth by slight deposition on crest and seaward slope; dunefoot	14.07

	gentle retreat on average		progression on average	
44.25	gradual increase in height; variable dunefoot	6.51	stable; limited deposition	1.90
44.50	slight increase in height of crest (top and back); since 2000 slight dune erosion	8.04	stable; some dune erosion since 2001	-1.50
44.75	since 1980 progression, slight increase in height of crest; dune erosion in 2005	4.56	stable with variable dunefoot; some deposition	5.30
45.00	since 1970 slight progression in increase in height; 2005 retreat	6.18	since 2000 stable; erosion in 2004	5.79
45.25	between 1980 and 1990 slight retreat, since 1990 slight progression and increase in height	3.95	stable dunefoot; slight but gradual deposition on crest	9.34
45.50	slight progression until 1980; dune erosion between 1980 and 1995; since 1995 stronger progression, slight increase in height of crest and seaward slope	7.92	gradual building of new foredunes; slight deposition on crest and seaward slope until 2001	18.27
45.75	slight progression of seaward slope before 1985; 1985-1995 erosion; since 1995 strong progression of dunefoot and increase in height of crest	4.70	gradual accretion of new foredunes; limited deposition on crest	20.82
46.00	Rolling foredune between 1970 and 1975? Landward movement of crest and deposition at the back. Gradual increase of height; progression since 1995.	12.36	gradual accretion of new foredunes; slight deposition behind new dunes until 2000	23.13

WL | Delft Hydraulics

Rotterdamseweg 185
postbus 177
2600 MH Delft
telefoon 015 285 85 85
telefax 015 285 85 82
e-mail info@wldelft.nl
internet www.wldelft.nl

Rotterdamseweg 185
p.o. box 177
2600 MH Delft
The Netherlands
telephone +31 15 285 85 85
telefax +31 15 285 85 82
e-mail info@wldelft.nl
internet www.wldelft.nl